PEOPLE'S DEMOCRATIC REPUBLIC OF ALGERIA
MINISTERY OF HIGHER EDUCATION AND SCIENTIFIC RESEARCH
UNIVERSITY OF MOHAMED SEDDIK BEN YAHIA - JIJEL

FACULTY OF EXACT SCIENCES AND COMPUTER SCIENCE
DEPARTEMENT OF PHYSICS

Série :.....

Title :

Identifying Higgs-Gauge couplings (HVV) via the $b\bar{b}$ final State at Leptonic Colliders

By

Bougherira Wiam

A dissertation submitted in partial fulfillment of the requirements for the degree of :

Master in Physics

Option: Theoretical Physics

Defended on: June 30th, 2018.

The jury:

President :	Pr. Bouaziz Djamil	Univ. MSBY, Jijel
Supervisor:	Pr. Amine AHRICHE	Univ. MSBY, Jijel
Examiners :	Dr. Med Sadek Zidi	Univ. MSBY, Jijel
	Mr. Nabil Baouche	Univ. YF, Medea

ملخص

في هذه المذكرة لنيل شهادة الماستر، تحققنا من وجود انحرافات عن النموذج المعياري، و بالتالي تأكيد وجود فيزياء جديدة في المصادم الخطي الدولي (ILC) من أجل طاقة مركز الكتل تساوي بالتقريب 1 TeV ، و ذلك من خلال التفاعل $e^-e^+ \to b\bar{b} + \mathrm{E_{miss}}$. من أجل تحقيق هذا الهدف قمنا بإدخال تعديل بسيط في المفصلين HZZ و HWW ثم فرضنا مجموعة من التخفيضات للمتغيرات الحركية، بعد ذلك قمنا بتوليد التوزيعات. في النهاية حددنا عدد الأحداث و الإشارة.

Résumé

Dans ce mémoire du master, nous avons étudié la possibilité de trouver des déviations par rapport au modèle standard, et donc l'existence d'une nouvelle physique au Collisionneur Linéaire International, pour une énergie de centre de mass de 1 TeV a travers le processus $e^-e^+ \to b\bar{b} + \mathrm{E_{miss}}$. Pour cela, nous avons considéré une simple modification sur les deux vertex HZZ et HWW, puis définissé un ensemble de coupures, après nous avons généré des différents distributions. En fin nous avons défini le nombre d'événements et la signification du signal.

Abstract

In this Master's thesis, we studied the possibility of finding deviations from the standard model, and thus the existence of a new physics within the International Linear Collider, for a center of mass energy of about 1 TeV through the process $e^-e^+ \to b\bar{b} + \mathrm{E_{miss}}$. To realize that, we considered a simple modification on the two vertices HZZ and HWW, then we defined a set of cuts, after that, we generated the different distributions. Finally we defined the number of events and the the signal significance.

Contents

Acknowledgments

◦ I want to thank the person with the greatest indirect contribution to this work, my mother. I want to thank, my father, my sister Nada, my brothers Ziad and Nizar, as well as to my uncles Farid and Aissa, and my aunts Sabah, Rabiha and Sofia, not forgiving my dear Salwa for their encouragement. I am deeply indebted to Miss Lamri Houria who helped me enormously.

◦ I want to show my acknowledgment to my supervisor, Dr. Amine Ahriche, who provided me with excellent guidance and precious advice, for his caring and patience during these months, my sincere thanks to you for everything.

◦ I am deeply grateful to Dr. Djamil Bouaziz and Dr. Mohamed Sadek Zidi who accepted to be in my examination jury.

◦ I am so thankful to my professors Dr. S. Houat, Dr. N. Ferkous, Dr. Kh. Nouicer, Dr. T. Boujedaa, Dr. A. Bounames, and to the head of the physics department, Dr. A. Berbadj.

◦ Finally, I thank all my friends and my colleagues Ahlem, Rania, Chahra, Noussaiba, Nesrine, Abir, Rahma, Omar, Hichem and Hilal.

Chapter 1

Introduction

The Standard Model (SM) of particle physics describes the basic constituents of matter and their interactions, but it was able to describe only massless particles. Peter Higgs (and others) have postulated the existence of a new force field (Higgs field) associated with the Higgs boson, where the interaction of the elementary particles with this field generates the mass. This Higgs boson was observed in 2012 at the LHC with mass of 125 GeV [1, 2]. Despite the great successes of the SM, it is unable to answer many questions, such as dark matter nature, neutrino masses and their mixing, ..., etc. That makes physicists looking for a more comprehensive theory which they call " Beyond the Standard Model"

The measurement of the Z and W masses at LEP in 1983, allowed both the HZZ and HWW vertices to be determined. The ILC, which is proposed especially for discovering a new physics beyond the SM, where it has a baseline center of mass energy of 250-500 GeV upgradeable to 1TeV [3, 4, 5] with high-luminosity, can measure these vertices through the interaction $e^-e^+ \to HZ$ with very large precision contrary to the LHC, where there will always remain an uncertainty related to the complex structure of the proton.

In this work, we will look at the HZZ and HWW couplings by interacting$e^-e^+ \to HZ$, trying to find a discovery or a deviation from the SM. To do this, we make a simple modification in the vertices where $2\frac{M_W^2}{\nu}(HWW) \to 2\frac{M_W^2}{\nu}(1+\alpha) \equiv 2\kappa_W\frac{M_W^2}{\nu}$ and $2\frac{M_Z^2}{\nu}(HZZ) \to 2\frac{M_Z^2}{\nu}(1+\beta) \equiv 2\kappa_Z\frac{M_Z^2}{\nu}$ [6, 7, 8]($\alpha = \beta = 0$ is the SM case) using CalcHEP package [13], where we propose a set of values for α and β with relevant cuts that make background reduced while keeping the signal cross section values and maximize the significance, then measuring the cross section of the reactions, and then determine the number of events and the signal significance (S), where, when $S > 3$ is the result, physicists express this result as a deviation from the SM, but when it is greater than 5, that means a new discovery.

It is within the ILC collider that the work presented in this dissertation was carried out. The next chapter presents a brief review of the SM, the Higgs mechanism of spontaneous symmetry breaking, and the general lagrangean of the model,

it presents also its limitations (for a review, see [9, 10, 11, 12]). The third chapter is devoted to the description of some colliders, as LHC, Tevatron, LEP, ILC, ..., etc, as well as to a brief overview of the CalcHEP [13] program and its composition, which will be used in Chapter 4, and brief definitions to one of the most important characteristics of colliders " the luminosity" and to kinematic variables used in accelerators physics. The last chapter concentrates on studying the interaction $e^-e^+ \rightarrow HZ$ where the final state include $b\bar{b}$+E_{miss} in which the missing energy $E_{miss} \equiv v_i\bar{v}_i$ $(i = e, \mu, \tau)$, with summarizing and discussing the results that we have received. Finally we conclude.

Chapter 2

The Standard Model: brief review

2.1 Structure of the Standard Model

The Standard Model (SM) (for review see [10]) of particle physics is a Quantum field theory (QFT) that describes phenomena of particle physics as three types of interaction: strong interactions that make the nucleis of atoms cohesive, weak interactions that cause nuclear disintegrations which are measured as radioactivity, and the electromagnetic interactions that make atoms cohesive with each other and describes the light behavior. There is a fourth force, the gravitational one, but it is not described by this theory. The known particles that the universe is made of are classified by SM into two classes: elementary particles named fermions (leptons and quarks) that build up matter and gauge bosons that are responsible for mediating these interactions.

Fermions:

As said before, fermions are elementary particles of spin $1/2$, in unit of $\hbar$, build up matter, obey the Fermi-Dirac statistic and subdue to Pauli exclusion principle. This means that two identical fermions could not be found at the same quantum state. In the SM, there exist 12 fermions (6 leptons and 6 quarks) grouped two by two into families or generations (Tab. 2.1), (Tab. 2.2):

Generation	Flavor	electric charge	Mass (MeV)	Main Decays
1^{st}	electron (e)	-1	0.510999	-
	e neutrino (ν_e)	0	0	-
2^{nd}	muon (μ)	-1	105.659	$e\nu_e\overline{\nu}_e$
	μ neutrino (ν_μ)	0	0	-
3^{rd}	tau (τ)	-1	1776.99	$e\nu_\tau\overline{\nu}_e, \mu\nu_\tau\overline{\nu}_\mu, \pi^-\nu_\tau$
	τ neutrino (ν_τ)	0	0	-

Table 2.1: Leptons of the SM.

Generation	Flavor	Electric charge	Mass (MeV)
1^{st}	down (d)	$-\frac{1}{3}$	7
	up (u)	$\frac{2}{3}$	3
2^{nd}	strange (s)	$-\frac{1}{3}$	120
	charm (c)	$\frac{2}{3}$	1200
3^{rd}	bottom (b)	$-\frac{1}{3}$	4300
	top (t)	$\frac{2}{3}$	174000

Table 2.2: Quarks of the SM

If we consider the helicity of these particles, each fermion would have two spin states, left-handed $'L'$ for directions of spin and directions of motion opposite, and right-handed $'R'$ for parallel directions, except neutrinos. Massive particles have both L and R components, but neutrinos have only the L component (Tab. 2.3).

1^{st} generation	2^{nd} generation	3^{rd} generation	Y	I_3	Q
$\begin{pmatrix} e^- \\ \nu_e \end{pmatrix}_L$	$\begin{pmatrix} \mu^- \\ \nu_\mu \end{pmatrix}_L$	$\begin{pmatrix} \tau^- \\ \nu_\tau \end{pmatrix}_L$	-1	$-\frac{1}{2}$	-1
				$\frac{1}{2}$	0
e_R^-	μ_R^-	τ_R^-	-2	0	-1
$\begin{pmatrix} u \\ d \end{pmatrix}_L$	$\begin{pmatrix} c \\ s \end{pmatrix}_L$	$\begin{pmatrix} t \\ b \end{pmatrix}_L$	$\frac{1}{3}$	$-\frac{1}{2}$	$\frac{2}{3}$
				$\frac{1}{2}$	$-\frac{1}{3}$
u_R	c_R	t_R	$\frac{4}{3}$	0	$\frac{2}{3}$
d_R	s_R	b_R	$-\frac{2}{3}$	0	$-\frac{1}{3}$

Table 2.3: Eigenvalues of Y , Q and I_3 for different SM fermions. Here, Y is the hypercharge, Q is the electric charge and I_3 is the third component of the isospin.

The hypercharge, the electric charge and the third component of the isospin are related by the so-called Gell-Mann–Nishijima formula

$$Q = I_3 + \frac{1}{2}Y. \tag{2.1}$$

Gauge Bosons:

The gauge bosons are the particles associated with the interactions fields between elementary fermions (Tab. 2.4). For electromagnetic force, the interaction occurs between electrically charged particles via the exchange of the massless photon. The mediator of strong interactions, between quarks, between gluons and between quarks and gluons, is the massless gluon gauge boson. Both gluons and quarks has color charge (red, blue and green) under the color gauge group $SU(3)_C$. The only three massive gauge bosons are the charged $W^{\pm}$, and the neutral Z, which mediate the weak interactions. The postulated graviton is the mediator of gravitational interactions, but, they are not considered by the SM.

Force	Theory	mediator	Electric charge	Mass (GeV)	Spin
Strong	QCD	8 gluons (g)	0	0	1
Electromagnetic	QED	photon (γ)	0	0	1
Weak	Flavor dynamics	$W^{\pm}$	± 1	80.420	1
		Z	0	91.190	1
Gravitational	Geometrodynamics	Gravitons	0	0	2

Table 2.4: Gauge bosons of the SM. Here, the graviton does not belong to the SM.

The theory of SM is a collection of three related theories: theory of quantum electrodynamics QED (of electromagnetic), theory of quantum chromodynamics QCD (of strong interactions) and the Glashow-Weinberg-Salam GWS electroweak theory EW. Moreover, it is a gauge theory based on the local gauge symmetry group (in fact, the direct product of three sub-groups) $SU(3)_C \otimes SU(2)_L \otimes U(1)_Y$ that has 12 generators, where $SU(3)_c$ or color group, describes strong interaction, $SU(2)_L$ is the weak isospin group where $'L'$ expresses the left-hunded chirality, which describes weak interactions. Here both weak and electromagnetic interactions are described together within the so-called electroweak theory that is described by the gauge group $SU(2)_L \otimes U(1)_Y$. Then after the spontaneous symmetry breaking, weak and electromagnetic interactions are separated and only QED symmetry $U(1)_{em}$ is maintained which results the masslessness of the photon.

2.2 The Standard Model Lagrangian

Here, we present the full Lagrangian of the SM that includes all the fields and obey the gauge group $SU(3)_C \otimes SU(2)_L \otimes U(1)_Y$.

QCD

The theory QCD is described by the following lagrangian

$$\mathcal{L}_{QCD} = -\frac{1}{4} F^i_{\mu\nu} F^{i\mu\nu} + \sum \bar{q}_{r\alpha} i \not{D}^{\alpha}_{\beta} q^{\beta}_{r}, \tag{2.2}$$

where α, β are generation indices, and $F^i_{\mu\nu}$ is the field strength tensor for the gluon fields G^i_μ, which is given by:

$$F^i_{\mu\nu} = \partial_\mu G^i_\nu - \partial_\nu G^i_\mu - g_s f_{ijk} G^j_\mu G^k_\nu, \tag{2.3}$$

with g_s is the QCD gauge coupling, and f_{ijk} $(i, j, k = 1..8)$ are called antisymmetric structure constants, that are defined as:

$$[\lambda^i, \lambda^j] = 2i f_{ijk} \lambda^k. \tag{2.4}$$

The generators λ are eight 3×3 matrices, normalized by:

$$Tr(\lambda^i\lambda^j) = 2\delta^{ij}. \tag{2.5}$$

According to (Eq. 2.3), there could be triple and quadruple gluon vertices.

The electroweak theory

The electroweak model is a description of both weak and electromagnetic interactions before the electroweak symmetry gets broken. It is described by the direct product of two groups: $SU(2)_L \times U(1)_Y$, and results massive gauge bosons and a massless photon. The electroweak Lagrangean is given by:

$$\mathcal{L}_{EW} = \mathcal{L}_{Yuk} + \mathcal{L}_{gauge} + \mathcal{L}_{\phi} + \mathcal{L}_f. \tag{2.6}$$

The gauge Lagrangean is :

$$\mathcal{L}_{gauge} = -\frac{1}{4}B_{\mu\nu}B^{\mu\nu} - \frac{1}{4}W^i_{\mu\nu}W^{i\mu\nu}, \tag{2.7}$$

where $B_{\mu\nu}$, $W^i_{\mu\nu}$ are the field strengths:

$$\begin{aligned} B_{\mu\nu} &= \partial_\mu B_\nu - \partial_\nu B_\mu \\ W^i_{\mu\nu} &= \partial_\mu W^i_\nu - \partial_\nu W^i_\mu - g\epsilon_{ijk}W^j_\mu W^k_\nu, \quad i = 1...3 \end{aligned} \tag{2.8}$$

with: $B_\mu(x)$ is the gauge boson of $U(1)_Y$, $W^a_\mu(x)$ are the three bosons vectors $SU(2)_L$, and g is the gauge coupling of the $SU(2)_L$ gauge group.

The scalar part is given by:

$$\mathcal{L}_\phi = (D^\mu\phi)^\dagger(D_\mu\phi) - \underbrace{(\mu^2\phi^\dagger\phi + \lambda(\phi^\dagger\phi)^2)}_{=V(\phi)}, \tag{2.9}$$

where

$$\phi = \begin{pmatrix} \phi^+ \\ \phi^0 \end{pmatrix}, \tag{2.10}$$

is the Higgs complex scalar $SU(2)_L$ field doublet, and λ is the positive scalar quartic coupling. The scalar doublet covariant derivative is written as

$$D_\mu\phi = (\partial_\mu + \frac{i}{2}g\sigma^i W^i_\mu + \frac{i}{2}g'B_\mu)\phi. \tag{2.11}$$

The fermions Lagrangian Part is:

$$\begin{aligned} \mathcal{L}_f &= \sum_m (\overline{q}^0_{mL} i\not{D} q^0_{mL} + \overline{l}^0_{mL} i\not{D} l^0_{mL} + \overline{u}^0_{mR} i\not{D} u^0_{mR} \\ &+ \overline{d}^0_{mR} i\not{D} d^0_{mR} + \overline{e}^0_{mR} i\not{D} e^0_{mR} + \overline{v}^0_{mR} i\not{D} v^0_{mR}). \end{aligned} \tag{2.12}$$

Here, the label " L" refers to the left-handed chirality $\psi_L = \frac{1}{2}(1-\gamma_5)\psi$ and " R" refers to the right-handed chirality $\psi_R = \frac{1}{2}(1+\gamma_5)\psi$ where the matrices $\frac{1}{2}(1\pm\gamma_5)$ are the left- and right-handed projectors. The fermions of left-handed-chirality

$$l^0_{mL} = \begin{pmatrix} v^0_m \\ e^{-0}_m \end{pmatrix}_L, q^0_{mL} = \begin{pmatrix} u^0_m \\ d^0_m \end{pmatrix}_L, \tag{2.13}$$

are classified in doublets according to $SU(2)_L$. While, the right–handed fermions v^0_{mR}, e^{-0}_{mR}, u^0_{mR} and d^0_{mR} are singlets under the same gauge group.

The $U(1)_Y$ charges for these fermions are $y_{q_L} = \frac{1}{6}$, $y_{l_L} = -\frac{1}{2}$, $y_{\psi_R} = q_\psi$. Then, the covariant derivatives of the SM fermionic representations are:

$$\begin{aligned} D_\mu l^0_{mL} &= (\partial_\mu + i\frac{g}{2}\vec{\sigma}\vec{W}_\mu + i\frac{g'}{2}B_\mu)l^0_{mL}, \\ D_\mu q^0_{mL} &= (\partial_\mu + i\frac{g}{2}\vec{\sigma}\vec{W}_\mu + i\frac{g'}{6}B_\mu)q^0_{mL}, \end{aligned} \tag{2.14}$$

and

$$\begin{aligned} D_\mu u^0_{mR} &= (\partial_\mu + i\frac{2g'}{3}B_\mu)u^0_{mR}, \\ D_\mu d^0_{mR} &= (\partial_\mu - i\frac{g'}{3}B_\mu)d^0_{mR}, \\ D_\mu e^0_{mR} &= (\partial_\mu - ig'B_\mu)e^0_{mR}, \\ D_\mu v^0_{mR} &= \partial_\mu v^0_{mR}. \end{aligned} \tag{2.15}$$

The Yukawa Lagrangian is:

$$\mathcal{L}_{Yuk} = -\sum_{m,n=1}^{F}[\Gamma^u_{mn}\bar{q}^0_{mL}\tilde{\phi}u^0_{nR} + \Gamma^d_{mn}\bar{q}^0_{mL}\phi d^0_{nR} + \Gamma^e_{mn}\bar{l}^0_{mL}\phi e^0_{nR} \tag{2.16}$$

$$+ \Gamma^v_{mn}\bar{l}^0_{mL}\tilde{\phi}v^0_{nR}] + h.c., \tag{2.17}$$

where F represents the number of families ($F \geq 3$), m and n are flavors indices, Γ_{mn} are the Yukawa coupling matrices between the Higgs ϕ and various fermionic representations.

2.3 Spontaneous Symmetry Breaking

The mass terms are not allowed in the Lagrangean because of its invariance under gauge transformations. To make gauge bosons or chiral fermions acquire masses, the gauge invariance must be broken spontaneously. The system vacuum of the Higgs field ($\langle h \rangle = 0$) is supposed to make the gauge symmetry invariant under

$SU(2)_L \otimes U(1)_Y$. However, if the Higgs field acquires a vacuum expectation value (vev) system vacuum ($\langle h \rangle \neq 0$), then the symmetry is spontaneously broken.

Let's consider the Lagrangian of the $\lambda\phi^4$ theory (Eq. 2.9), which is invariant under a global symmetry $U(1)$ with,

$$V(\phi) = \mu^2 |\phi|^2 + \lambda |\phi|^4, \tag{2.18}$$

with

$$\phi = \frac{1}{\sqrt{2}}(\varphi_1 + i\varphi_2) = \frac{1}{\sqrt{2}} |\phi_0| e^{i\theta}. \tag{2.19}$$

The symmetry breaking could be spontaneously if μ^2 is slashedative. Then the potential gets a vev at $|\phi_0|^2 = \frac{-\mu^2}{\lambda}$ by imposing the conditions $\frac{\partial V}{\partial \varphi_{1,2}} = 0$, or $\frac{\partial V}{\partial \phi_0} = \frac{\partial V}{\partial \theta} = 0$.

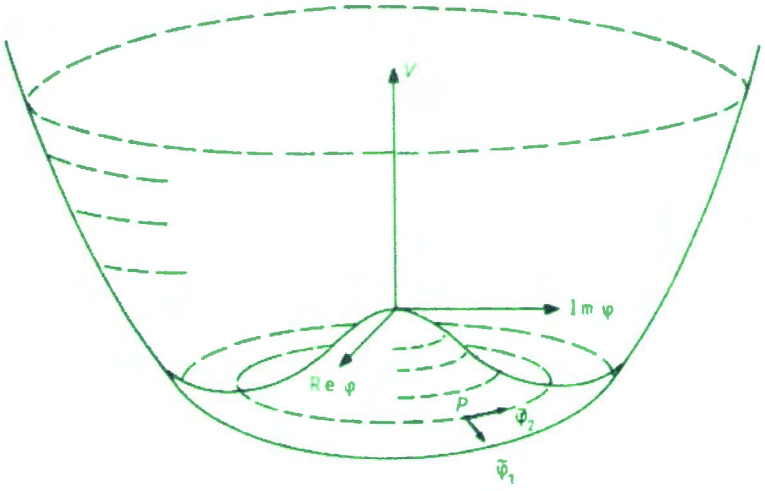

Figure 2.1: The form of $V(\phi)$ for $\mu^2 < 0$.

Here, there is an infinite number of vacua, so we choose the simple case:

$$\Longrightarrow \phi_0 = v = \sqrt{\frac{-\mu^2}{\lambda}}. \tag{2.20}$$

In the SM, the electroweak symmetry is broken when the neutral component of the Higgs doublet (Eq. 2.10) get a vev, i.e.,

$$\phi(x) = \frac{1}{\sqrt{2}} \begin{pmatrix} 0 \\ v + H \end{pmatrix}. \tag{2.21}$$

Since the vacuum is neutral, then one must have ($I = \frac{1}{2}, I_3 = -\frac{1}{2}$), and as $Q = I_3 + \frac{1}{2}Y$, the choice that Y equal to 1 breaks the $SU(2)_L \times U(1)_Y$.

After expanding the expression of the Higgs kinetic term, one gets

$$\begin{aligned}(D_\mu\phi)^\dagger(D_\mu\phi) &= \left|(\partial_\mu + \frac{i}{2}g\sigma^i W_\mu^i + \frac{i}{2}g'B_\mu)\frac{1}{\sqrt{2}}\begin{pmatrix}0\\ v+H\end{pmatrix}\right|^2 \\ &= \frac{1}{2}(\partial_\mu H)(\partial^\mu H) + \frac{(v+H)^2}{8}\left\{g^2\left(\left(W_\mu^1\right)^2 + \left(W_\mu^2\right)^2\right) + \left(gW_\mu^3 - g'B_\mu\right)^2\right\} \quad (2.22)\end{aligned}$$

In the electroweak theory, W^1 and W^2 identify the charged gauge boson $W^\pm$, and W^3 and B mix to form the neutral bosons Z and the photon; i.e. the physical particles with the masses:

$$\begin{aligned}W_\mu^\pm &= \frac{1}{\sqrt{2}}\left(W_\mu^1 \mp iW_\mu^2\right) \; M_W = \frac{gv}{2}, \\ Z_\mu &= \frac{1}{\sqrt{g^2+g'^2}}\left(gW_\mu^3 - g'B_\mu\right) \; M_Z = \frac{v}{2}\sqrt{g^2+g'^2} = \frac{M_W}{\cos\theta_W}, \\ A_\mu &= \frac{1}{\sqrt{g^2+g'^2}}\left(g'W_\mu^3 - gB_\mu\right) \; M_A = 0. \quad (2.23)\end{aligned}$$

Here, we have,

$$\begin{aligned}A_\mu &= \cos\theta_W B_\mu + \sin\theta_W W_\mu^3, \\ Z_\mu &= -\sin\theta_W B_\mu + \cos\theta_W W_\mu^3, \quad (2.24)\end{aligned}$$

or

$$\begin{aligned}W_\mu^3 &= \sin\theta_W A_\mu + \cos\theta_W Z_\mu, \\ B_\mu &= \cos\theta_W A_\mu - \sin\theta_W Z_\mu, \quad (2.25)\end{aligned}$$

with

$$e = g\sin\theta_W = g'\cos\theta_W \;\Rightarrow \tan(\theta_W) = \frac{g'}{g}, \quad (2.26)$$

where θ_W is the Winberg mixing angle.

2.4 The Higgs and Yukawa Interactions:

The Lagrangian Higgs term in (Eq. 2.9) can be written after the electroweak symmetry breaking as:

$$\begin{aligned}\mathcal{L}_\phi &= \frac{1}{2}(\partial_\mu\phi)^2 - V(\phi) \\ &+ M_W^2 W^{\mu+}W_\mu^-(1+\frac{H}{v})^2 + \frac{1}{2}M_Z^2 Z^\mu Z_\mu(1+\frac{H}{v})^2, \quad (2.27)\end{aligned}$$

and the Higgs potential is:

$$V(\phi) \supset -\mu^2 H^2 + \frac{1}{4}\lambda H^4 + \lambda v H^3. \tag{2.28}$$

After SSB, we get the Higgs real scalar field H with the mass $M_H = \sqrt{-2\mu^2} = \sqrt{2\lambda}v$.

The second third and the fourth terms in (Eq. 2.27) give $HHZZ$, $HHWW$, HZZ and HWW interactions (Fig. 2.2).

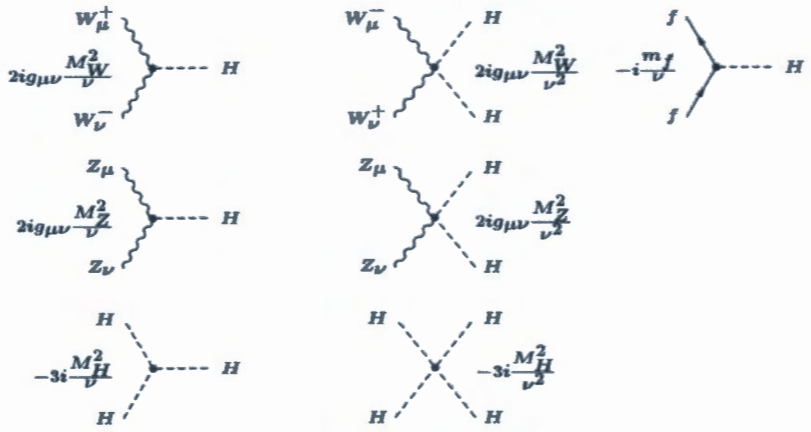

Figure 2.2: The Higgs interactions vertices.

The Yukawa part becomes:

$$\begin{aligned}\mathcal{L}_{Yuk} &\rightarrow -\sum_{m,n=1}^{F} \overline{u}^0_{mL}\Gamma^u_{mn}(\frac{v+H}{\sqrt{2}})u^0_{mR} + (d,e) \text{ terms} + h.c. \\ &= \overline{u}^0_L(M^u + h^u H)u^0_R + (d,e) \text{ terms} + h.c,\end{aligned} \tag{2.29}$$

where: $\overline{u}^0_L = (\overline{u}^0_{1L}\overline{u}^0_{2L}...\overline{u}^0_{FL})^T$ and $\overline{u}^0_R = (\overline{u}^0_{1R}\overline{u}^0_{2R}...\overline{u}^0_{FR})^T$ are F-components column vectors, $M^u = \frac{\Gamma^u_{mn}v}{\sqrt{2}}$ is a $F \times F$ fermion mass matrix, and $h^u = \frac{M^u}{v} = \frac{gM^u}{2M_W}$ is the Yukawa coupling matrix.

2.5 The Charged and Neutral Currents

The Charged Current

The interaction of the charged bosons W to quarks and leptons is:

$$\mathcal{L} = -\frac{g}{2\sqrt{2}}(J^\mu_W W^-_\mu + J^{\mu\dagger}_W W^+_\mu), \tag{2.30}$$

where

$$J_W^{\mu\dagger} = \sum_{m=1}^{F} [\overline{\nu}_m^0 \gamma^\mu (1-\gamma^5) e_m^0 + \overline{u}_m^0 \gamma^\mu (1-\gamma^5) d_m^0]$$
$$= (\overline{\nu}_e \overline{\nu}_\mu \overline{\nu}_\tau) \gamma^\mu (1-\gamma^5) V_l \begin{pmatrix} e^- \\ \mu^- \\ \tau^- \end{pmatrix} + (\overline{u}\overline{c}\overline{t}) \gamma^\mu (1-\gamma^5) V_q \begin{pmatrix} d \\ s \\ b \end{pmatrix}, \quad (2.31)$$

is the weak charge raising current. It has a $V-A$ form, with, V is the Cabibbo-Kobayashi-Maskawa (CKM) matrix [17]. The fermions gauge vertices shown in (Fig. 2.3), and g_A, g_V are given in the following table

Fermion	g_V	g_A
ν_e, ν_μ, ν_τ	$\frac{1}{2}$	$\frac{1}{2}$
e^-, μ^-, τ^-	$-\frac{1}{2} + 2\sin^2\theta_W$	$-\frac{1}{2}$
u, c, t	$\frac{1}{2} - \frac{4}{3}\sin^2\theta_W$	$\frac{1}{2}$
d, s, b	$-\frac{1}{2} + \frac{2}{3}\sin^2\theta_W$	$-\frac{1}{2}$

Table 2.5: The coupling constants values of the W gauge boson to the SM fermions.

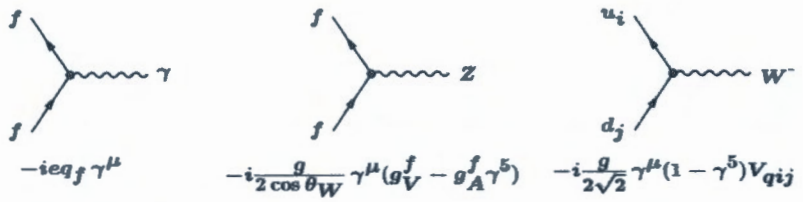

Figure 2.3: The fermion gauge vertices in the EW theory.

The Neutral Current

The weak neutral current is a class of gauge interaction, where the combination of its fields is the neutral boson Z

$$\mathcal{L} = -\frac{\sqrt{g^2+g'^2}}{2} J_Z^\mu (-\sin\theta_W B_\mu + \cos\theta_W W_\mu^3)$$
$$= -\frac{g}{2\cos\theta_W} J_Z^\mu Z_\mu \;/\; \cos\theta_W = \frac{g}{\sqrt{g^2+g'^2}} \quad (2.32)$$

where

$$J_Z^\mu = \sum_{m,n=1}^{F} [\overline{u}_{mL}^0 \gamma^\mu u_{mL}^0 - \overline{d}_{mL}^0 \gamma^\mu d_{mL}^0 + \overline{\nu}_{mL}^0 \gamma^\mu \nu_{mL}^0 - \overline{e}_{mL}^0 \gamma^\mu e_{mL}^0] - 2\sin\theta_W J_Q^\mu$$
$$= \sum_{m,n=1}^{F} [\overline{u}_{mL} \gamma^\mu u_{mL} - \overline{d}_{mL} \gamma^\mu d_{mL} + \overline{\nu}_{mL} \gamma^\mu \nu_{mL} - \overline{e}_{mL} \gamma^\mu e_{mL}] - 2\sin\theta_W J_Q^\mu \quad (2.33)$$

2.6 Limitations of the SM

None can deny the great experimental and theoretical success of the SM in particle physics, especially in describing the electroweak theory. Effectively, it predicted the existence of $W^{\pm}$and Z bosons, and the top quark before their detecting in CERN(1983) and in tevatron(1995) respectively, also the discovering of the Higgs boson but that does not mean that this theory is without failure:

*Gravitational force stays a missed piece in SM theory till now.

*The kinematics of galaxies indicate the existence of non-luminous matter (dark matter), and dark energy which account for 95% of the matter in this universe in addition to the ordinary particles described by SM. Till now, the SM can not define any scalar particle has characteristics that make it considered as a dark matter component.

*Contrary to the supersymmetric SM which proves the possibility of unifying coupling constants g_1, g_2, g' of the symmetry groups $U_Y(1)$, $SU_L(2)$ and $SU_C(3)$ respectively, SM is unable to unify them

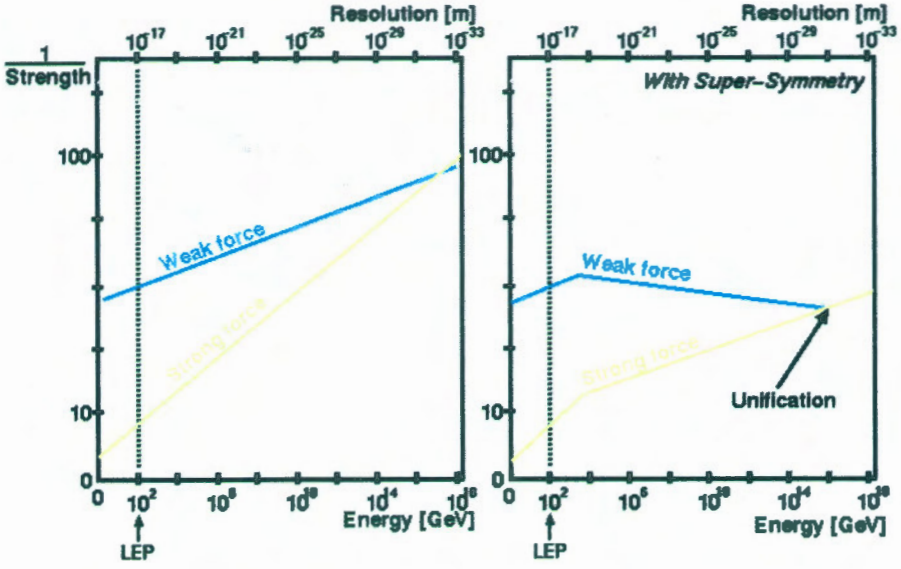

Figure 2.4: The interaction strengths evolution with respect to the energy scale.

* Neutrinos postulated in 1933 by Pauli, and baptized by Fermi who shows that neutrino mass is very smaller then the mass of electron or it is a zero mass. Landau, Yang and lee, and Salam supposed then that neutrino is a massless particle and that it has both right and left components. After observing that neutrinos oscillate from flavor to other, the beliefs that those particles are massless changed. In the SM, neutrinos, that interacts only via weak interactions through the exchange of W and Z bosons, are massive and only left-handed. In fact, the measured value is the difference between square of eigenstates of mass and not the individual masses of neutrinos. If we suppose that this mass is really exist, neutrinos will be Dirac

fermions and may be Majorana fermions, but the mass terms of Dirac and Majorana are not allowed because they vacate the invariance of the system??

*Basic interactions of the standard are defined by the direct product of three symmetry groups $SU(3) \otimes SU(2) \otimes U(1)$, so it exists three fundamental scales of energy. The problem here [9] is the long disparity between these scales ($\Lambda_{QCD} \simeq 100\ MeV$ for strong coupling, $M_{Planck} \simeq 10^{19} GeV$ and the scale $M_W \simeq 100 GeV$ of SSB of the electroweak sector)

*SM can not explain what is the mechanism that explains the orders of magnitude separating the masses of the three generations of fermions, and why there are only three generations.

*SM can not explain the asymmetry between matter and anti-matter, exactly the asymmetry between baryons and antybaryons in this universe.

Chapter 3

Physics at Colliders

3.1 Overview on Particles Colliders

Experiences of particle physics depend to particle accelerators, that used as colliders or as synchrotron light sources. They may be under two types: linear and circular accelerators (Fig. 3.1), The objective of a collider is to accelerate particles to high energy, and make them collide between each other to create new particles (short-lived particles). Colliders depend of some parameters like luminosity, dimensions, life cycle, ...etc. It exists many colliders:

* Hadrons Colliders (Tevatron and LHC ... etc)
* Electron-Positron Colliders (like LEP).
* Electron-Proton Colliders (like Hera).

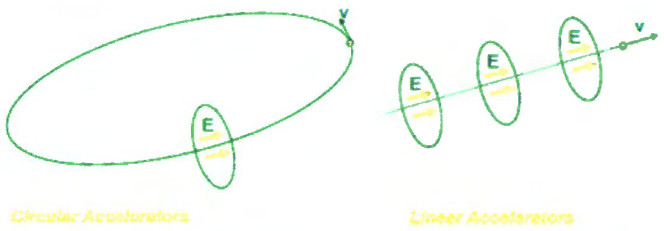

Figure 3.1: Circular and linear accelerators.

Recent colliders:

Tevatron:

Fermilab tevatron(1987) is a circular collider, its objective was to accelerate protons and antiproton in a ring of 6.28 Km to very high center of mass energy of about 2TeV (tera electron volt). The discovery of Top-quark particle, with m$\simeq$175GeV, was in this collider in 1994.

HERA:

HERA (Hadron-Electron Ring Accelerator) is the only highest energy Lepton-Hadron , more precisely, it is a Proton-Electron collider, used super-conductivity

applications. In this collider, electrons collide with protons at a center of mass energy of about 320 GeV.

Understanding the QCD dynamics and elucidating the structure of the proton, the discovery of slow partons in the proton and the sizable diffractive cross section at large four-momentum squared Q^2, can be noted as a great success for HERA.

LEP:

The Large Electron-Positrons collider began running in 1989 at CERN (European Organization for Nuclear Research) -Switzerland, with initial energy around 45.6 GeV, so that, it would be able to produce and study the three massive bosons Z and $W^{\pm}$, that were observed at the Super Proton-Antiproton Synchrotron (SPS Proton-anti-proton collider). It succeeded in measuring characteristics of these bosons with excellent precision; moreover, it proved that there are three types of neutrinos, and so only three fundamental generations of fermions.

LEP was deactivated in 2000, and replaced by the Large Hadron Collider LHC.

Present & Future Colliders

LHC:

LHC started its operation on November 2009, in the 27 Km ring tunnel of the LEP. Its aim is accelerating two proton beams to the speed of light, then makes them collide at center of mass energy of 14 TeV (7 TeV for each beam), also colliding heavy ions (Pb-Pb collisions) and providing Pb-p collisions, in order to look for evidence of supersymmetry, the nature of dark matter and the origin of the mass of elementary particles.

In 2012, the discovery of a new elementary particle, similar to the Higgs boson, was officially announced at LHC.

LHC includes six experiments/detectors [19] with a Monopole and Exotics Detector (MoEDAL) :

ATLAS and CMS:

ATLAS (**A** Toroidal LHC Apparatu **S**) and CMS (**C**ompact **M**uon **S**olenoid), are two large particles detectors constructed at the LHC, their first objective was to discover the Higgs boson. Now that it is reached, they will accurately measure the properties of this particle, and study physics theories beyond the SM: supersymmetry, ...

ALICE and LHCb:

ALICE (**A** Large Ions Collider Experiment) concentrates on heavy ions collisions, where, the encounter of two heavy ions results a high energy in the form of heat and radiation to produce quark–gluon plasma, and that allows the study of strong interaction between quarks. LHCB (**LHC** Beauty Experiment) studies hadrons containing a heavy quark (charm or beauty). Its precision measurements make it possible to examine the Standard Model (violations of the charge conjugation and parity symmetries).

TOTEM and LHCf:

TOTEM (Total cross section, elastic scattering and diffraction dissociation), and LHCf (**LHC** forward) are the smallest LHC experiments, where, the objective of

TOTEM is to measure the total proton-proton cross section and study elastic scattering and diffractive dissociation, and the objective of LHCf is to measure the energy and numbers of neutral pions produced, and that will help in explaining the origin of ultra-high-energy cosmic rays.

ILC

Proton is a particle composed of quarks, the total energy of a proton at LHC is shared between its components and the energy available for a reaction between two component quarks is unknown. Contrary to the proton, electron and positron are elementary particles without internal structure, so that the energy of each collision in a electron-positron collider (ILC) will be precisely determinated, that is why ILC will be more accurate than LHC.

The International Linear Collider (ILC) [20], is a high-luminosity electron-positron collider of 31 km in length, with a center-of-mass energy of 250-500 GeV upgradeable to 1TeV, proposed to be constructed in Japan, it should be linear to avoid energy losses, due to synchrotron radiation, from circular geometry. It consists of two 12 Km linear accelerators (Linacs) facing each other and propelling electrons to positrons, at the speed of light, plus two damping rings with a circumference of 6.7 km for each ring, and an interaction area. ILC should provide information on a series of unanswered questions in particle physics, like the nature of dark matter, unification of all forces, the Higgs bosons properties (mass, spin and the strength of their interactions with the other elementary particles), the existence of hypothetical elementary particles, ...etc.

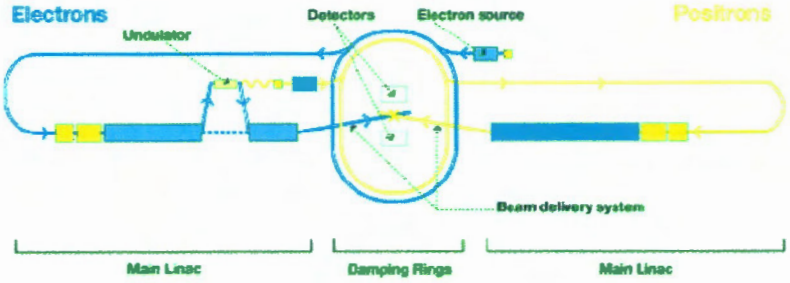

Figure 3.2: The International Linear Collider (ILC).

3.2 Collider Kinematic Variables

In this section, we will show different kinematic variables that are measured, directly and indirectly, at collider detectors [22].

Pseudorapidity, is a dimensionless variable, used in experimental particle physics to describe the angle of a particle relative to the beam axis, it is defined by [22]:

$$\eta = -\ln\left|\tan\frac{\theta}{2}\right| = \frac{1}{2}\ln\left(\frac{\left|\vec{P}\right| + P_Z}{\left|\vec{P}\right| - P_Z}\right)$$

where P_Z is the component of the momentum along the beam axis (Z)

Invariant mass is the mass of one particle or more in state of rest, given by:

$$M^2 = \left(\sum_i E_i\right)^2 - \left(\sum_{i=1} \vec{P}_i\right)^2$$

where E is the energy of particles and P is the quantity of motion

Transverse Momentum is a dynamical variable, it can be measured at leptonic colliders, at the transverse level of detector, it is defined as:

Energy is the energy of one particle or more in state of rest

Transverse Energy is an invariant quantity under Lorentz transformations along the direction of the beam axis Z, given by:

$$E_T = \sqrt{M^2 + P_T^2} \tag{3.1}$$

once the particle is massless, transverse energy will be equal to the Transverse momentum

Transverse Mass, is an important quantity in particle physics, it is invariant under Lorentz transformations along the direction of the beam axis Z, given by:

$$M_T^2 = M^2 + P_x^2 + P_y^2 = E^2 - P_Z^2 \tag{3.2}$$

where P_x, P_y are the components of the momentum perpendicular to the beam axis

Jet cone angle is the quantity describes the separation between cones of hadrons and other particles produced by the hadronization of a quark and gluon, it is defined as:

$$\triangle R = \sqrt{\triangle\eta^2 + \triangle\phi^2} \tag{3.3}$$

where ϕ is the azimuthal angle and η is the pseudorapidity.

we will use these variables as Cuts and Distributions in the next chapter.

3.3 Data Analysis

Collider which consists of two synchrotrons where the particles are accelerated in opposite directions, is one of the most efficient since the energy available in the center of mass is very large. However, the probability of an interaction when two beams arrive face-to-face is much weaker than in the case of a fixed target collision

because of the density of the beams in particular. This probability is parameterized by a quantity called luminosity.

The luminosity L is one of the High Energy colliders characteristics, it is obtained from the ratio N/σ [21], where N is the number of events produced and σ is the process cross section:

$$N = L\sigma, \tag{3.4}$$

also it can be expressed as follow:

$$N = L\int d\sigma = L\int \frac{d\sigma}{dX}dX, \tag{3.5}$$

where X expresses the kinetic variables described in the previous section, and $\frac{dN}{dX}$ is the distribution function of the number of events in relation to the variable X, this ratio describes the experimental results obtained by data analyzers, in order to evaluate the physical significance of the signal. The general signal significance is defined by:

$$S = \frac{N_S}{\sqrt{N_S + N_B}} \tag{3.6}$$

with N_S is the signal event number, and N_B is the background number of events. In our work, since we are interested in looking for event excess with respect to the SM due to Higgs-gauge coupling modifications, then N_S and N_B are given by:

$$\begin{aligned} N_S &= L(\sigma^M - \sigma^B), \\ N_B &= L\sigma^B \end{aligned} \tag{3.7}$$

where, σ^M is the modified model cross section, σ^B is the SM background cross section, and $L = \int Ldt$ is the integrated luminosity. If the signal and background events numbers are comparable, it would be better to the significance definition [23] rather than (Eq. 3.6).

$$S = \sqrt{2 \times \left[(N_S + N_B) \times \log(1 + \frac{N_S}{N_B}) - N_S\right]} \tag{3.8}$$

3.4 HEP Tools: CalcHEP Package

CalcHEP (Calculations in High Energy Physics) is [13] a useful package for the computation of cross sections, evaluation of decay and scattering processes in elementary particle physics, it is the development of CompHep package, which was created by Alexander Pukhov with Neil Christense and Alexander Belyaev. CalcHEP consists of two parts, which are written in the C programming language, a part of symbolic calculations and a part of numeric calculation.

Installation of CalcHEP:

To install CalcHEP we should:

1-download it from the web site:

http://theory.sinp.msu.ru/~pukhov/calchep.html.

2-unpack the download file: tar -xvzf CalcHEP_3.3.6.tgz .

3-compile it by running " make" or " gmake" .

we need a C compiler with the X11 graphics library to avoid any compilation problem; getting it by installing Libx11-dev.

4- create a working directory by running ./mk WORK dir/directory-name.

once this directory is created, the subdirectories bin/, results/, tmp/ and models/ should be created automatically.

*bin/: a symbolic link to CalcHEP executables.

*results/: is for CalcHEP output

*tmp/: for temporal files

*models/: contains a set of files define theoretical particle physics models:

-prtcls#.mdl for particle definition

-vars#.mdl for independent parameters

- func#.mdl for dependent parameters

- lgrng#.mdl for interactions, and

-extlib#.mdl for external routines

we can modify or add any model.

In addition to these files, we find two scripts: ./calchep for launching the Graphical User Interface (GUI), and ./calchep_batch for launching batch sessions.

Running CalcHEP:

To go to the Graphical User Interface, we should execute ./calchep script in a terminal. the main menu of CalcHEP will be opened

For studying any interaction, we should follow the steps bellow:

1-choose a model from the original models of CalcHEP or import new ones.

2-select " Enter process" , then write the expression of the process using the equivalent notations from the list of particles above. As we do not need to exclude any diagram or particle, we let them empty:

If the subdirectory results/ contains any result, it will ask to " delete" or " rename" it.

3- all possible Feynman diagrams will be plotted by CalcHEP, display them by selecting " view diagrams" :

4- to go to the numerical session, select " Square diagrams" , then to " Make & launch n_calchep" , that will open a new window.

5- it is possible to change the model parameters, CM energy, kinematical scheme, and impose regularizations and cuts

The variables used as cuts in CalcHEP are the same to the variables used in accelerators physics; E is the energy of the particle set (here is the missing energy), M is the mass of particle set (invariant mass of the bottom quark and its antiquark in this case), T is the transverse momentum, and J is the jet cone angle, which is defined as $\sqrt{\triangle\eta^2 + \triangle\phi^2}$, where $\triangle\phi$ is the azimuthal angle difference and $\triangle\eta$ is the pseudorapidity difference. There are other variables, we can find them by pressing " F1"

6-select " Monte Carlo Simulation" , then go to " Set Distributions" , insert all possible distributions and click on " Start Integration" to get the cross section values. * once we add cuts, kinematics and regularizations, computation of the total cross section will be fast and more accurate. CalcHEP can then plot distributions, click on " Display Distributions" to show them:

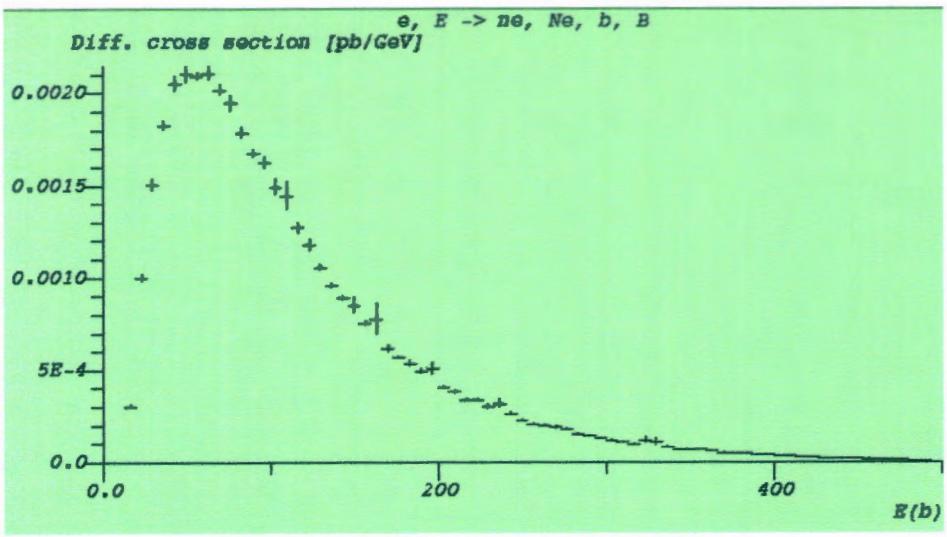

Figure 3.3: Differential cross section variation with energy.

Running batch sessions:

All the previous steps of calculation take a long time, they can be done in batch mode by one command
./calchep_batch file_name , the batch_file contains all the informations about the reaction: model informations, process informations, momentum informations, parameter informations, run informations, cuts informations, regularization informations, events generations, distribution informations, parallelization informations, and Vegas. Control of calculation and progress informations can be found in the html directory. We will see an example in the next chapter.

Chapter 4

Identifying Higgs-Gauge couplings

4.1 The final state $b\bar{b} + E_{miss}$ at leptonic collider

In this work, we are interesting by the study of the process $e^-e^+ \to HZ$ (Fig. 4.1) via HZZ and HWW couplings, at the future e^-e^+ collider ILC. we propose that the final state include $b\bar{b}$ pair from the Higgs decays, with missing energy $E_{miss} = v_i\bar{v}_i$ $(i = e, \mu, \tau)$ from Z boson decays to study the possibility of a deviation from the SM.

We suppose a simple change on the vertices HZZ and HWW where:

$$2\frac{M_W^2}{v}(HWW) \to 2\frac{M_W^2}{v}(1+\alpha) \equiv 2\kappa_W\frac{M_W^2}{v}, \tag{4.1}$$

$$2\frac{M_Z^2}{v}(HZZ) \to 2\frac{M_Z^2}{v}(1+\beta) \equiv 2\kappa_Z\frac{M_Z^2}{v} \tag{4.2}$$

here we supposed that $(1+\alpha)$ and $(1+\beta)$ are equivalents to the coupling scale factors κ_W and κ_Z respectively [24], and we can return to the SM by putting $\alpha = \beta = 0$ or $\kappa_W = \kappa_Z = 1$ The measurement of $\lambda_{WZ} \equiv \frac{\kappa_W}{\kappa_Z}$ gives:

Within the LHC RUN I:

$-1.10 \leq \lambda_{WZ} \leq -0.73$ or $0.72 \leq \lambda_{WZ} \leq 1.10$

while in LHC RUN II:

$-1.39 \leq \lambda_{WZ} \leq -0.97$ or $0.92 \leq \lambda_{WZ} \leq 1.37$

we start by varying the center of mass energy from 250 GeV to 1 TeV to calculate the background cross section σ^B, then taking the value of $\sqrt{S} = E_{cm}$ that corresponds to σ^B maximal (Fig. 4.2), which will be equal to 1 TeV.

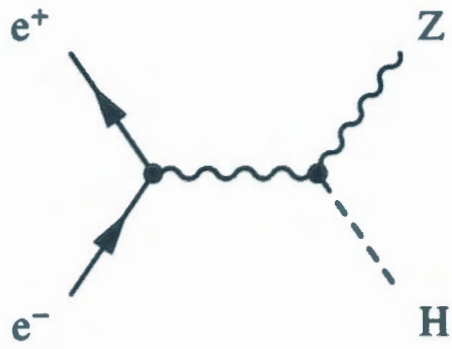

Figure 4.1: Feynman diagram for the process $e^-e^+ \rightarrow HZ$.

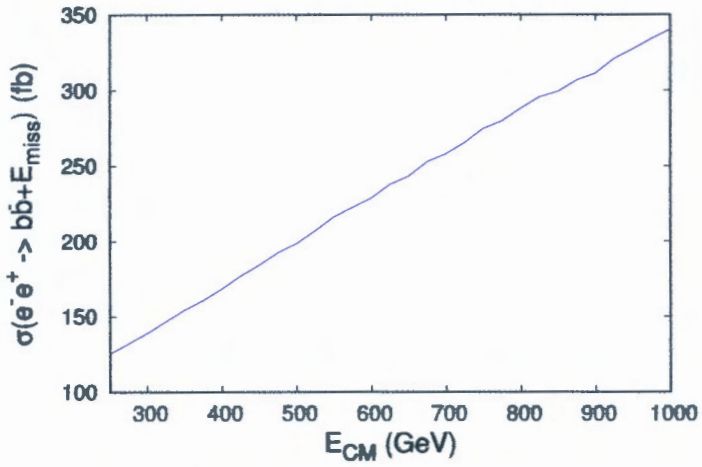

Figure 4.2: The cross section of the background as a function of center of mass energy

4.2 Constraints on Modified Higgs-Gauge Couplings

We can organize the squared amplitude of the process presented in (Fig. 4.1) as:

$$| M |^2 = | M_{HWW} |^2 (1+\alpha)^2 + | M_{HZZ} |^2 (1+\beta)^2 + | M_{rest} |^2$$
$$+2Re(M_{HWW}M_{HZZ})(1+\alpha)(1+\beta) + 2Re(M_{HWW}M_{rest})(1+\alpha) + 2Re(M_{HZZ}M_{rest})(1+\beta)$$

Where:

M_{HWW} involves the HWW coupling,
M_{HZZ} involves the HZZ coupling,
M_{rest} involves the *rest* ,
$Re(M_{HWW}M_{HZZ})$, $Re(M_{HWW}M_{rest})$ and $Re(M_{HZZ}M_{rest})$ the interferences.

The total cross section with HWW and HZZ couplings can be expressed then as:

$$\begin{aligned}\sigma_{tot} &= \sigma_{HWW}(1+\alpha)^2 + \sigma_{HZZ}(1+\beta)^2 + \sigma_{rest} \\ &+2\sigma_{HWW,HZZ}(1+\beta)(1+\alpha) + 2\sigma_{HWW,rest}(1+\alpha) + \sigma_{HZZ,rest}(1+\beta) \quad (4.3)\end{aligned}$$

To calculate σ_{tot} we consider firstly six values for α and for β
for$(\alpha=-1,\beta=-1), \sigma_{tot} \equiv \varkappa_1 = \sigma_{rest}$
for $(\alpha=0,\beta=-1), \sigma_{tot} \equiv \varkappa_2 = \sigma_{HWW} + \sigma_{rest} + \sigma_{HWW,rest}$
for $(\alpha=1,\beta=-1), \sigma_{tot} \equiv \varkappa_3 = 4\sigma_{HWW} + \sigma_{rest} + 2\sigma_{HWW,rest}$
for $(\alpha=-1,\beta=0), \sigma_{tot} \equiv \varkappa_4 = \sigma_{HZZ} + \sigma_{rest} + \sigma_{HZZ,rest}$
for $(\alpha=-1,\beta=1), \sigma_{tot} \equiv \varkappa_5 = 4\sigma_{HZZ} + \sigma_{rest} + \sigma_{HZZ,rest}$
for $(\alpha=1,\beta=0), \sigma_{tot} \equiv \varkappa_6 = 4\sigma_{HWW} + \sigma_{HZZ} + \sigma_{rest} + 2\sigma_{HWW,HZZ} + 2\sigma_{HWW,rest} + \sigma_{HZZ,rest}$.

That gives :

$$\begin{aligned}\sigma_{HWW} &= \frac{1}{2}\varkappa_1 - \varkappa_2 + \frac{1}{2}\varkappa_3 \\ \sigma_{HZZ} &= \frac{1}{2}\varkappa_1 - \varkappa_4 + \frac{1}{2}\varkappa_5 \\ \sigma_{rest} &= \varkappa_1 \\ \sigma_{HWW,rest} &= -\frac{3}{2}\varkappa_1 + 2\varkappa_2 - \frac{1}{2}\varkappa_3 \\ \sigma_{HZZ,rest} &= -\frac{3}{2}\varkappa_1 - \frac{1}{2}\varkappa_5 + 2\varkappa_4 \\ \sigma_{HWW,HZZ} &= \frac{1}{2}\varkappa_6 - \frac{1}{2}\varkappa_4 - \frac{1}{2}\varkappa_3 + \frac{1}{2}\varkappa_1 \quad (4.4)\end{aligned}$$

In order to compute σ_{HWW}, σ_{HZZ}, σ_{rest}, $\sigma_{HWW,HZZ}$, $\sigma_{HWW,rest}$ and $\sigma_{HZZ,rest}$ and then the total cross sections for the background ($\alpha=\beta=0$) and for the signal, we use CalcHEP package to obtain the different values of $\varkappa$, taking into account a set of cuts:

$E_{CM} = 1TeV$	$15 < P_T^b$	$30 < \not{E}_T$	$71 < M^{b\bar{b}} < 145$	$0.4 < \Delta R_{b\bar{b}}$

where:

P_T^b is the transverse momentum of the bottom quark (b),
$\not{E}_T$ is the missing energy,
$M^{b\bar{b}}$ is the invariant mass of the bottom quark (b) and the bottom antiquark ($\bar{b}$),
$\Delta R_{b\bar{b}}$ is the jet cone angle.

The corresponding values of $\varkappa$ are:

$$\begin{aligned}
\varkappa_1 &= 139.14(fb) \\
\varkappa_2 &= 290.47(fb) \\
\varkappa_3 &= 577.59(fb) \\
\varkappa_4 &= 143.86(fb) \\
\varkappa_5 &= 148.29(fb) \\
\varkappa_6 &= 560.50(fb)
\end{aligned}$$

by replacing this values in (Eq. 4.4), and then (Eq. 4.4) in (Eq. 4.3), we get the following figures (Fig. 4.3):

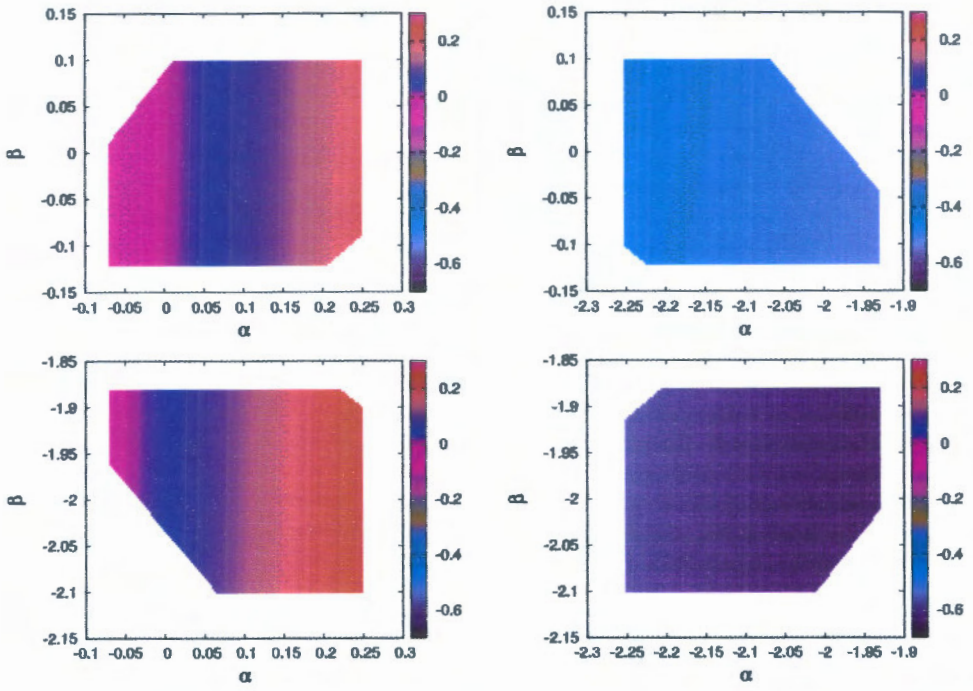

Figure 4.3: The Palette represents the allowed values of $(\sigma^S - \sigma^B)/\sigma^S$ as a function of α and β

.

At High Luminosity LHC (HL LHC), we can not see any diviation at: $\alpha, \beta = 0$ and $\alpha, \beta = -2$ We choose values for α and β that should be predicted by the SM, and fulfilling the conditions [25]:

$$\frac{\delta\kappa_W}{\kappa_W} \leq 5\%, \frac{\delta\kappa_Z}{\kappa_Z} \leq 4\% \tag{4.5}$$

4.3 Analysis and Discussion

We consider the following Benchmarks:

B1: $\alpha = 0.04, \quad \beta = 0.04$
B2: $\alpha = 0.04, \quad \beta = -2.04$
B3: $\alpha = -2.04, \quad \beta = -0.04$
B4: $\alpha = -2.04, \quad \beta = -1.96,$

with the pre-cuts above and generate different distributions to define new cuts that make the significance (Eq. 3.8) maximal.

By imposing all these cuts, parameters, distributions.. in batch_files (APPENDIX A.2), we get the following results:

$E_{CM}(GeV)$	$\sigma^B(fb)$	Models	$\sigma^S(fb)$
		B1	278.03
1000	268.54	B2	278.25
		B3	278.22
		B4	277.70

Table 4.1: The cross section values of the background and the considered Benchmarck points.

From the distributions obtained in this case, we choose kinematical variables that make background reduced while keeping the signal cross section values.

* Firstly we take all the possible cuts:

$15 < P_T^b, \quad 71 < M^{b\bar{b}} < 145, \quad 0.4 < \triangle R_{b\bar{b}}, \quad 520 < \not{E}_T < 880,$
$120 < E^{b,\bar{b}} < 430, \quad 120 < E_T^{b,\bar{b}} < 260, \quad P_T^{\not{E}_T} < 250, \quad M^{b,\not{E}_T} > 500,$
$D^{b\bar{b}} < 400, \quad W^{b,\not{E}_T} < 600.$

After applying these cuts, we get the following cross section values (Tab. 4.2):

$E_{CM}(GeV)$	$\sigma'^B(fb)$	Models	$\sigma'^S(fb)$
		B1	180.72
1000	172.05	B2	180.98
		B3	181.01
		B4	180.86

Table 4.2: Signal and background cross sections after applying the all possible cuts

Comparing these results (Tab. 4.2) with the results obtained by applying the pre-cuts (Tab. 4.1), we notice that both the background and the signal cross sections get reduced a bit. We show also the relevant distributions (from (Fig. 4.4) to (Fig. 4.18)), that are:

-The polar angle between bottom-antibottom jets.
-The jet energy.
-The jet transverse energy.
-The jet transverse momentum.
-The transverse mass of the bottom-antibottom jets.
-The invariant mass of the missing energy with a jet.
-The jet pseudorapidity.
-The two jets pseudorapidity.
-The jet separation.
-The transverse momentum of the missing energy with a jet.

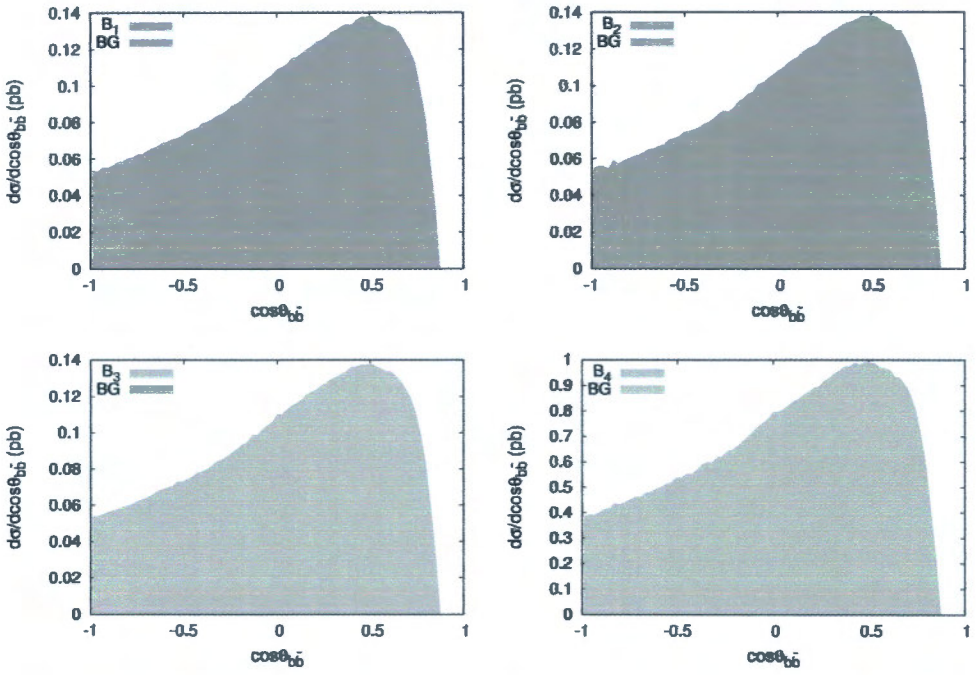

Figure 4.4: Distributions of the angle between the jets for the four benchmarks.

By comparing between the different Benchmarks and the background shapes (from (Fig. 4.4) to (Fig. 4.18)), we remark a clear difference. We take the signal cross section values for the different Benchmarks, with the background value, and replacing them in (Eq. 3.8) then estimate the signal significance S by varying integrated luminosity L from 10 to 1000(fb^{-1}). We show in (Fig. 4.19) the signal significance

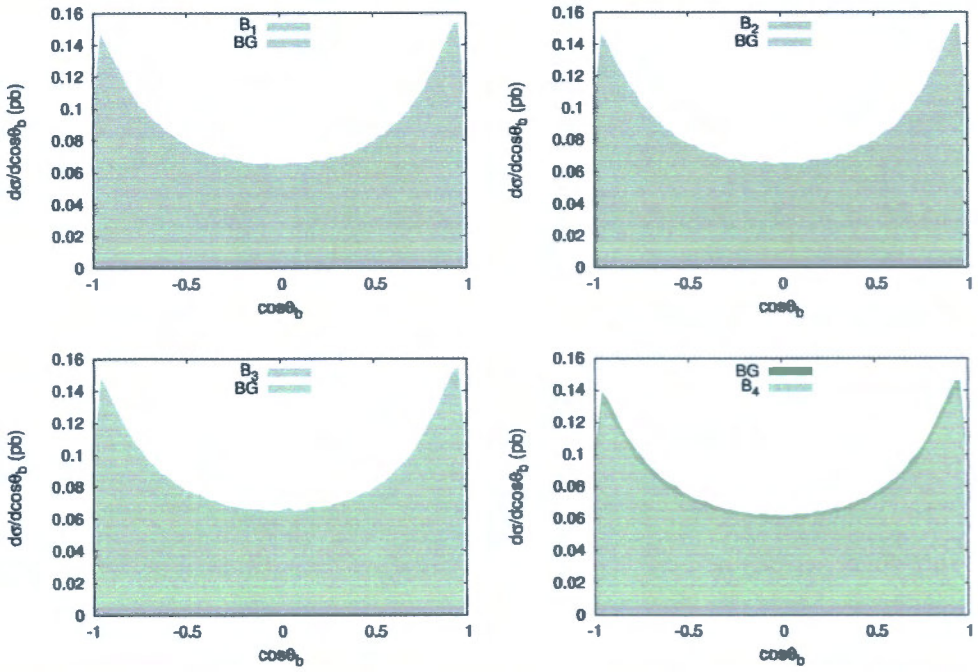

Figure 4.5: Distributions of the angle of the jest for the four benchmarks.

for different Benchmarks:

In (Fig. 4.19), we notice a deviation ($3 \leq S < 5$) from the SM at luminosity $L = 32.69(\ fb^{-1})$ for all Benchmarks. At $L = 90(\ fb^{-1})$, $S \geq 5$,, so we can clearly see a discovery for all Benchmarks. Finally, we calculate the signal significance at $L = 10, 100, 300, 1000(\ fb^{-1})$

$E_{CM}(GeV)$	Models	$\sigma'^S(fb)$	$\sigma'^B(fb)$	S_{10}	S_{100}	S_{300}	S_{1000}
	B1	180.72		2.039	6.449	11.171	20.395
1000	B2	180.98	172.05	2.099	6.638	11.497	20.991
	B3	181.01		2.106	6.666	11.535	21.060
	B4	180.86		2.0716	6.551	11.347	20.716

and display the signal significance (in palette) (from (Fig. 4.20) to (Fig. 4.23)) as a function of the parameters α and β

*We take now only the transverse energy with the pre-cuts and redoing the same steps:

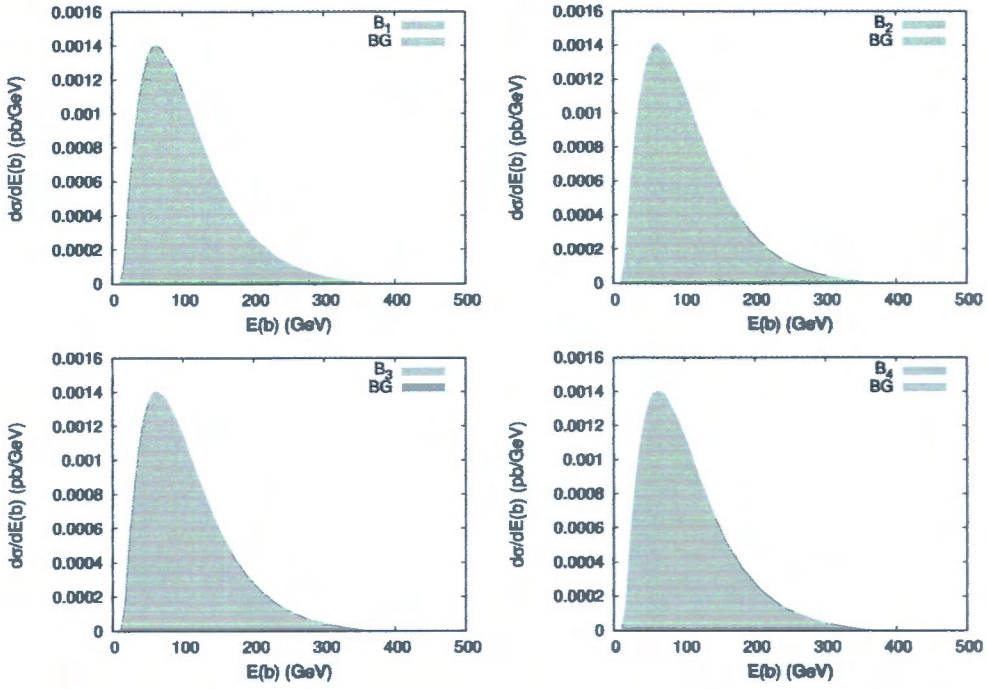

Figure 4.6: Distributions of the jet energy for the four benchmarks.

$$15 < P_T^b, \quad 71 < M^{b\bar{b}} < 145, \quad 0.4 < \Delta R_{b\bar{b}}, \quad 30 < \not{E}_T,$$
$$120 < E_T^{b,\bar{b}} < 260,$$

After applying these cuts, we get the following values (Tab. 4.3):

$E_{CM}(GeV)$	$\sigma'^B(fb)$	Models	$\sigma'^S(fb)$
		B1	201.31
1000	192.19	B2	201.44
		B3	201.82
		B4	201.36

Table 4.3: Signal and background cross sections after applying only the transverse energy with the pre-cuts

Comparing the results in (Tab. 4.3) with the results obtained by applying the pre-cuts(Tab. 4.1), we notice that both the background and the signal cross sections also get reduced a bit. We show also the same relevant distributions (from (Fig. 4.24) to (Fig. 4.38)) presented previously.

By comparing between the different Benchmarks and the background shapes (from (Fig. 4.24) to (Fig. 4.38)), we remark a clear difference.

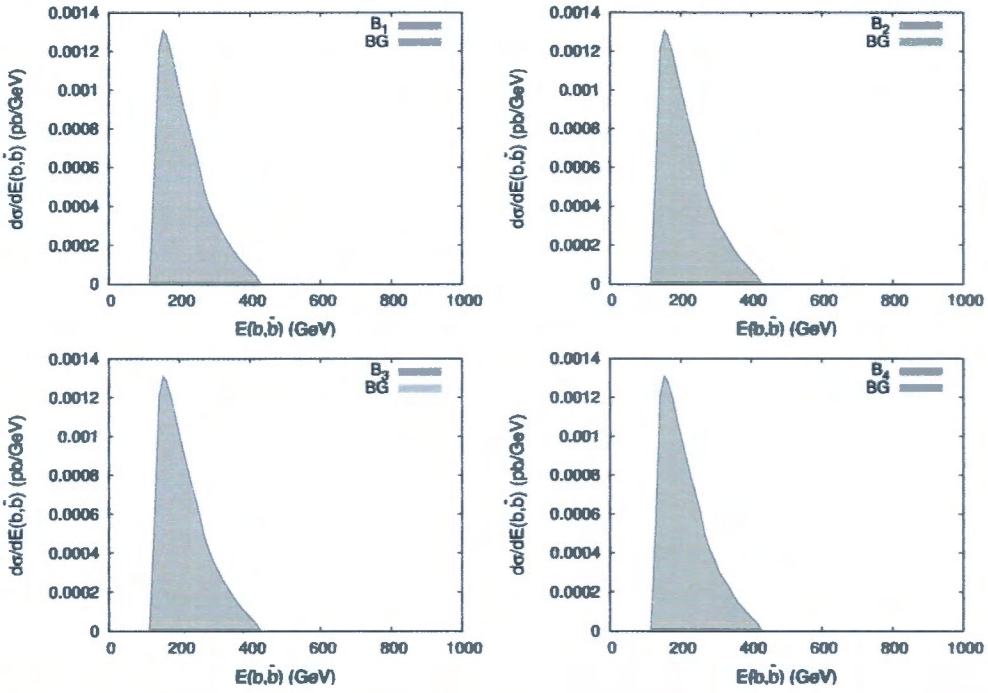

Figure 4.7: Distributions of the two jets energy for the four benchmarks.

We estimate again the signal significance S by varying integrated luminosity L from 10 to 1000(fb^{-1}). We show in (Fig. 4.39) the signal significance for different Benchmarks:

In (Fig. 4.39), we notice a deviation ($3 \leq S < 5$) from the SM at luminosity $L = 30.9(\ fb^{-1})$ for the Benchmark B3, and $L = 33.2(\ fb^{-1})$ for the the other Benchmarks. For $L = 84.5(\ fb^{-1})$ for the Benchmark B3, and $L = 91.4(\ fb^{-1})$ for the the other Benchmarks, $S \geq 5$,, so we can clearly see a discovery for all Benchmarks.

Finally, we calculate the signal significance at $L = 10, 100, 300, 1000(\ fb^{-1})$

$E_{CM}(GeV)$	Models	$\sigma^{\prime\prime S}(fb)$	$\sigma^{\prime\prime B}(fb)$	S_{10}	S_{100}	S_{300}	S_{1000}
	B1	201.31		2.033	6.428	11.133	20.326
1000	B2	201.44	192.19	2.061	6.517	11.288	20.610
	B3	201.82		2.144	6.779	11.741	21.436
	B4	201.36		2.043	6.462	11.193	20.435

and display the signal significance (in palette) (from (Fig. 4.40) to (Fig. 4.43)) as a function of the parameters α and β :

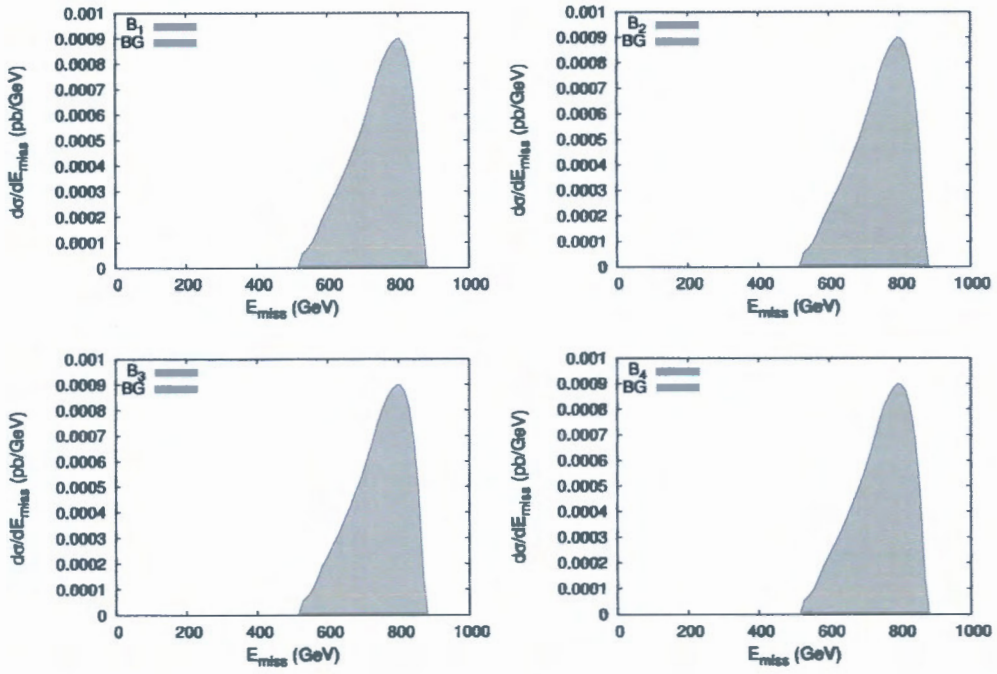

Figure 4.8: Distributions of the missing energy for the four benchmarks.

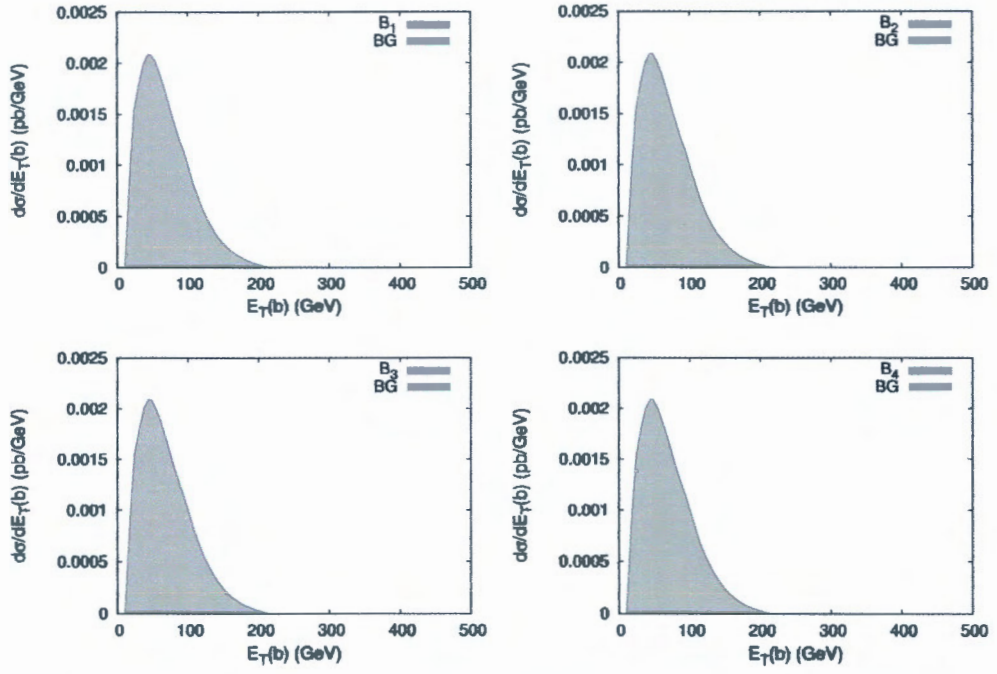

Figure 4.9: Distributions of the jet missing transverse momentum for the four benchmarks.

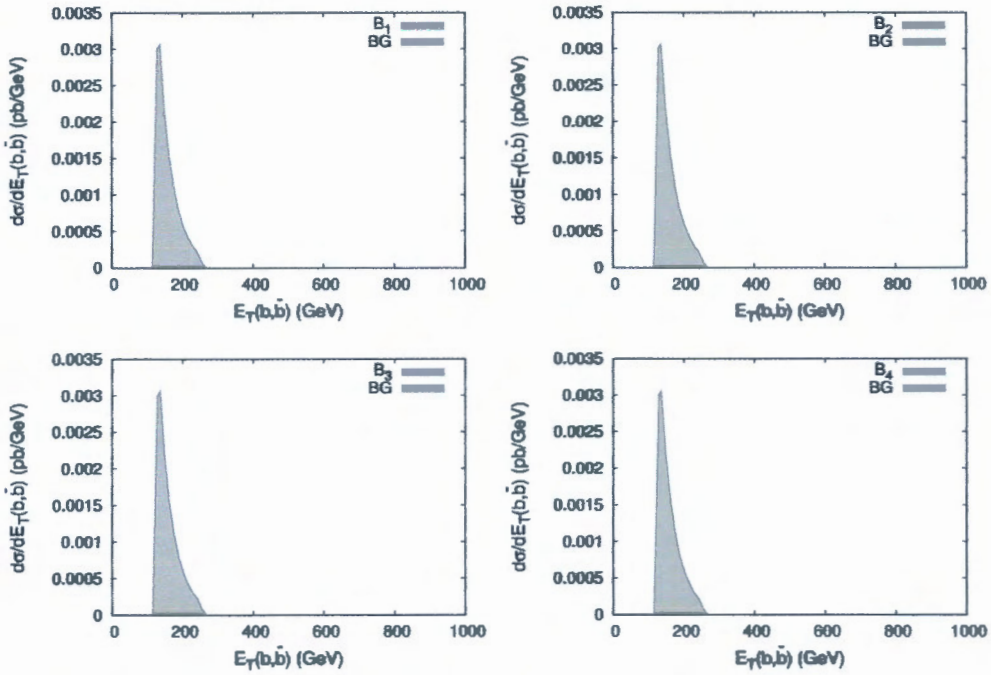

Figure 4.10: Distributions of the two jets energy for the four benchmarks.

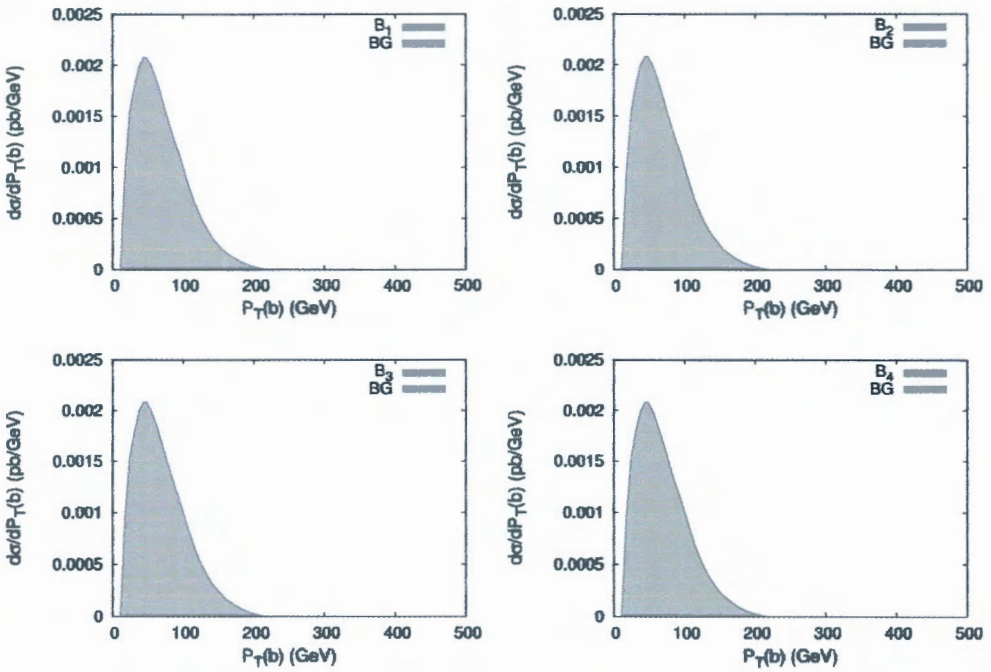

Figure 4.11: Distributions of the jet transverse momentum for the four benchmarks.

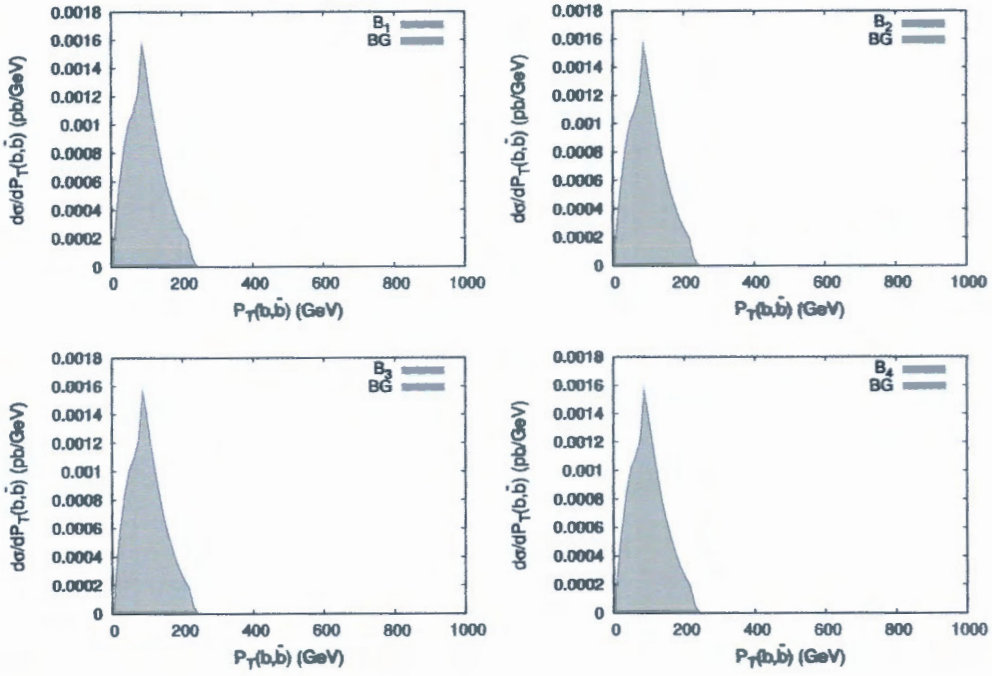

Figure 4.12: Distributions of the two jets transverse momentum for the four benchmarks.

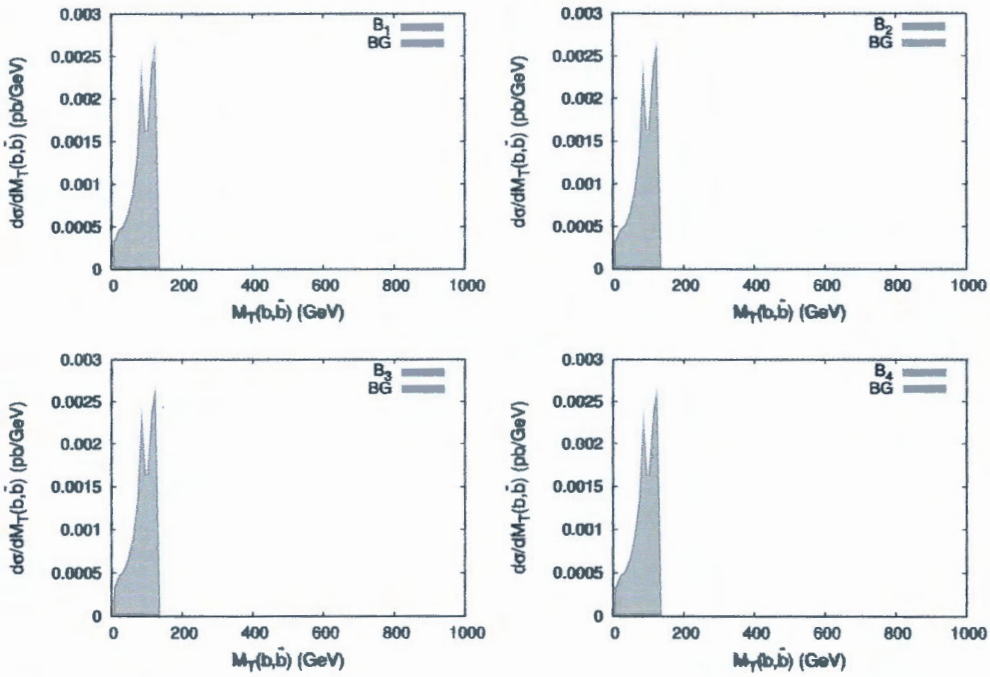

Figure 4.13: Distributions of the two jets transverse mass for the four benchmarks.

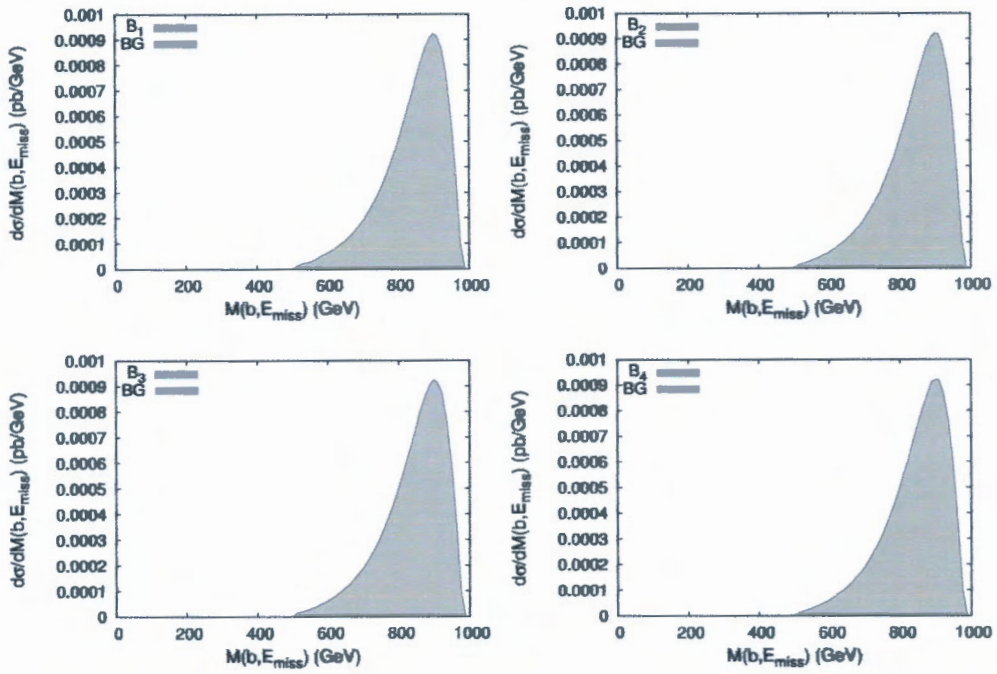

Figure 4.14: Distributions of the jet plus missing energy invariant mass for the four benchmarks.

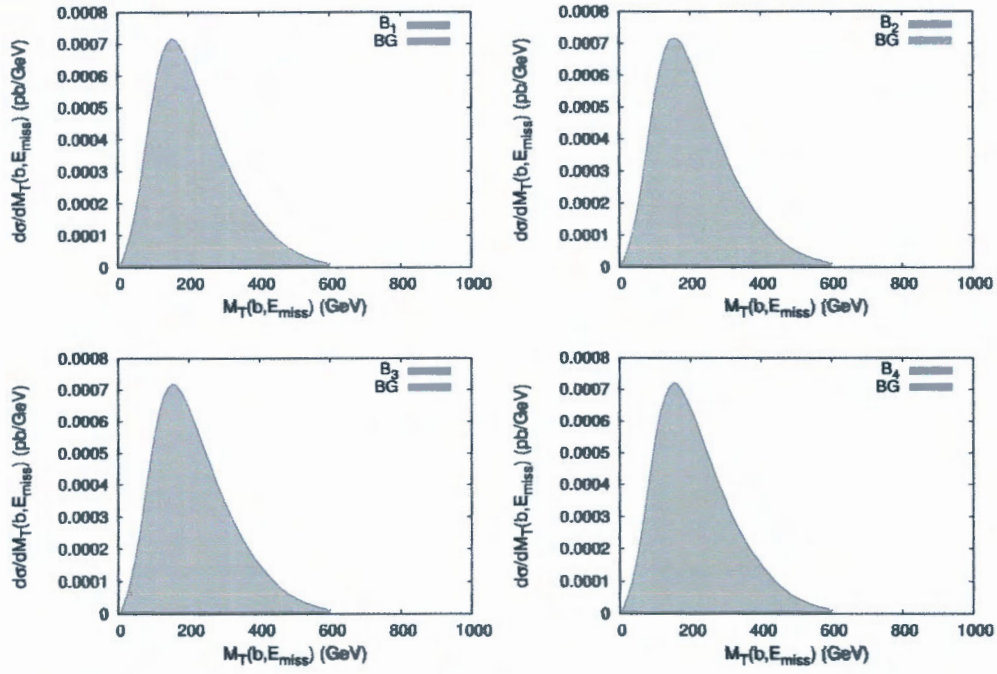

Figure 4.15: Distributions of the jet plus missing energy transverse mass for the four benchmarks.

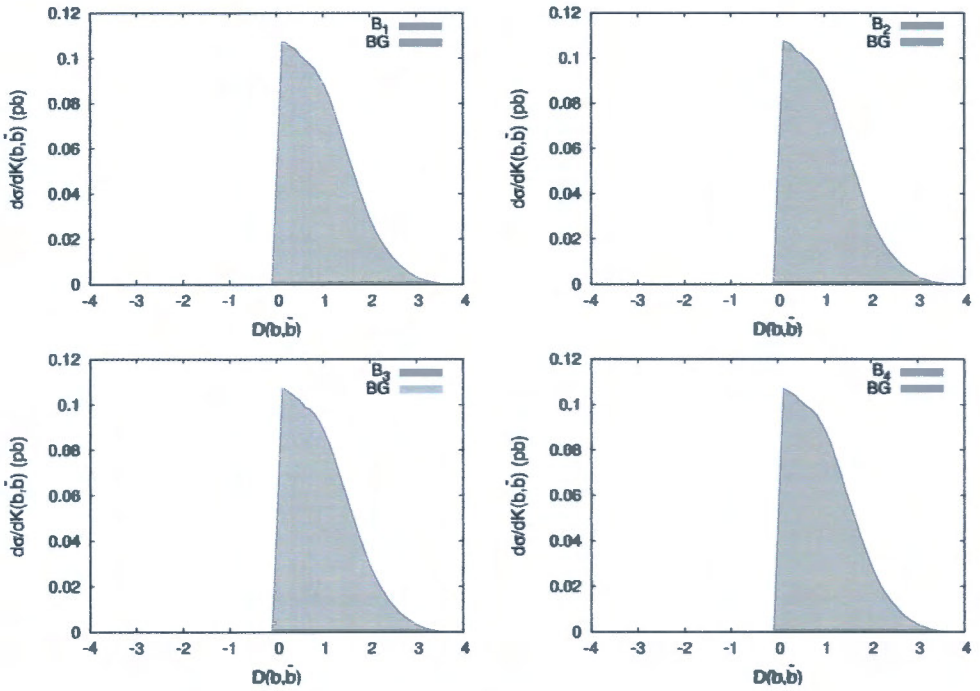

Figure 4.16: Distributions of pseudorapidity difference between the two jets for the four benchmarks.

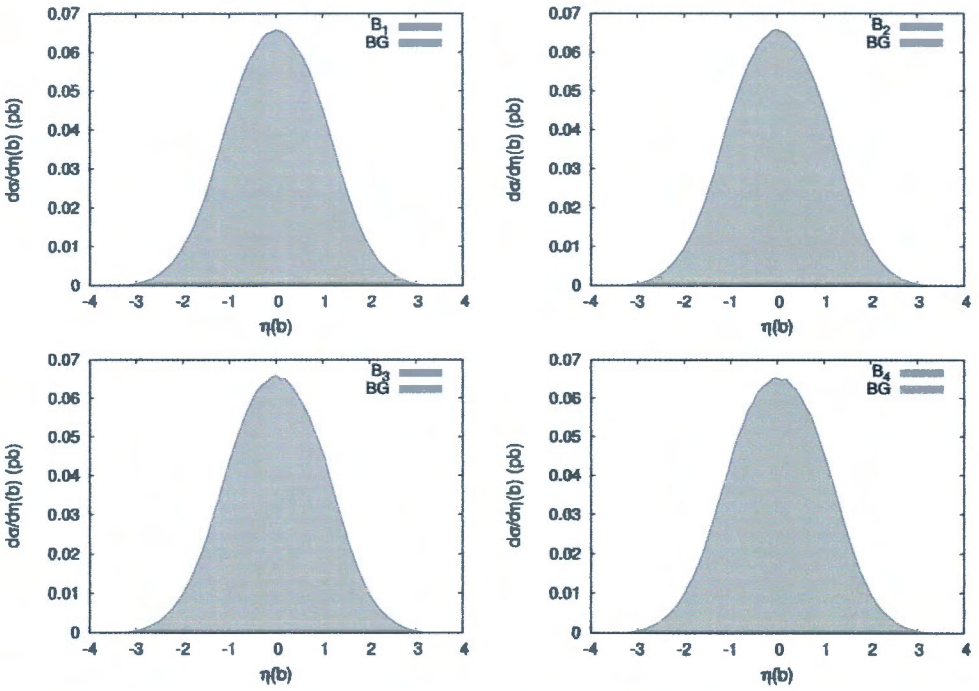

Figure 4.17: Distributions of the jet pseudorapidity for the four benchmarks.

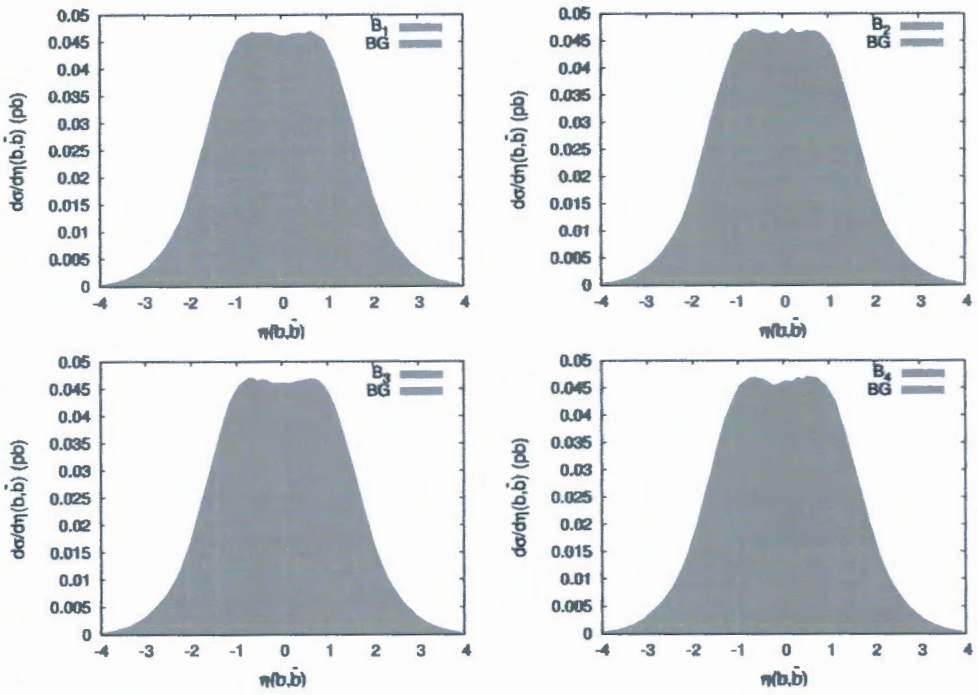

Figure 4.18: Distributions of the two jets pseudorapidity for the four benchmarks.

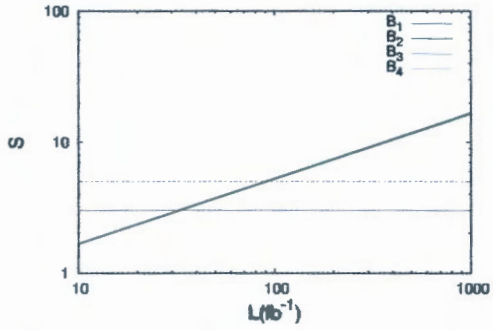

Figure 4.19: The significance as a function of integrated luminosity L. The two dashed lines represent S=3 and S=5

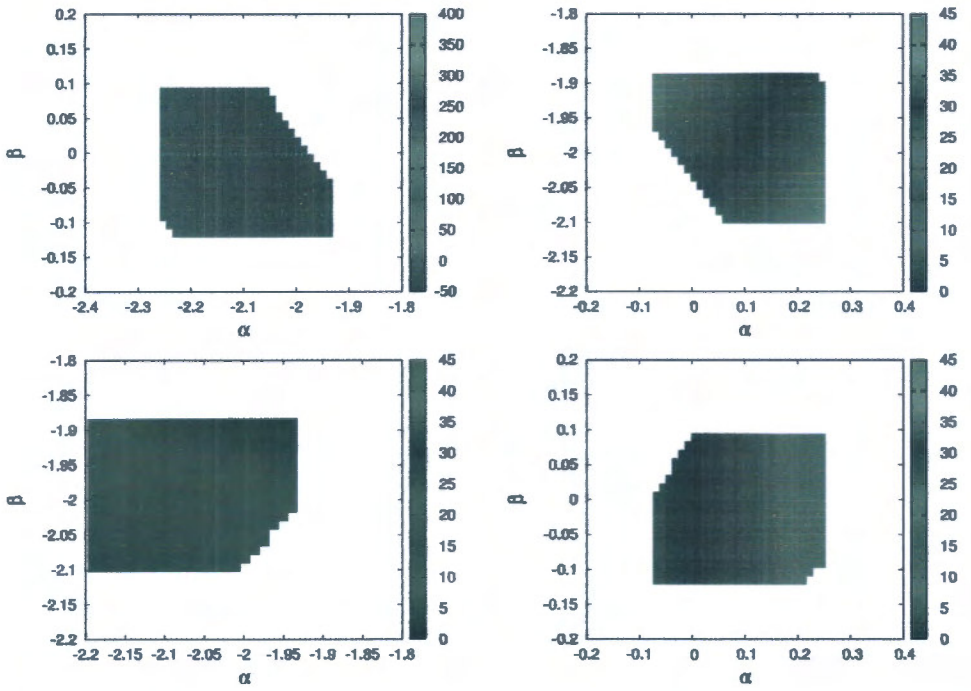

Figure 4.20: The signal significance for $L = 10(\ fb^{-1})$ as a function of parameters β and α.

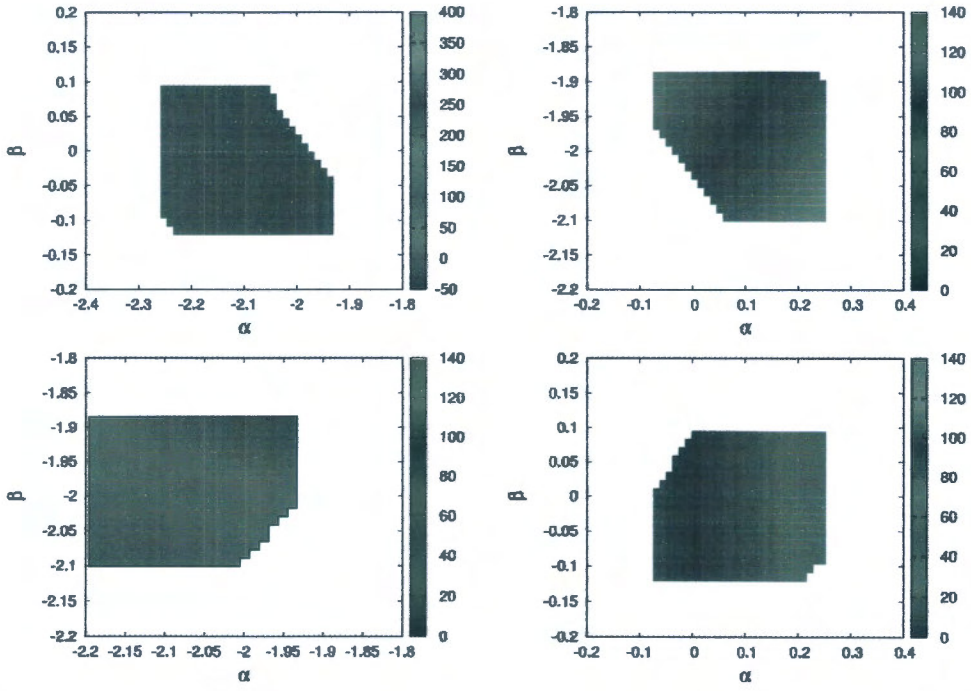

Figure 4.21: The signal significance for $L = 100(\ fb^{-1})$ as a function of parameters β and α.

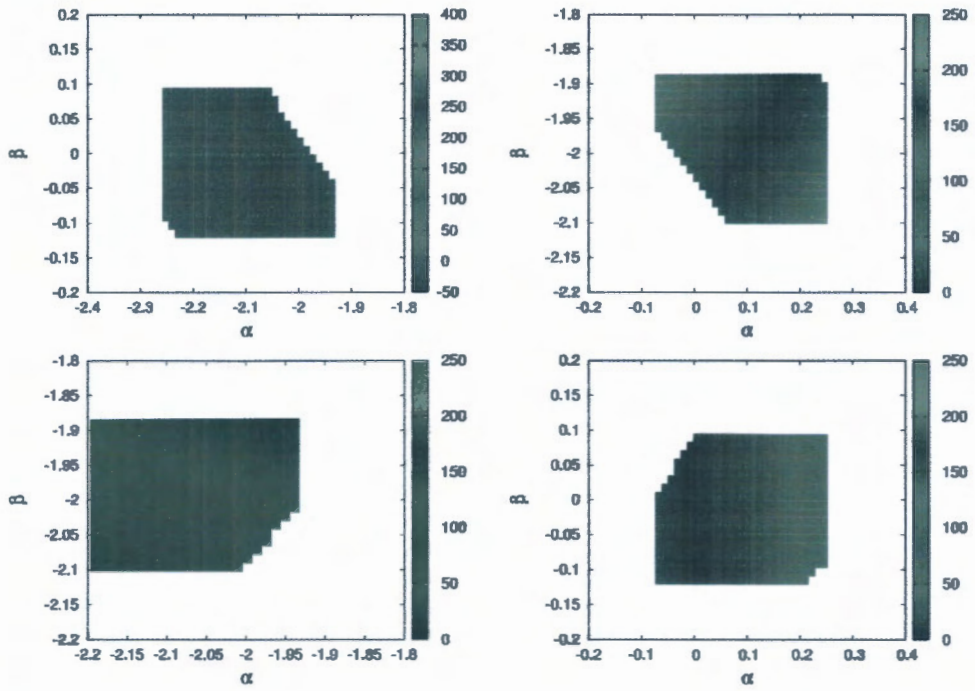

Figure 4.22: The signal significance for $L = 300(\ fb^{-1})$ as a function of parameters β and α.

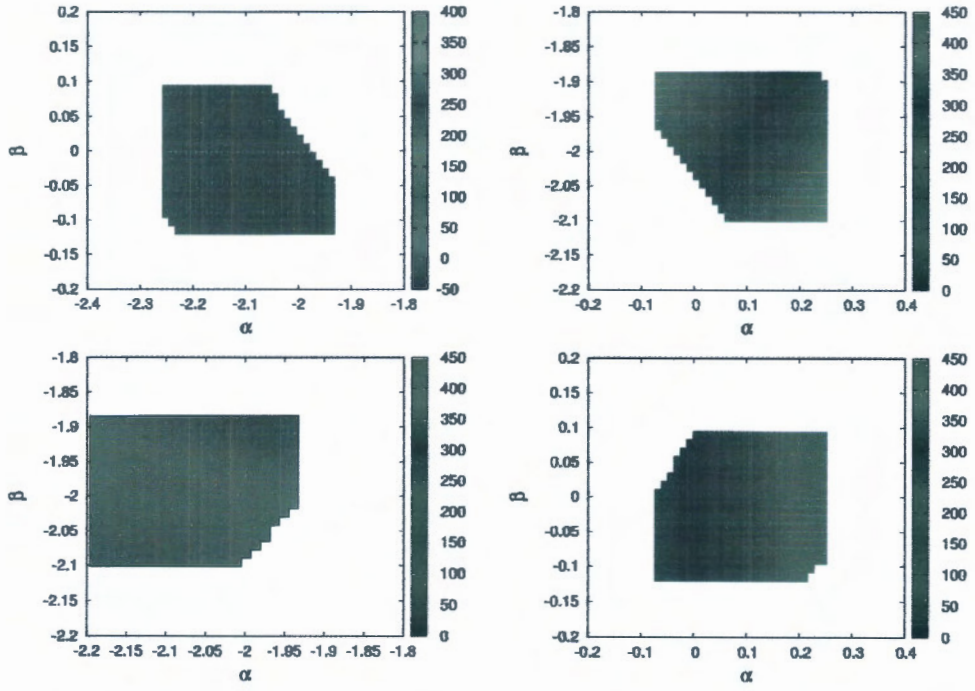

Figure 4.23: The signal significance for $L = 1000(\ fb^{-1})$ as a function of parameters β and α.

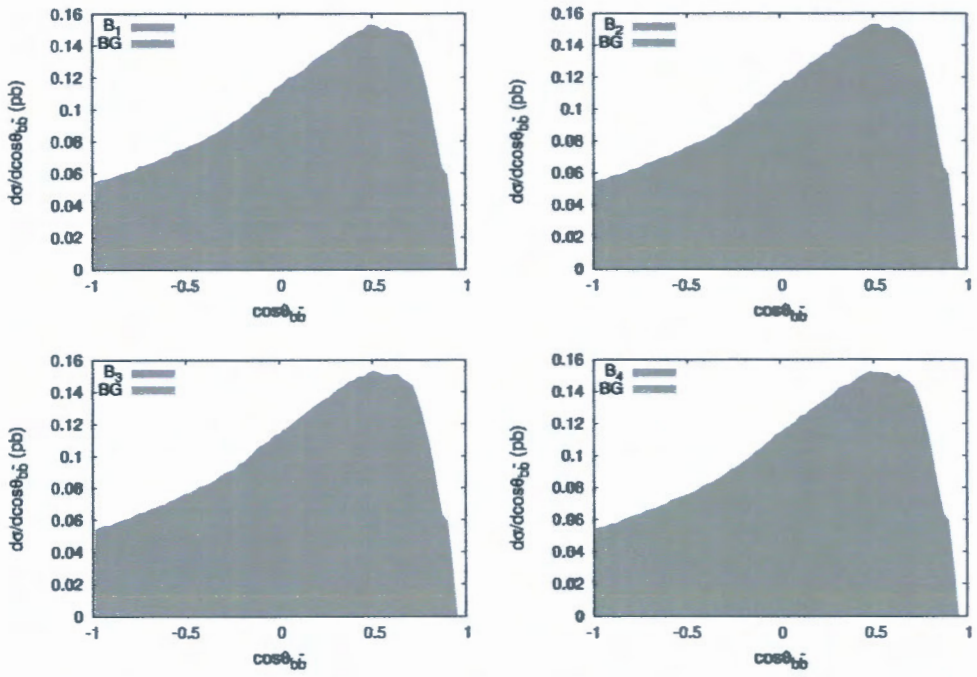

Figure 4.24: Distributions of the angle between the jets for the four benchmarks.

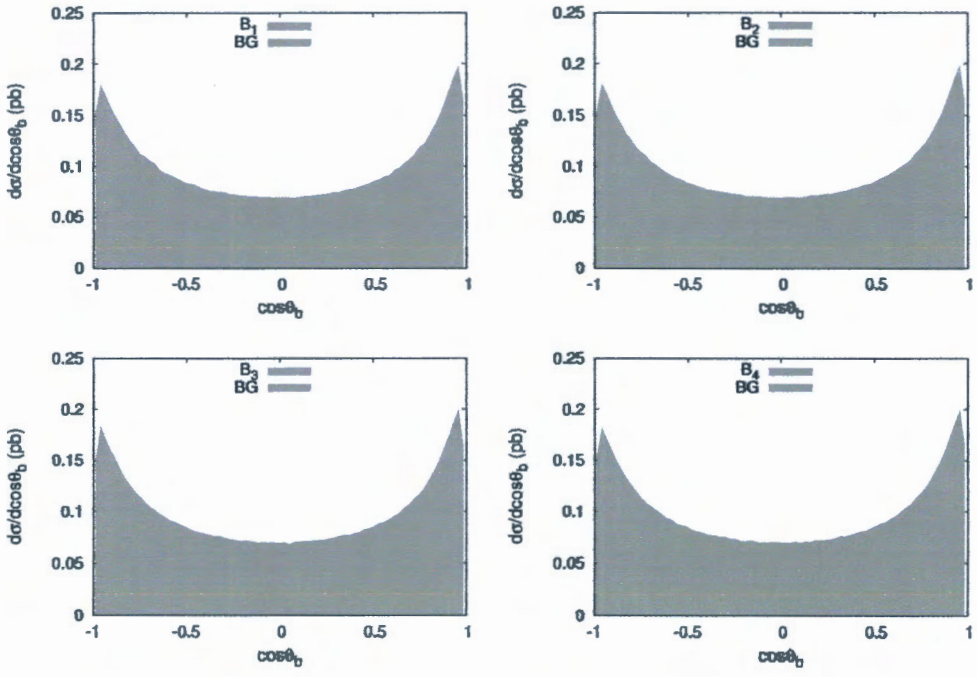

Figure 4.25: Distributions of the angle of the jest for the four benchmarks.

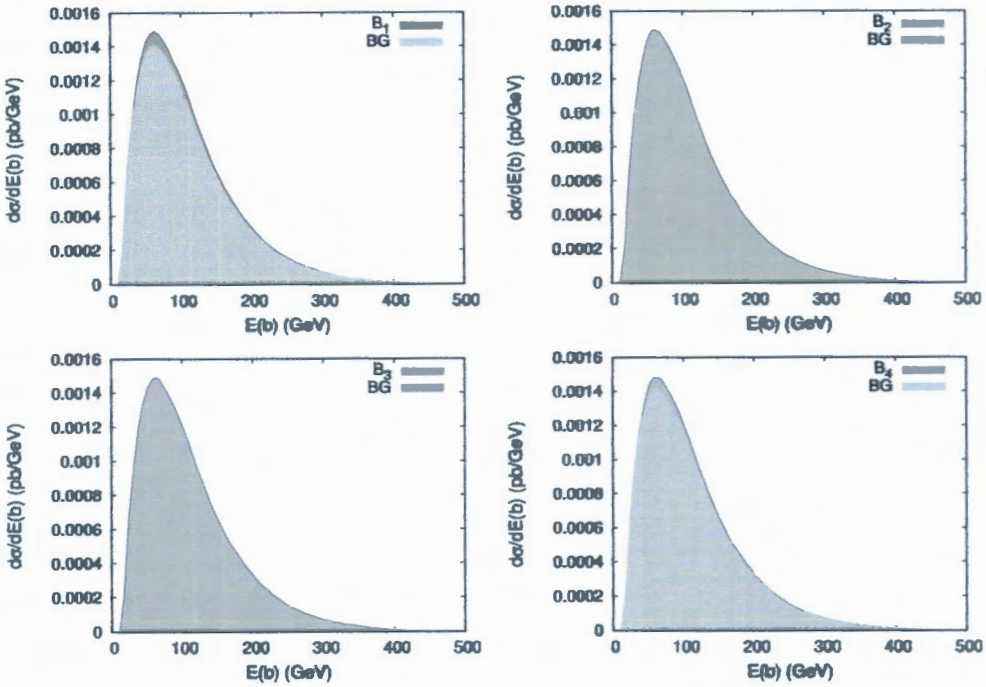

Figure 4.26: Distributions of the jet energy for the four benchmarks.

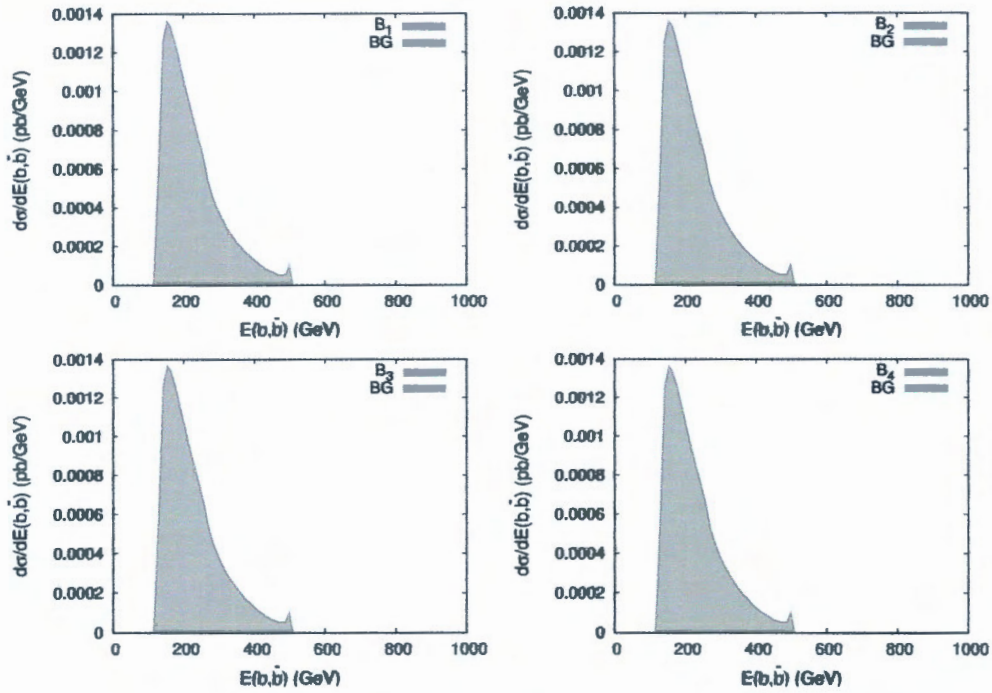

Figure 4.27: Distributions of the missing energy for the four benchmarks.

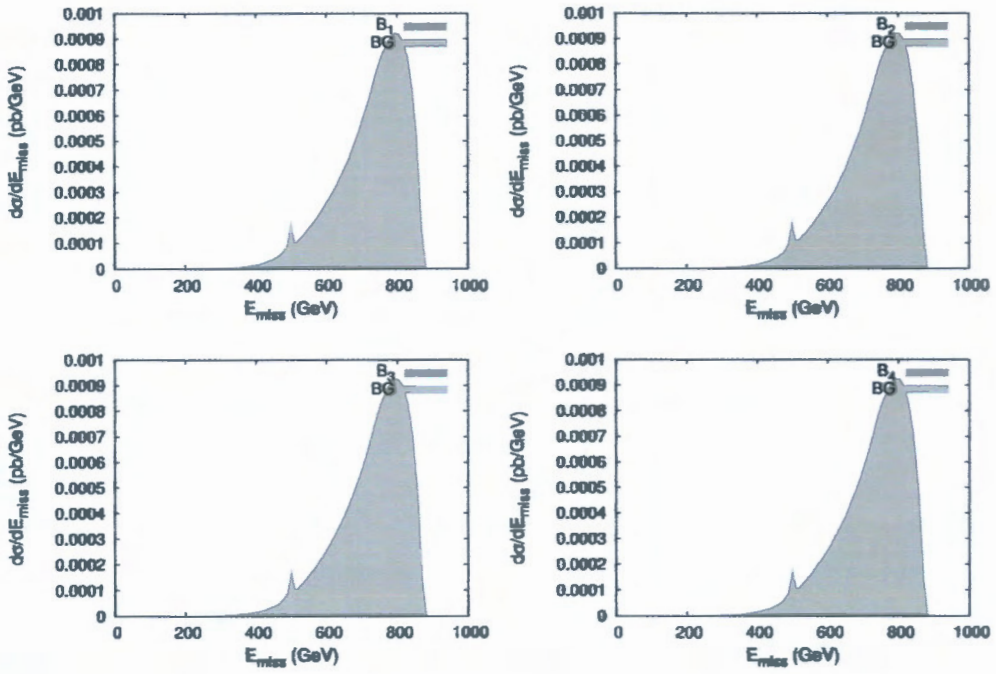

Figure 4.28: Distributions of the jet missing energy for the four benchmarks.

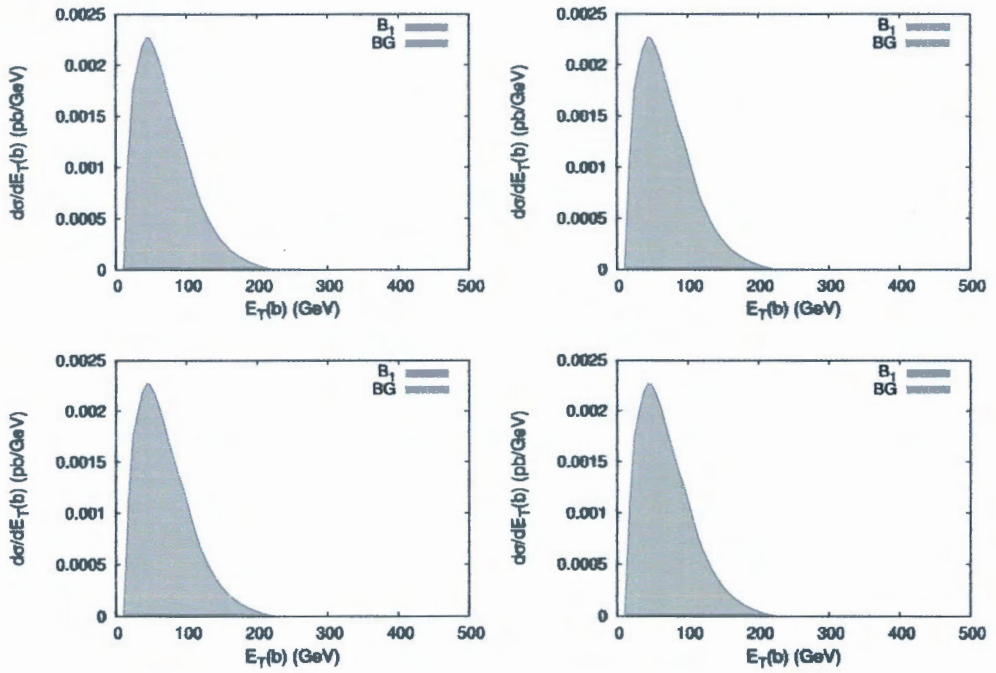

Figure 4.29: Distributions of the jet missing transverse momentum for the four benchmarks.

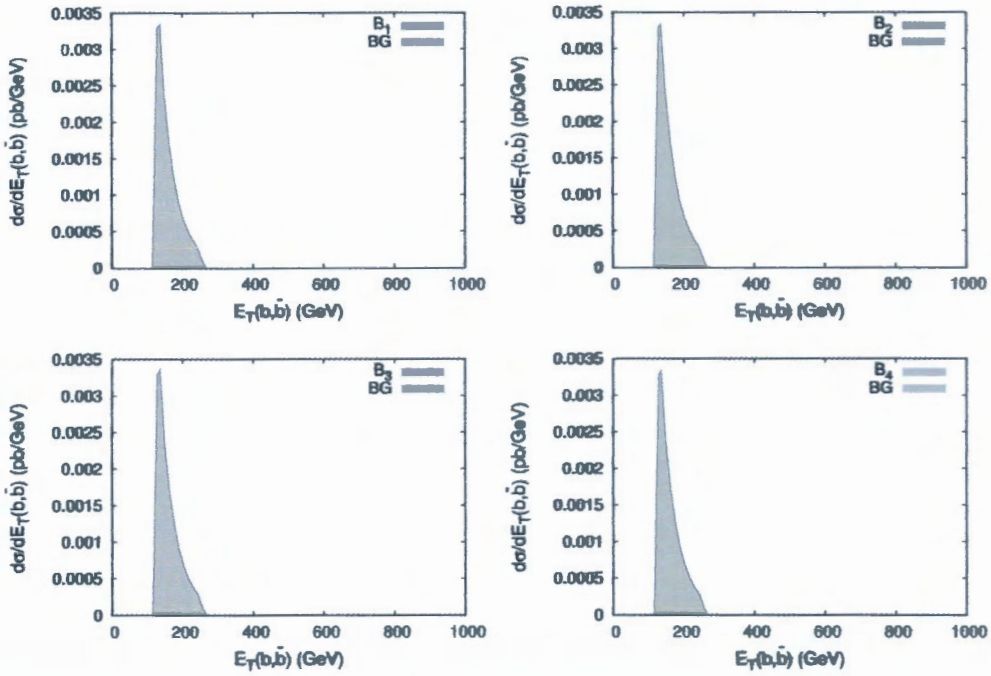

Figure 4.30: Distributions of the two jets energy for the four benchmarks.

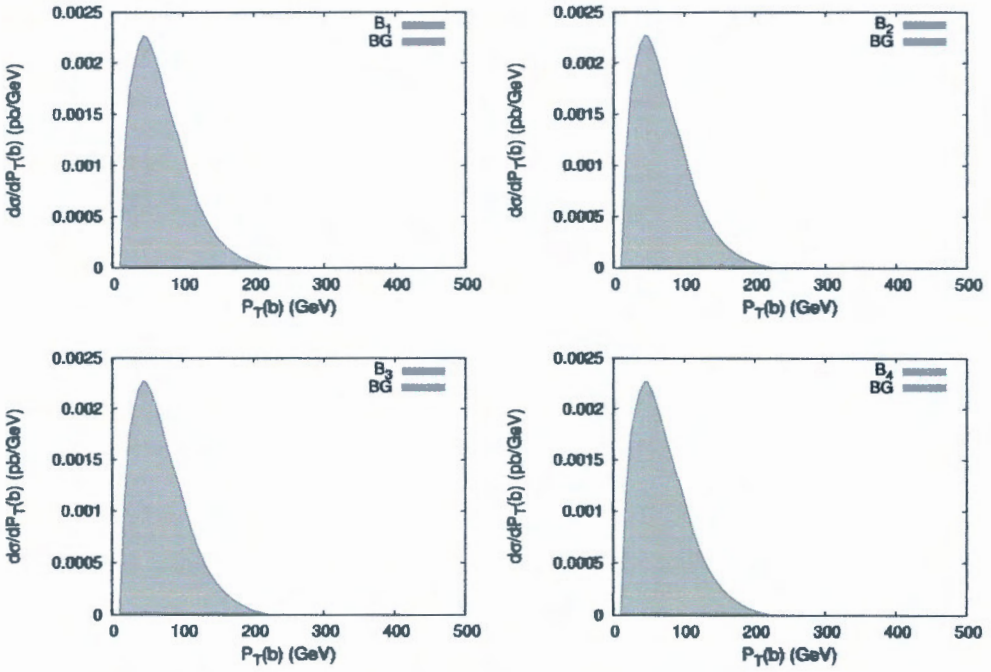

Figure 4.31: Distributions of the jet transverse momentum for the four benchmarks.

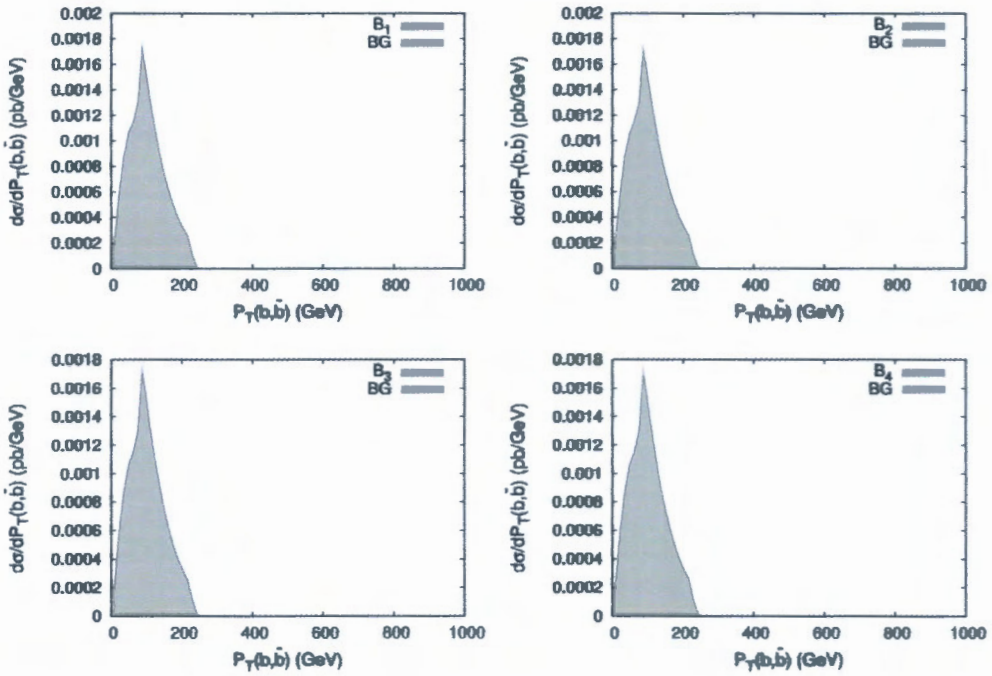

Figure 4.32: Distributions of the two jets transverse momentum for the four benchmarks.

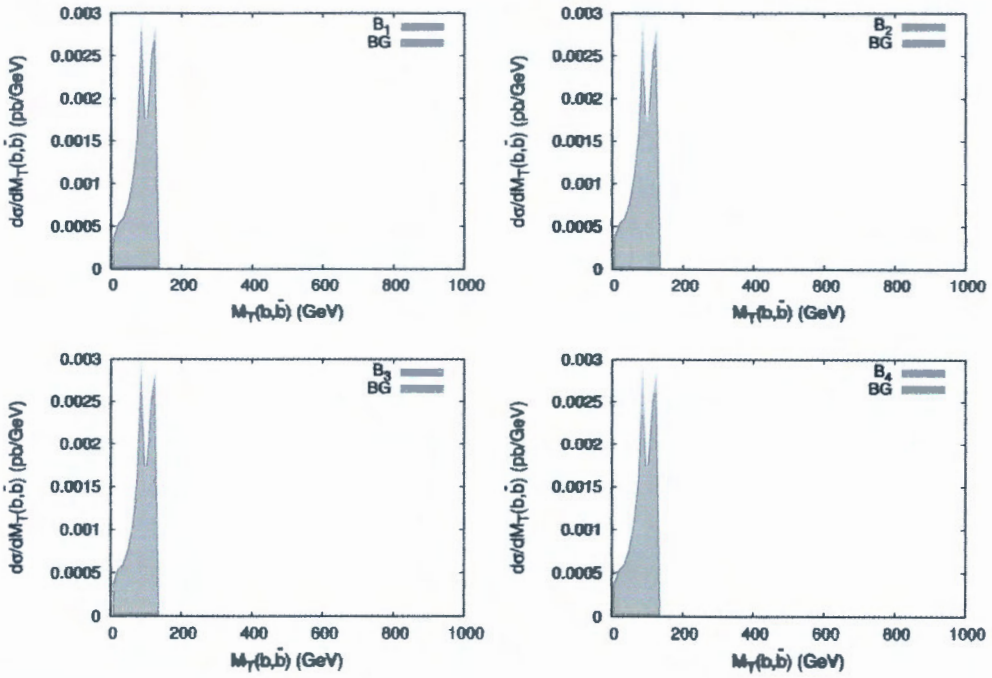

Figure 4.33: Distributions of the two jets transverse mass for the four benchmarks.

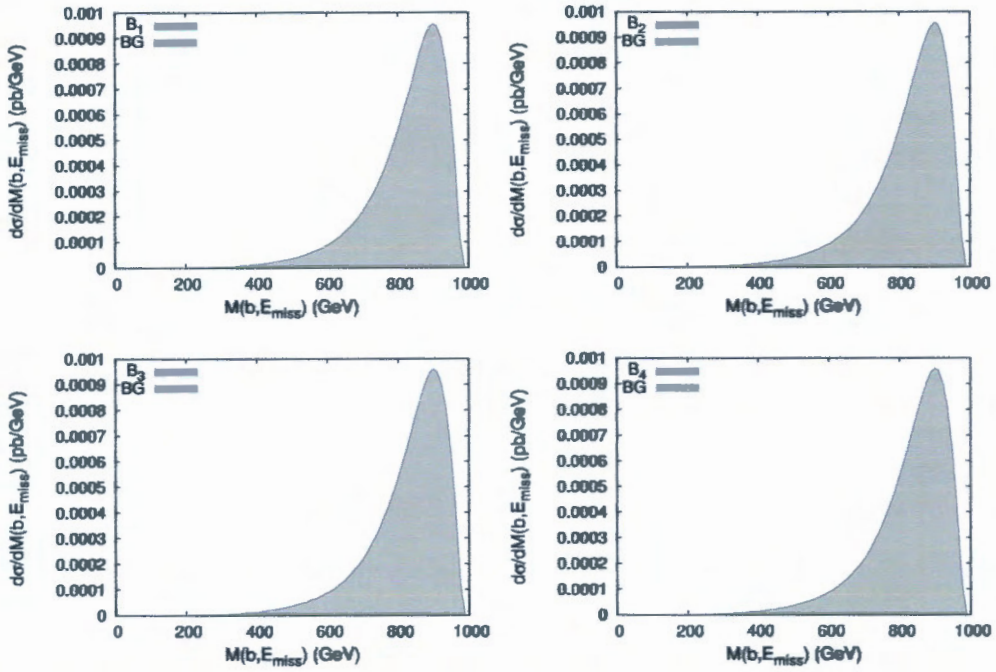

Figure 4.34: Distributions of the jet plus missing energy invariant mass for the four benchmarks.

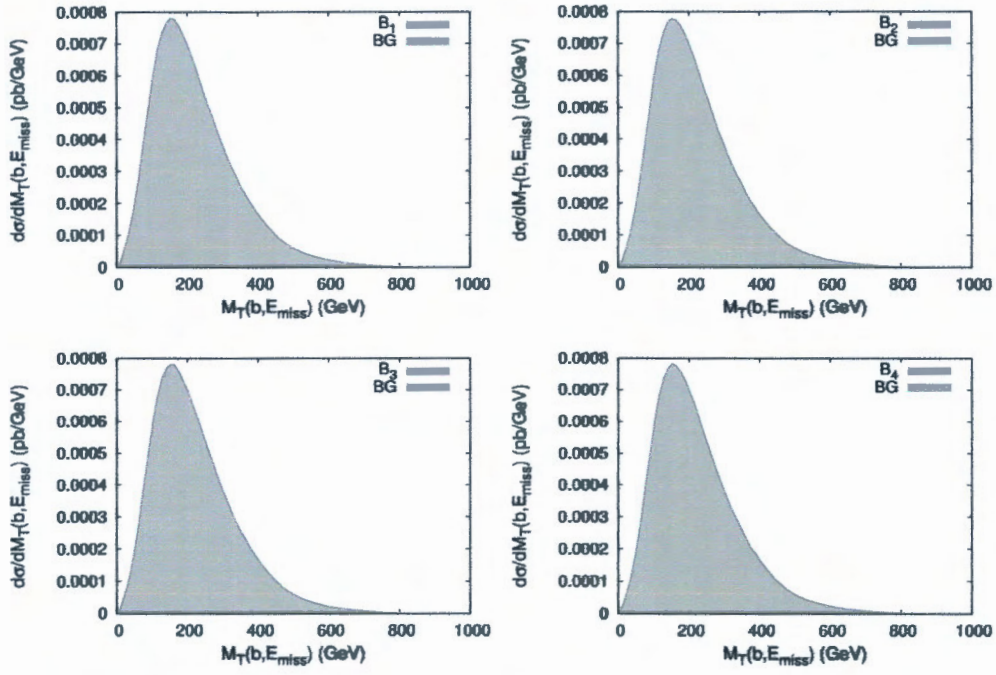

Figure 4.35: Distributions of the jet plus missing energy transverse mass for the four benchmarks.

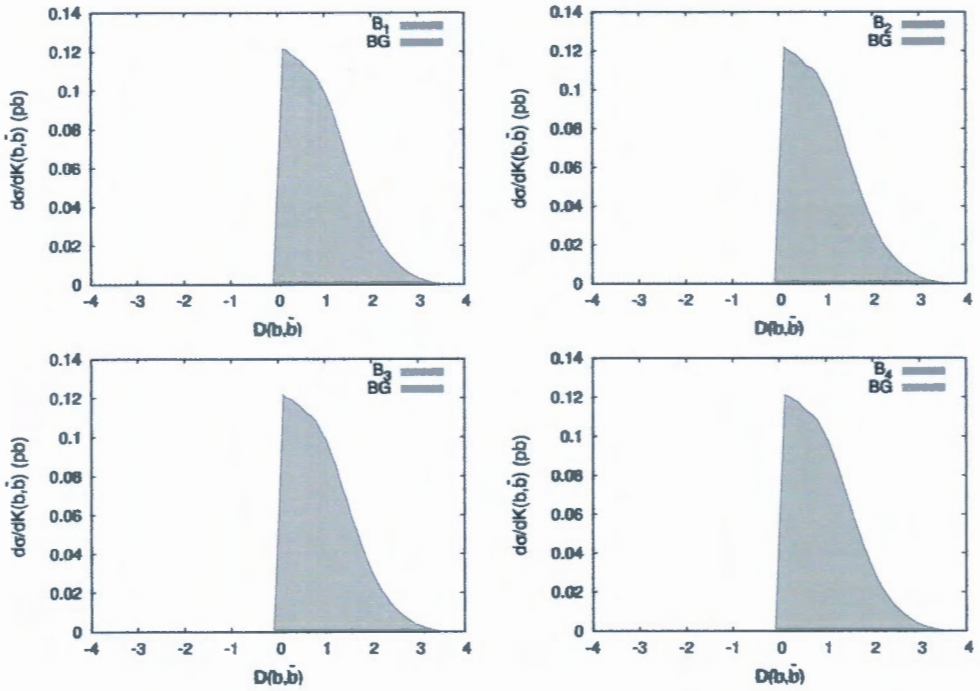

Figure 4.36: Distributions of pseudorapidity difference between the two jets for the four benchmarks.

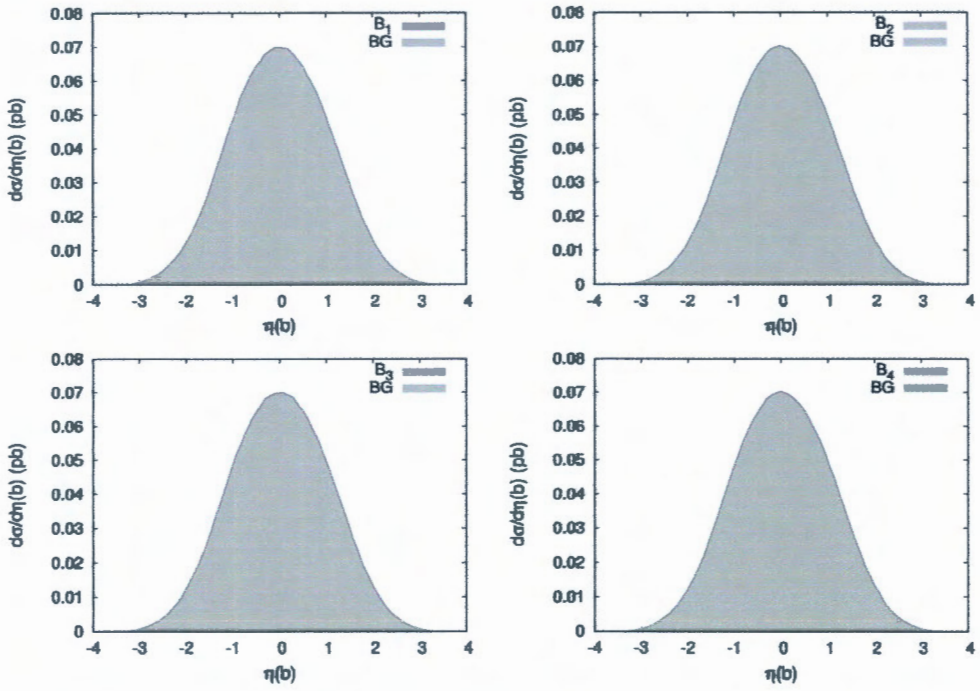

Figure 4.37: Distributions of the jet pseudorapidity for the four benchmarks.

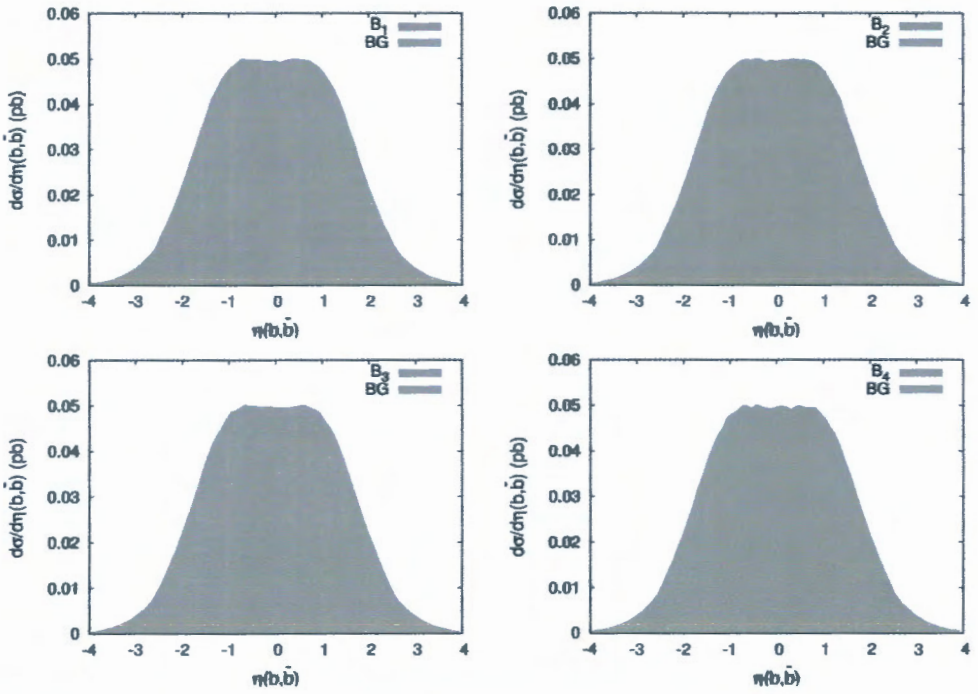

Figure 4.38: Distributions of the two jets pseudorapidity for the four benchmarks.

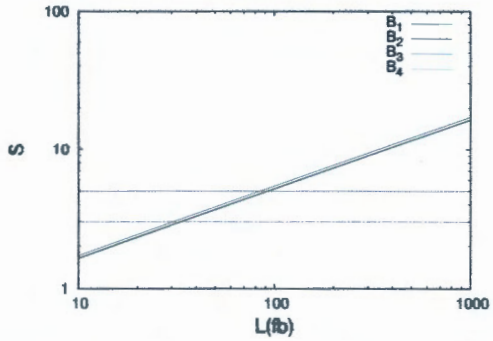

Figure 4.39: The significance as a function of integrated luminosity L. The two dashed lines represent S=3 and S=5

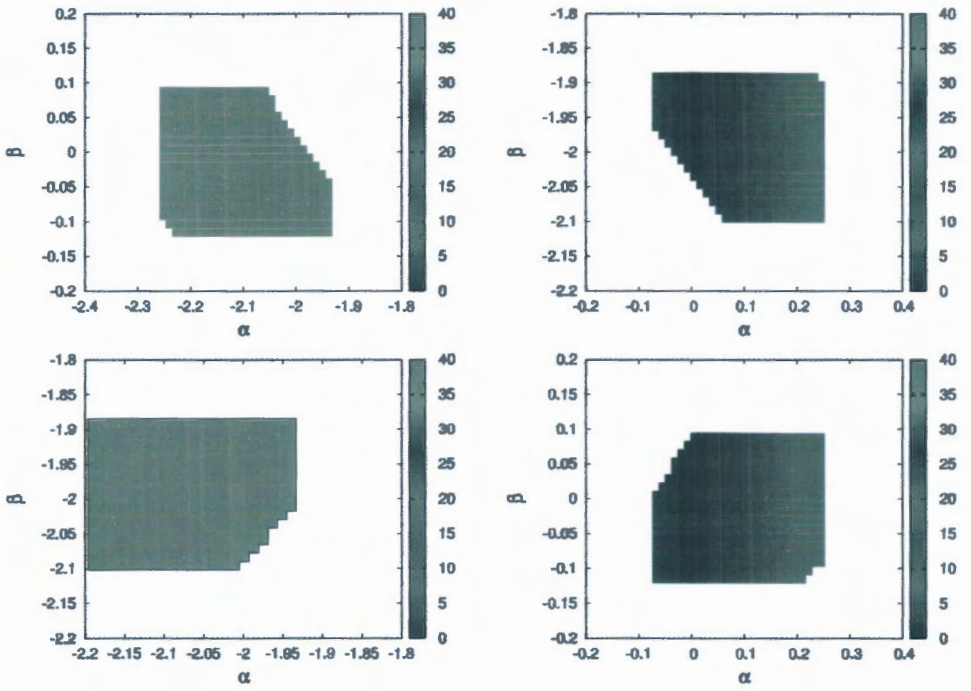

Figure 4.40: The signal significance for $L = 10(\ fb^{-1})$ as a function of parameters β and α.

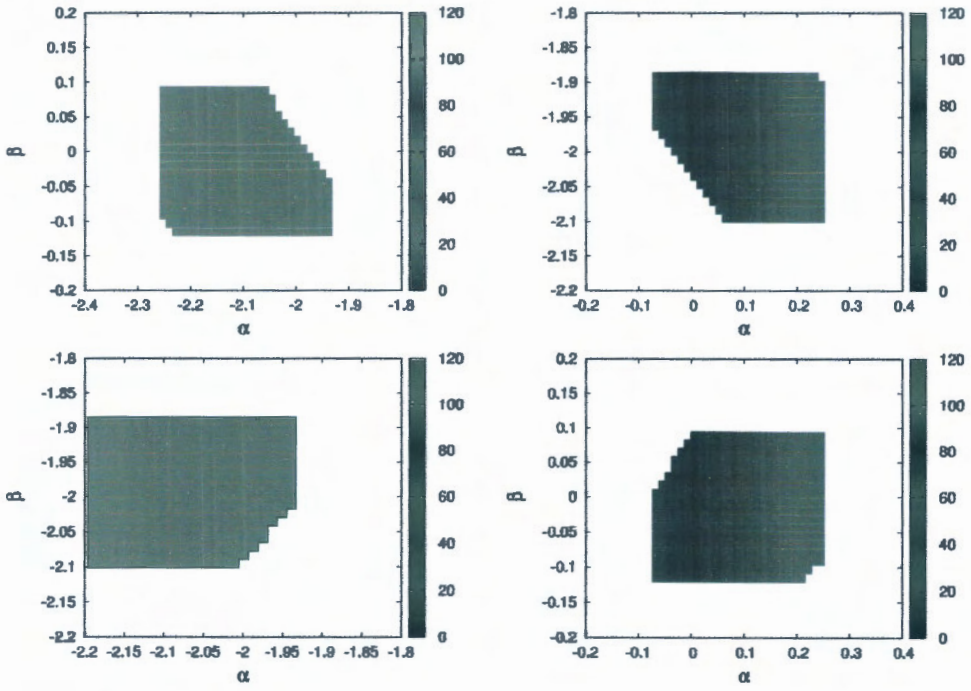

Figure 4.41: The signal significance for $L = 100(\ fb^{-1})$ as a function of parameters β and α.

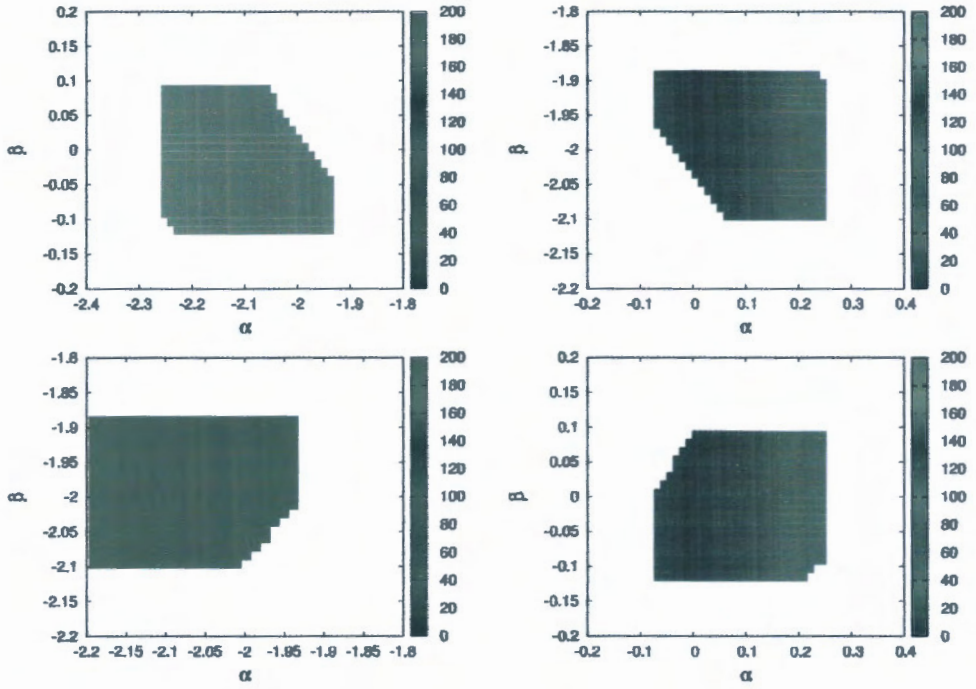

Figure 4.42: The signal significance for $L = 300(\ fb^{-1})$ as a function of parameters β and α.

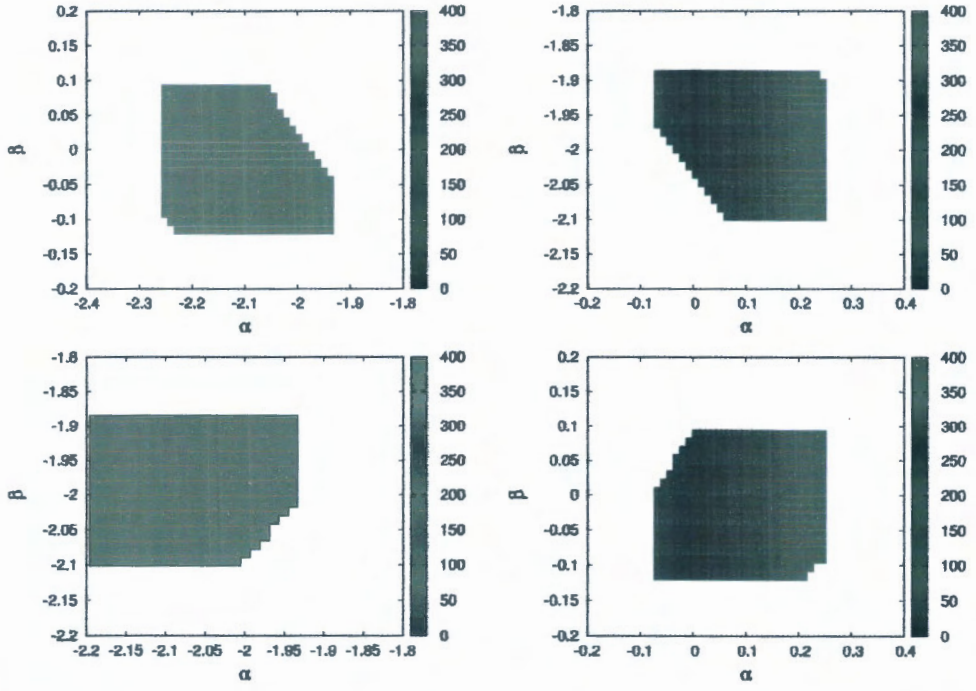

Figure 4.43: The signal significance for $L = 1000(\ fb^{-1})$ as a function of parameters β and α.

Chapter 5

Conclusion

In our work, we have investigated the possibility of discovering a new physics beyond the standard model at future leptonic collider ILC. To realize this task, we considered the process $e^-e^+ \rightarrow HZ \rightarrow b\bar{b}$+$E_{miss}$ at center of mass energy $E_{CM} = 1000GeV$, where $E_{miss} = \upsilon_i\bar{\upsilon}_i$ $(i = e, \mu, \tau)$, then concidered two parameters α and β where α, β are real numbers that can express any possible deviation from the SM, for the couplings HWW and HZZ, respectively. Of course, before began this study, we started by giving a brief review for the SM, the Higgs mechanism, and the general lagrangean of the model, after that, we talked about its limitations. Then, we gave a simple description for CalcHEP, the package used in this study, and defined the kinematic variables used in accelerators physics, we described also some colliders.

In this work, and by using CalcHEP package, we fixed the parameter values, and then generated the differential cross section for both the background (SM) and the signal (the four Benchmarks B_i), where we were able to produce a set of different distributions in order to define a new set of cuts that maximize the significance. We showed that at the choosen cuts and at the α and β chosen values in B1, B2, B3 and B4, and within estimating the cross section of different benchmarks and the background, and then estimating the signal by variating integrated luminosity, there was a deviation from the standard model at minimum of $L = 30\ fb^{-1}$ and we saw clearly a discovery at minimum of $L = 84\ fb^{-1}$. Finaly, We then translated the values of the measured cross sections in each case to a palette of signal significance in terms of α and β by taking four values for luminosity ($L = 10\ fb^{-1}$, $L = 100\ fb^{-1}$, $L = 300\ fb^{-1}$, $L = 1000\ fb^{-1}$), we detected a discovery signal.

We conclude that the reaction $e^-e^+ \rightarrow HZ \rightarrow b\bar{b}$+$E_{miss}$ is excellent for investigating the possibility of discovering a new physics beyond the standard model at future leptonic collider ILC.

Appendix A

CalcHEP model files & Batch files

A.1 CalcHEP model files

Here we show the SM CalcHEP model files where the HVV couplings are modified.

```
SMm
 Particles
 Full  name  |A   |A+  | number |2*spin| mass  |width |color|aux|>LaTex(A)<|>LaTeX(A+)   <|
gluon        |G   |G   |21      |2     |0      |0     |8    |G  |g         |g
photon       |A   |A   |22      |2     |0      |0     |1    |G  |\gamma    |\gamma
Z-boson      |Z   |Z   |23      |2     |MZ     |wZ    |i    |G  |Z         |Z
W-boson      |W+  |W-  |24      |2     |MW     |wW    |1    |G  |W+        |W-
Higgs        |h   |h   |25      |0     |Mh     |wh    |1    |   |h         |h
electron     |e   |E   |ii      |i     |Me     |0     |i    |   |e         |\bar{e}
e-neutrino   |ne  |Ne  |12      |1     |0      |0     |1    |L  |\nu_e     |\bar{\nu}_e
muon         |m   |M   |i3      |i     |Mm     |0     |i    |   |\mu       |\bar{\mu}
m-neutrino   |nm  |Nm  |14      |1     |0      |0     |1    |L  |\nu_\mu   |\bar{\nu}_\mu
tau-lepton   |l   |L   |i5      |i     |Ml     |0     |i    |   |\tau      |\bar{\tau}
t-neutrino   |nl  |Nl  |16      |1     |0      |0     |1    |L  |\nu_\tau  |\bar{\nu}_\tau
d-quark      |d   |D   |1       |1     |0      |0     |3    |   |d         |\bar{d}
u-quark      |u   |U   |2       |1     |0      |0     |3    |   |u         |\bar{u}
s-quark      |s   |S   |3       |1     |0      |0     |3    |   |s         |\bar{s}
c-quark      |c   |C   |4       |1     |Mcp    |0     |3    |   |c         |\bar{c}
b-quark      |b   |B   |5       |1     |Mbp    |0     |3    |   |b         |\bar{b}
t-quark      |t   |T   |6       |1     |Mtp    |wt    |3    |   |t         |\bar{t}
=============================================================================================
```

```
SMm
 Parameters
  Name   <| Value          <|> Comment                                                    <|
 alphaSMZ |0.1184           |Srtong alpha(MZ) for running mass calculation
 EE       |0.31343          |elecromagnetic constant
 Me       |0.000511         |electron mass
 Mm       |0.1057           |muon mass
 Ml       |1.777            |tau-lepton mass
 Q        |100              |scale for running mass calculation
 McMc     |1.23             | Mc(Mc)  MS-BAR
 MbMb     |4.25             | Mb(Mb)  MS-BAR
 Mtp      |173.07           |t-quark pole mass
 Mh       |125.09           |higgs mass
 wt       |1.59             |t-quark width        (tree level 1->2x)
 MZ       |91.188           |Z-boson mass
 MW       |80.385           |Sine of electro-weak mixing angle (MS_bar)
 bb       |0                | hZZ
 aa       |0                | hWW
 v        |246.22           | Higgs vev
```

```
 s12       |0.221            |Parameter of C-K-M matrix  (PDG96)
 s23       |0.041            |Parameter of C-K-M matrix  (PDG96)
 s13       |0.0035           |Parameter of C-K-M matrix  (PDG96)
 wt        |1.59             |t-quark width        (tree level 1->2x)
 wZ        |2.49444          |Z-boson width        (tree level 1->2x)
 wW        |2.08895          |W-boson width        (tree level 1->2x)
=============================================================================================================

SMm
 Constraints
 Name       |  Expression                                                                              <|
CW          |MW/MZ                          % on-shell cos of the Weinberg angle
SW          |sqrt(1-CW^2)                   % sin of the Weinberg angle
GF          |EE^2/(2*SW*MW)^2/Sqrt2         % Fermi constant (not used below)
c12         |sqrt(1-s12^ 2)                 % parameter  of C-K-M matrix
c23         |sqrt(1-s23^ 2)                 % parameter  of C-K-M matrix
c13         |sqrt(1-s13^ 2)                 % parameter  of C-K-M matrix
Vud         |c12*c13                        % C-K-M matrix element
Vus         |s12*c13                        % C-K-M matrix element
Vub         |s13                            % C-K-M matrix element
Vcd         |-s12*c23-c12*s23*s13           % C-K-M matrix element
Vcs         |c12*c23-s12*s23*s13            % C-K-M matrix element
Vcb         |s23*c13                        % C-K-M matrix element
Vtd         |s12*s23-c12*c23*s13            % C-K-M matrix element
Vts         |-c12*s23-s12*c23*s13           % C-K-M matrix element
Vtb         |c23*c13                        % C-K-M matrix element
Mb          |MbEff(Q)
Mt          |MtEff(Q)
Mc          |McEff(Q)
VEV         |2*MW*SW/EE
LamQCD      |initQCD5(alphaSMZ,McMc,MbMb,Mtp)
Mcp         | McMc*(1+4/3*alphaQCD(McMc)/pi)  % 1 loop formula like in Hdecay
Mbp         | MbMb*(1+4/3*alphaQCD(MbMb)/pi)  % 1 loop formula like in Hdecay
aQCDh       |alphaQCD(Mh)/pi
Rqcdh       |sqrt(1+149/12*aQCDh+68.6482*aQCDh^2-212.447*aQCDh^3)
LGGh        |-cabs(hGGeven(Mh, aQCDh,3, 1,3,Mtp,1/VEV,  1,3,Mbp,1/VEV, 1,3,Mcp,1/VEV))
Quq         | 4/9
Qdq         | 1/9
LAAh        |-cabs( hAAeven(Mh,aQCDh,2, 2,1,MW,-2/VEV, 1,1,Ml,1/VEV)+Quq*hAAe)
=============================================================================================================

SMm
 Vertices
A1   |A2   |A3   |A4   |>          Factor                          <|>  Lorentz part
G    |G    |G    |     |GG                                          |m1.m2*(p1-p2).m3+m2.m3*(p2-p3).m1+m3.m1*(p3-p
G    |G    |G.t  |     |GG/Sqrt2                                    |m1.M3*m2.m3-m1.m3*m2.M3
W+   |W-   |A    |     |-EE                                         |m1.m2*(p1-p2).m3+m2.m3*(p2-p3).m1+m3.m1*(p3-p
W+   |W-   |Z    |     |-EE*CW/SW                                   |m1.m2*(p1-p2).m3+m2.m3*(p2-p3).m1+m3.m1*(p3-p
W+   |W-   |Z    |Z    |-(EE*CW/SW)^ 2                              |2*m1.m2*m3.m4-m1.m3*m2.m4-m1.m4*m2.m3
W+   |W+   |W-   |W-   |(EE/SW)^ 2                                  |2*m1.m2*m3.m4-m1.m3*m2.m4-m1.m4*m2.m3
W+   |W-   |A    |Z    |-EE^ 2*CW/SW                                |2*m1.m2*m3.m4-m1.m3*m2.m4-m1.m4*m2.m3
W+   |W-   |A    |A    |-EE^ 2                                      |2*m1.m2*m3.m4-m1.m3*m2.m4-m1.m4*m2.m3
h    |h    |h    |     |-(3/2)*EE*Mh^2/(MW*SW)                      |1+cc
h    |W+   |W-   |     |EE*MW/SW                                    |(1+aa)*m2.m3
h    |Z    |Z    |     |EE/(SW*CW^ 2)*MW                            |(1+bb)*m2.m3
h    |fi   |fi   |     |-cs*v                                       |1
h    |h    |h    |h    |(-3/4)*(EE*Mh/(MW*SW))^ 2                   |1
h    |h    |Z    |Z    | (1/2)*(EE/(SW*CW))^ 2                      |m3.m4
h    |h    |W+   |W-   | (1/2)*(EE/SW)^ 2                           |m3.m4
M    |m    |h    |     |-EE*Mm/(2*MW*SW)                            |1
L    |l    |h    |     |-EE*Ml  /(2*MW*SW)                          |1
C    |c    |h    |     |-EE*Mc/(2*MW*SW)                            |1
B    |b    |h    |     |-EE*Mb/(2*MW*SW)                            |1
T    |t    |h    |     |-EE*Mt  /(2*MW*SW)                          |1
E    |e    |A    |     |-EE                                         |G(m3)
M    |m    |A    |     |-EE                                         |G(m3)
L    |l    |A    |     |-EE                                         |G(m3)
Ne   |e    |W+   |     |EE/(2*Sqrt2*SW)                             |G(m3)*(1-G5)
Nm   |m    |W+   |     |EE/(2*Sqrt2*SW)                             |G(m3)*(1-G5)
```

```
Nl  |l    |W+   |      |EE/(2*Sqrt2*SW)                    |G(m3)*(1-G5)
E   |ne   |W-   |      |EE/(2*Sqrt2*SW)                    |G(m3)*(1-G5)
M   |nm   |W-   |      |EE/(2*Sqrt2*SW)                    |G(m3)*(1-G5)
L   |nl   |W-   |      |EE/(2*Sqrt2*SW)                    |G(m3)*(1-G5)
E   |e    |Z    |      |-EE/(4*SW*CW)                      |G(m3)*(1-G5)-4*(SW^ 2)*G(m3)
M   |m    |Z    |      |-EE/(4*SW*CW)                      |G(m3)*(1-G5)-4*(SW^ 2)*G(m3)
L   |l    |Z    |      |-EE/(4*SW*CW)                      |G(m3)*(1-G5)-4*(SW^ 2)*G(m3)
Ne  |ne   |Z    |      |EE/(4*SW*CW)                       |G(m3)*(1-G5)
Nm  |nm   |Z    |      |EE/(4*SW*CW)                       |G(m3)*(1-G5)
Nl  |nl   |Z    |      |EE/(4*SW*CW)                       |G(m3)*(1-G5)
U   |u    |A    |      |(2/3)*EE                           |G(m3)
D   |d    |A    |      |(-1/3)*EE                          |G(m3)
C   |c    |A    |      |(2/3)*EE                           |G(m3)
S   |s    |A    |      |(-1/3)*EE                          |G(m3)
B   |b    |A    |      |(-1/3)*EE                          |G(m3)
T   |t    |A    |      |(2/3)*EE                           |G(m3)
U   |u    |Z    |      |-EE/(12*SW*CW)                     |-3*G(m3)*(1-G5)+8*(SW^ 2)*G(m3)
D   |d    |Z    |      |-EE/(12*SW*CW)                     |+3*G(m3)*(1-G5)-4*(SW^ 2)*G(m3)
C   |c    |Z    |      |-EE/(12*SW*CW)                     |-3*G(m3)*(1-G5)+8*(SW^ 2)*G(m3)
S   |s    |Z    |      |-EE/(12*SW*CW)                     |+3*G(m3)*(1-G5)-4*(SW^ 2)*G(m3)
B   |b    |Z    |      |-EE/(12*SW*CW)                     |+3*G(m3)*(1-G5)-4*(SW^ 2)*G(m3)
T   |t    |Z    |      |-EE/(12*SW*CW)                     |-3*G(m3)*(1-G5)+8*(SW^ 2)*G(m3)
U   |d    |W+   |      |EE*Vud/(2*Sqrt2*SW)                |G(m3)*(1-G5)
U   |s    |W+   |      |EE*Vus/(2*Sqrt2*SW)                |G(m3)*(1-G5)
U   |b    |W+   |      |EE*Vub/(2*Sqrt2*SW)                |G(m3)*(1-G5)
C   |d    |W+   |      |EE*Vcd/(2*Sqrt2*SW)                |G(m3)*(1-G5)
C   |s    |W+   |      |EE*Vcs/(2*Sqrt2*SW)                |G(m3)*(1-G5)
C   |b    |W+   |      |EE*Vcb/(2*Sqrt2*SW)                |G(m3)*(1-G5)
T   |d    |W+   |      |EE*Vtd/(2*Sqrt2*SW)                |G(m3)*(1-G5)
T   |s    |W+   |      |EE*Vts/(2*Sqrt2*SW)                |G(m3)*(1-G5)
T   |b    |W+   |      |EE*Vtb/(2*Sqrt2*SW)                |G(m3)*(1-G5)
D   |u    |W-   |      |EE*Vud/(2*Sqrt2*SW)                |G(m3)*(1-G5)
S   |u    |W-   |      |EE*Vus/(2*Sqrt2*SW)                |G(m3)*(1-G5)
B   |u    |W-   |      |EE*Vub/(2*Sqrt2*SW)                |G(m3)*(1-G5)
D   |c    |W-   |      |EE*Vcd/(2*Sqrt2*SW)                |G(m3)*(1-G5)
S   |c    |W-   |      |EE*Vcs/(2*Sqrt2*SW)                |G(m3)*(1-G5)
B   |c    |W-   |      |EE*Vcb/(2*Sqrt2*SW)                |G(m3)*(1-G5)
D   |t    |W-   |      |EE*Vtd/(2*Sqrt2*SW)                |G(m3)*(1-G5)
S   |t    |W-   |      |EE*Vts/(2*Sqrt2*SW)                |G(m3)*(1-G5)
B   |t    |W-   |      |EE*Vtb/(2*Sqrt2*SW)                |G(m3)*(1-G5)
U   |u    |G    |      |GG                                 |G(m3)
D   |d    |G    |      |GG                                 |G(m3)
C   |c    |G    |      |GG                                 |G(m3)
S   |s    |G    |      |GG                                 |G(m3)
T   |t    |G    |      |GG                                 |G(m3)
B   |b    |G    |      |GG                                 |G(m3)
U   |b    |W+.f |      |-i*EE*Vub/(2*Sqrt2*MW*SW)          |Mb*(1+G5)
C   |d    |W+.f |      |-i*EE*Vcd/(2*Sqrt2*MW*SW)          |          -Mc*(1-G5)
C   |b    |W+.f |      |-i*EE*Vcb/(2*Sqrt2*MW*SW)          |Mb*(1+G5)-Mc*(1-G5)
T   |d    |W+.f |      |-i*EE*Vtd/(2*Sqrt2*MW*SW)          |          -Mt  *(1-G5)
T   |b    |W+.f |      |-i*EE*Vtb/(2*Sqrt2*MW*SW)          |Mb*(1+G5)-Mt  *(1-G5)
D   |c    |W-.f |      |-i*EE*Vcd/(2*Sqrt2*MW*SW)          |Mc*(1+G5)
D   |t    |W-.f |      |-i*EE*Vtd/(2*Sqrt2*MW*SW)          |Mt  *(1+G5)
B   |u    |W-.f |      |-i*EE*Vub/(2*Sqrt2*MW*SW)          |           -Mb*(1-G5)
B   |c    |W-.f |      |-i*EE*Vcb/(2*Sqrt2*MW*SW)          |Mc*(1+G5)-Mb*(1-G5)
B   |t    |W-.f |      |-i*EE*Vtb/(2*Sqrt2*MW*SW)          |Mt  *(1+G5)-Mb*(1-G5)
C   |c    |Z.f  |      |-i*EE*Mc/(2*MW*SW)                 |G5
T   |t    |Z.f  |      |-i*EE*Mt  /(2*MW*SW)               |G5
B   |b    |Z.f  |      |i*EE*Mb/(2*MW*SW)                  |G5
M   |nm   |W-.f |      |-i*EE*Mm/(2*Sqrt2*MW*SW)           |-(1-G5)
L   |nl   |W-.f |      |-i*EE*Ml  /(2*Sqrt2*MW*SW)         |-(1-G5)
Nm  |m    |W+.f |      |-i*EE*Mm/(2*Sqrt2*MW*SW)           |(1+G5)
Nl  |l    |W+.f |      |-i*EE*Ml  /(2*Sqrt2*MW*SW)         |(1+G5)
M   |m    |Z.f  |      |i*EE*Mm/(2*MW*SW)                  |G5
L   |l    |Z.f  |      |i*EE*Ml  /(2*MW*SW)                |G5
h   |Z.f  |Z    |      |i*EE/(2*CW*SW)                     |(p2-p1).m3
h   |W-.f |W+   |      |i*EE/(2*SW)                        |(p2-p1).m3
h   |W+.f |W-   |      |i*EE/(2*SW)                        |(p2-p1).m3
Z.f |W+.f |W-   |      |EE/(2*SW)                          |-(p2-p1).m3
```

```
Z.f  |W-.f |W+   |     |EE/(2*SW)                                  |(p2-p1).m3
W-.f |W+.f |Z    |     |EE/(2*CW*SW)                               |(1-2*SW^ 2)* (p2-p1).m3
W-.f |W+.f |A    |     |EE                                         |(p2-p1).m3
W-.f |W+   |A    |     |-i*EE*MW                                   |m2.m3
W+.f |W-   |A    |     |-i*EE*MW                                   |-m2.m3
W-.f |W+   |Z    |     |-i*EE*MW*SW/CW                             |-m2.m3
W+.f |W-   |Z    |     |-i*EE*MW*SW/CW                             |m2.m3
W+.f |W-.f |h    |     |-EE*Mh^ 2/(2*MW*SW)                        |1
Z.f  |Z.f  |h    |     |-EE*Mh^ 2/(2*MW*SW)                        |1
W-.f |W+.f |A    |A    |2*EE^ 2                                    |m3.m4
W-.f |W+.f |Z    |Z    |(EE/(CW*SW))^ 2/2                          |(1-2*SW^ 2)^ 2*m3.m4
W-.f |W+.f |W-   |W+   |EE^ 2/(2*SW*SW)                            |m3.m4
W-.f |W+.f |Z    |A    |EE^ 2/(SW*CW)                              |(1-2*SW^ 2)*m3.m4
Z.f  |Z.f  |Z    |Z    |(EE/(SW*CW))^ 2/2                          |m3.m4
Z.f  |Z.f  |W-   |W+   |EE^ 2/(2*SW*SW)                            |m3.m4
W-.f |Z.f  |W+   |A    |-EE^ 2/(2*SW)                              |m3.m4
W+.f |Z.f  |W-   |A    |-EE^ 2/(2*SW)                              |m3.m4
W-.f |Z.f  |W+   |Z    |EE^ 2/(2*CW)                               |m3.m4
W+.f |Z.f  |W-   |Z    |EE^ 2/(2*CW)                               |m3.m4
W-.f |h    |W+   |A    |-i*EE^ 2/(2*SW)                            |m3.m4
W+.f |h    |W-   |A    |i*EE^ 2/(2*SW)                             |m3.m4
W-.f |h    |W+   |Z    |i*EE^ 2/(2*CW)                             |m3.m4
W+.f |h    |W-   |Z    |-i*EE^ 2/(2*CW)                            |m3.m4
Z.f  |Z.f  |Z.f  |Z.f  |-3*(EE*Mh/(2*MW*SW))^ 2                    |1
Z.f  |Z.f  |W-.f |W+.f |-(EE*Mh/(2*MW*SW))^ 2                      |1
W-.f |W-.f |W+.f |W+.f |- (EE*Mh/(MW*SW))^ 2/2                     |1
Z.f  |Z.f  |h    |h    |-(EE*Mh/(2*MW*SW))^ 2                      |1
W+.f |W-.f |h    |h    |-(EE*Mh/(2*MW*SW))^ 2                      |1
G.C  |G.c  |G    |     |-GG                                        |p1.m3
W-.C |Z.c  |W+   |     |EE*CW/SW                                   |p1.m3
W+.C |Z.c  |W-   |     |-EE*CW/SW                                  |p1.m3
Z.C  |W-.c |W+   |     |-EE*CW/SW                                  |p1.m3
Z.C  |W+.c |W-   |     |EE*CW/SW                                   |p1.m3
W-.C |W+.c |Z    |     |-EE*CW/SW                                  |p1.m3
W+.C |W-.c |Z    |     |EE*CW/SW                                   |p1.m3
W-.C |W+.c |A    |     |-EE                                        |p1.m3
W+.C |W-.c |A    |     |EE                                         |p1.m3
Z.C  |Z.c  |h    |     |-EE*MW/(2*SW*CW*CW)                        |1
W-.C |W+.c |h    |     |-EE*MW/(2*SW)                              |1
W+.C |W-.c |h    |     |-EE*MW/(2*SW)                              |1
W-.C |W+.c |Z.f  |     |i*EE*MW/(2*SW)                             |1
W+.C |W-.c |Z.f  |     |-i*EE*MW/(2*SW)                            |1
W-.C |Z.c  |W+.f |     |-i*EE*MW/(2*CW*SW)                         |1-2*SW^ 2
W+.C |Z.c  |W-.f |     |i*EE*MW/(2*CW*SW)                          |1-2*SW^ 2
Z.C  |W-.c |W+.f |     |i*EE*MW/(2*CW*SW)                          |1
Z.C  |W+.c |W-.f |     |-i*EE*MW/(2*CW*SW)                         |1
W-.C |A.c  |W+   |     |EE                                         |p1.m3
W+.C |A.c  |W-   |     |-EE                                        |p1.m3
A.C  |W-.c |W+   |     |-EE                                        |p1.m3
A.C  |W+.c |W-   |     |EE                                         |p1.m3
W-.C |A.c  |W+.f |     |-i*EE*MW                                   |1
W+.C |A.c  |W-.f |     |i*EE*MW                                    |1
G    |G    |h    |     |-4*LGGh*Rqcdh                              |(p1.p2*m1.m2-p1.m2*p2.m1)
G    |G    |G    |h    |-4*LGGh*GG*Rqcdh                           |m1.m2*(p1-p2).m3+m2.m3*(p2-p3).m1+m3.m1*(p3-p
A    |A    |h    |     |-4*LAAh                                    |(p1.p2*m1.m2-p1.m2*p2.m1)
=============================================================================================================
```

A.2 Batch files

Here we show the batch files where all cuts are considered.

```
Model: SMod
Model changed: False
```

```
Gauge: Feynman

Process: e,E->nn,Nn,b,B
Composite: nn=ne,nm,nl
Composite: Nn=Ne,Nm,Nl

pdf1: ISR & Beamstrahlung
pdf2: ISR & Beamstrahlung
Bunch x+y sizes (nm) : 560
Bunch length (mm) : 0.4
Number of particles : 2E+10

p1: 500
p2: 500

Parameter: aa=0.04
Parameter: bb=0.04

Kinematics : 12 -> 34 , 56
Kinematics : 34 -> 3 , 4
Kinematics : 56 -> 5 , 6

Regularization momentum: 34
Regularization mass: MZ
Regularization width: wZ
Regularization power: 2

Regularization momentum: 56
Regularization mass: MZ
Regularization width: wZ
Regularization power: 2

Regularization momentum: 56
Regularization mass: Mh
Regularization width: wh
Regularization power: 2

Breit Wigner range : 2.7
T-channel widths : ON
GI in T-channel : ON
GI in S-channel : ON

Cut parameter: E(nn,Nn)
Cut invert: False
Cut min: 520
Cut max: 880

Cut parameter: E(b,B)
Cut invert: False
Cut min: 120
Cut max: 430

Cut parameter: T(nn,Nn)
Cut invert: False
Cut min:
Cut max: 250

Cut parameter: T(b)
Cut invert: False
Cut min: 15
Cut max:

Cut parameter: T(B)
Cut invert: False
Cut min: 15
Cut max:

Cut parameter: M(b,B)
Cut invert: False
```

```
Cut min: 71
Cut max: 145

Cut parameter: M(b,nn,Nn)
Cut invert: False
Cut min: 500
Cut max:

Cut parameter: M(B,nn,Nn)
Cut invert: False
Cut min: 500
Cut max:

Cut parameter: J(b,B)
Cut invert: False
Cut min: 0.4
Cut max:

Cut parameter: Z(b,B)
Cut invert: False
Cut min: 120
Cut max: 260

Cut parameter: C(b,B)
Cut invert: False
Cut min:
Cut max: 0.86

Cut parameter: D(b,B)
Cut invert: False
Cut min: 400
Cut max:

Cut parameter: W(b,nn,Nn)
Cut invert: False
Cut min:
Cut max: 600

Cut parameter: W(B,nn,Nn)
Cut invert: False
Cut min:
Cut max: 600

Dist parameter: E(nn,Nn)
Dist min: 0
Dist max: 1000
Dist n bins: 300
Dist title: e,E->nn,Nn,b,B
Dist x-title: Emiss (GeV)

Dist parameter: E(b)
Dist min: 0
Dist max: 500
Dist n bins: 300
Dist title: e,E->nn,Nn,b,B
Dist x-title: E(b) (GeV)

Dist parameter: E(B)
Dist min: 0
Dist max: 500
Dist n bins: 300
Dist title: e,E->nn,Nn,b,B
Dist x-title: E(B) (GeV)

Dist parameter: E(b,B)
Dist min: 0
Dist max: 1000
Dist n bins: 300
Dist title: e,E->nn,Nn,b,B
```

```
Dist x-title: E(b,B) (GeV)

Dist parameter: T(nn,Nn)
Dist min: 0
Dist max: 1000
Dist n bins: 300
Dist title: e,E->nn,Nn,b,B
Dist x-title: Tmiss (GeV)

Dist parameter: T(b)
Dist min: 0
Dist max: 500
Dist n bins: 300
Dist title: e,E->nn,Nn,b,B
Dist x-title: T(b) (GeV)

Dist parameter: T(B)
Dist min: 0
Dist max: 500
Dist n bins: 300
Dist title: e,E->nn,Nn,b,B
Dist x-title: T(B) (GeV)


Dist parameter: T(b,B)
Dist min: 0
Dist max: 1000
Dist n bins: 300
Dist title: e,E->nn,Nn,b,B
Dist x-title: T(b,B) (GeV)

Dist parameter: Z(b)
Dist min: 0
Dist max: 500
Dist n bins: 300
Dist title: e,E->nn,Nn,b,B
Dist x-title: Z(b) (GeV)

Dist parameter: Z(B)
Dist min: 0
Dist max: 500
Dist n bins: 300
Dist title: e,E->nn,Nn,b,B
Dist x-title: Z(B) (GeV)


Dist parameter: Z(b,B)
Dist min: 0
Dist max: 1000
Dist n bins: 300
Dist title: e,E->nn,Nn,b,B
Dist x-title: Z(b,B) (GeV)

Dist parameter: M(b,B)
Dist min: 71
Dist max: 145
Dist n bins: 300
Dist title: e,E->nn,Nn,b,B
Dist x-title: M(b,B) (GeV)

Dist parameter: M(b,nn,Nn)
Dist min: 0
Dist max: 1000
Dist n bins: 300
Dist title: e,E->nn,Nn,b,B
Dist x-title: M(b,Emiss) (GeV)

Dist parameter: M(B,nn,Nn)
Dist min: 0
```

```
Dist max: 1000
Dist n bins: 300
Dist title: e,E->nn,Nn,b,B
Dist x-title: M(B,Emiss) (GeV)

Dist parameter: C(b,B)
Dist min: -1
Dist max: 1
Dist n bins: 300
Dist title: e,E->nn,Nn,b,B
Dist x-title: C(b,B)

Dist parameter: C(b)
Dist min: -1
Dist max: 1
Dist n bins: 300
Dist title: e,E->nn,Nn,b,B
Dist x-title: C(b)

Dist parameter: C(B)
Dist min: -1
Dist max: 1
Dist n bins: 300
Dist title: e,E->nn,Nn,b,B
Dist x-title: C(B)

Dist parameter: K(b,B)
Dist min: -4
Dist max: 4
Dist n bins: 300
Dist title: e,E->nn,Nn,b,B
Dist x-title: K(b,B)

Dist parameter: N(b)
Dist min: -4
Dist max: 4
Dist n bins: 300
Dist title: e,E->nn,Nn,b,B
Dist x-title: N(b) (GeV)

Dist parameter: N(B)
Dist min: -4
Dist max: 4
Dist n bins: 300
Dist title: e,E->nn,Nn,b,B
Dist x-title: N(B) (GeV)

Dist parameter: N(b,B)
Dist min: -4
Dist max: 4
Dist n bins: 300
Dist title: e,E->nn,Nn,b,B
Dist x-title: N(b,B) (GeV)

Dist parameter: D(b,B)
Dist min: 0
Dist max: 1000
Dist n bins: 300
Dist title: e,E->nn,Nn,b,B
Dist x-title: D(b,B) (GeV)

Dist parameter: W(b,B)
Dist min: 0
Dist max: 1000
Dist n bins: 300
Dist title: e,E->nn,Nn,b,B
Dist x-title: W(b,B) (GeV)

Dist parameter: W(b,nn,Nn)
```

```
Dist min: 0
Dist max: 1000
Dist n bins: 300
Dist title: e,E->nn,Nn,b,B
Dist x-title: W(b,Emiss) (GeV)

Dist parameter: W(B,nn,Nn)
Dist min: 0
Dist max: 1000
Dist n bins: 300
Dist title: e,E->nn,Nn,b,B
Dist x-title: W(B,Emiss) (GeV)

Number of events (per run step): 0
Filename: bB-B1-apre-CUT.distr
NTuple: False
Cleanup: False

Parallelization method: local

Max number of nodes: 8
Max number of processes per node: 4

sleep time: 3
nice level : 19

nSess_1: 5
nCalls_1: 300000
nSess_2: 15
nCalls_2: 1000000
```

Bibliography

[1] G. Aad et al. [ATLAS Collaboration], Phys. Lett. B 716, 1 (2012) [arXiv:1207.7214 [hep-ex]].

[2] S. Chatrchyan et al. [c.m.S Collaboration], Phys. Lett. B 716, 30 (2012) [arXiv:1207.7235 [hep-ex]].

[3] T. Behnke, C. Damerell, J. Jaros, A. Miyamoto et al. (ILC Collaboration), arXiv:0712.2356 [physics.ins-det].

[4] C. Adolphsen et al., arXiv:1306.6328 [physics.acc-ph]. III, IV B

[5] H. Baer et al., arXiv:1306.6352 [hep-ph].

[6] J. R. Andersen et al. (LHC Higgs Cross Section Working Group) (2013), 1307.1347.

[7] C. Mariotti and G. Passarino, Int. J. Mod. Phys. A32, 1730003 (2017), 1612.00269

[8] in Proceedings, 2013 Community Summer Study on the Future of U.S. Particle Physics: Snowmass on the Mississippi (CSS2013): Minneapolis, MN, USA, July 29-August 6, 2013, (2013), 1307.7135, URL https://inspirehep.net/record/1244669/files/arXiv:1307.7135.pdf.

[9] L.Marleau, " Introduction à la physique des particles" , Département de physique. Université Laval. Québec,Canada, 1998-2017.

[10] W.N.COTTINGHAM and D.A. GREENWOOD, " An introduction to the Standard Model of Particle Physics" . CAMBRIDGE UNIVERSITY PRESS.

[11] David Griffiths, " INTRODUCTION TO ELEMENTARY PARTICLES" , WILEY-VCH Verlag GmbH & Co. KGaA.

[12] P.Langacker, " Introduction to the Standard Model and Electroweak Physics" , arXiv:0901.0241 [hep-ph].

[13] A. Belyaev, N. D. Christensen, and A. Pukhov, "CalcHEP Calculator for High Energy Physics A package for the evaluation of feynman diagrams, integration

over multi-particle phase space, and event generation " right Comput. Phys. Commun. 184 1729 (2013), 1207.6082.

[14] Taizo Muta, " Foundations of quantum chromodynamics: An Introduction to Perturbative Methods in Gauge Theories" , World Scientific Publishing Co. Pte. Ltd, 1987

[15] Rikard Enberg, " Advanced Particle Physics 1FA355:Brief notes on gauge theory" , April 1, 2014; https://fr.scribd.com/document/358822505/Gauge-Theory

[16] Gordon L. Kane, " Modern elementary particle physics, the fundamental particles and forces" , Addison-Wcsley Publishing Company

[17] G. Altarelli, " Collider Physics within the Standard Model: A Primer" , arXiv:1303.2842.

[18] N. Baouche and A. Ahriche, "Identifying the nature of dark matter at e^-e^+ colliders," Phys. Rev. D **96**, no. 5, 055029 (2017) doi:10.1103/PhysRevD.96.055029 [arXiv:1707.05263 [hep-ph]].

[19] Joseph John Bevelacqua, " Health Physics in the 21st Century" , WILEY-VCH Verlag GmbH & Co. KGaA

[20] http://www.linearcollider.org/pdf/ilc_gateway_report.pdf

[21] S. Dawson, R.N Mohapatra, " COLLIDERS AND NEUTRINOS, The Window into Physics beyond the Standard Model" , World Scientific Publishing Co. Pte. Ltd, 2008.

[22] M. D. Schwartz, "TASI Lectures on Collider Physics," doi:10.1142/9789813233348002 arXiv:1709.04533 [hep-ph].

[23] G. Cowan, K. Cranmer, E. Gross and O. Vitells, "Asymptotic formulae for likelihood-based tests of new physics," Eur. Phys. J. C **71**, 1554 (2011) Erratum: [Eur. Phys. J. C **73**, 2501 (2013)] doi:10.1140/epjc/s10052-011-1554-0, 10.1140/epjc/s10052-013-2501-z [arXiv:1007.1727 [physics.data-an]].

[24] S. Heinemeyer *et al.* [LHC Higgs Cross Section Working Group], doi:10.5170/CERN-2013-004 arXiv:1307.1347 [hep-ph].

[25] C. W. Chiang, S. Kanemura and K. Yagyu, Phenomenology of the Georgi-Machacek model at future electron-positron colliders, Phys. Rev. D **93** (2016) no.5, 055002 [arXiv:1510.06297 [hep-ph]].

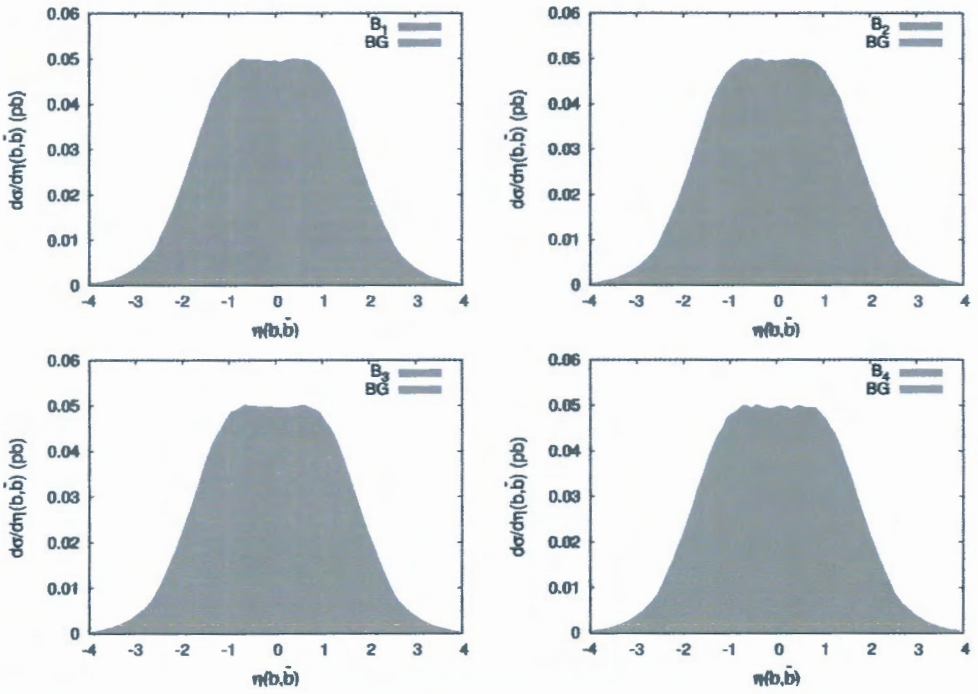

Figure 4.38: Distributions of the two jets pseudorapidity for the four benchmarks.

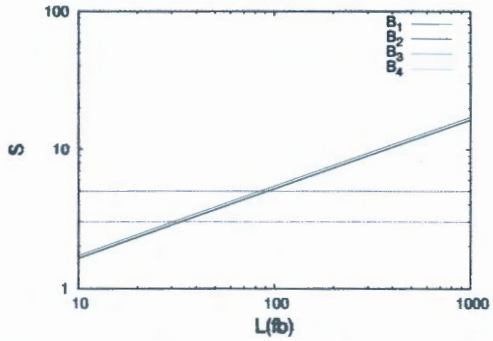

Figure 4.39: The significance as a function of integrated luminosity L. The two dashed lines represent S=3 and S=5

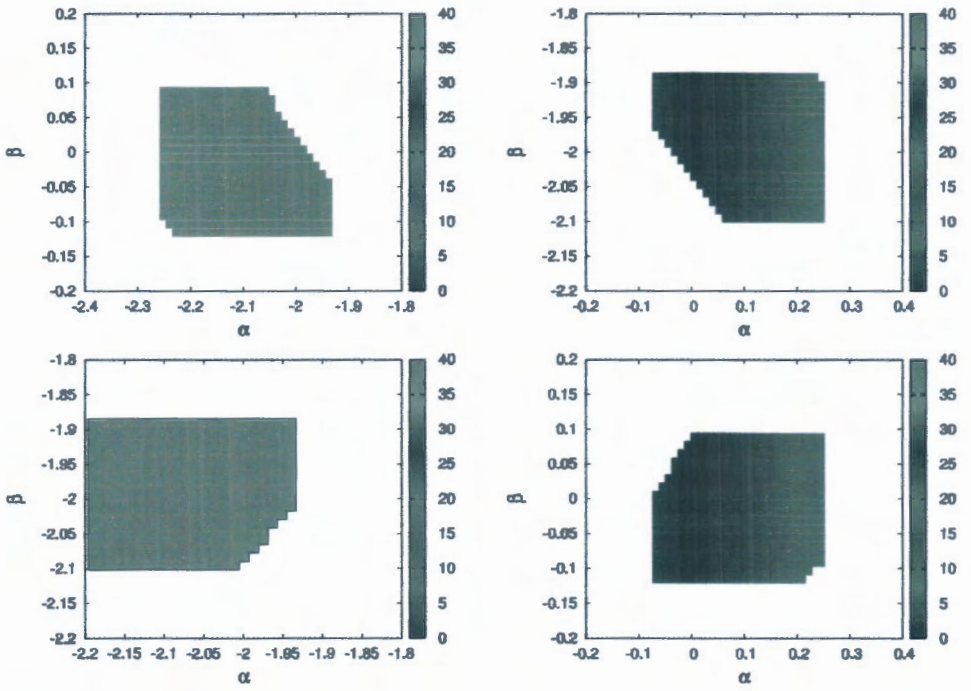

Figure 4.40: The signal significance for $L = 10(\ fb^{-1})$ as a function of parameters β and α.

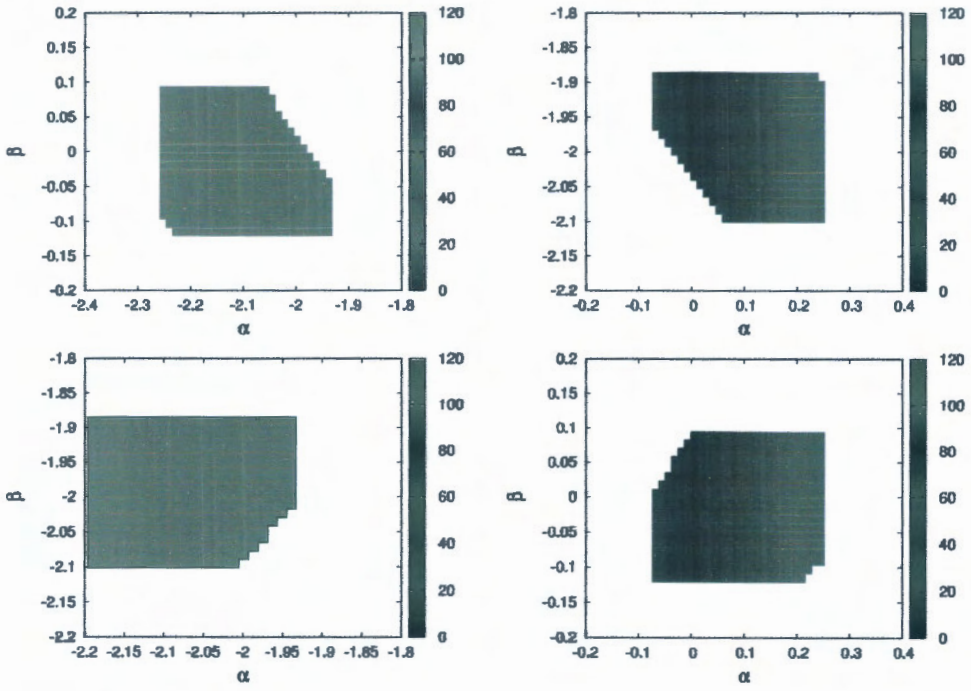

Figure 4.41: The signal significance for $L = 100(\ fb^{-1})$ as a function of parameters β and α.

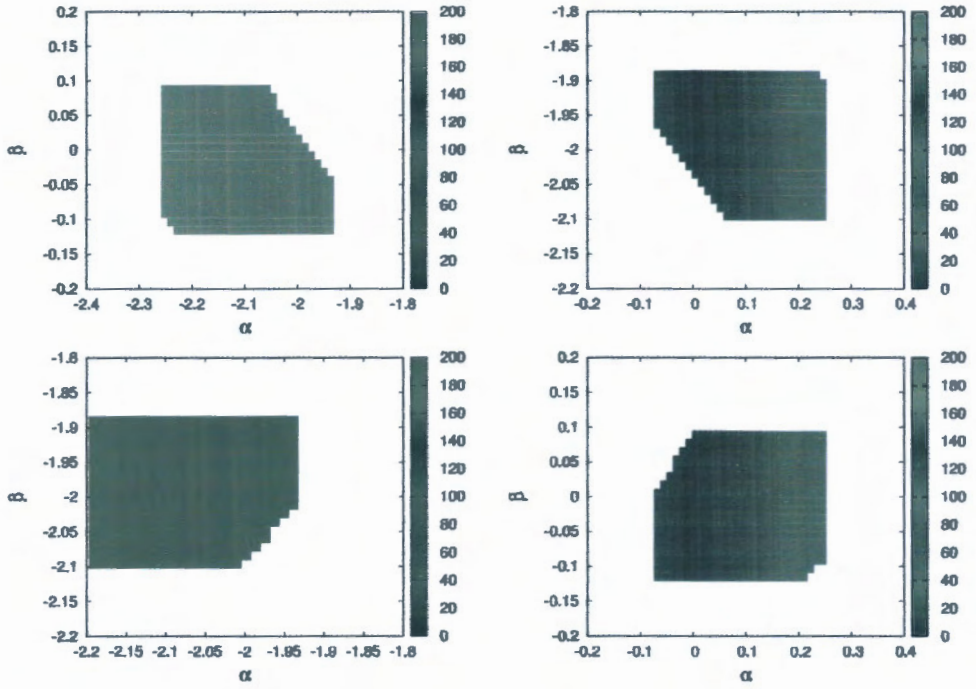

Figure 4.42: The signal significance for $L = 300(\ fb^{-1})$ as a function of parameters β and α.

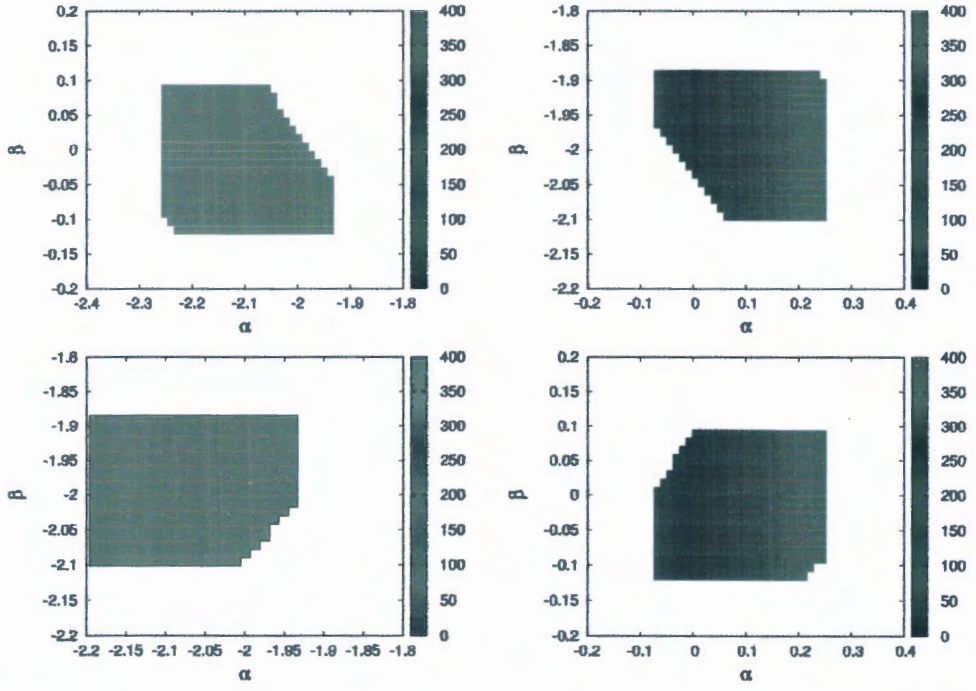

Figure 4.43: The signal significance for $L = 1000(\ fb^{-1})$ as a function of parameters β and α.

Chapter 5

Conclusion

In our work, we have investigated the possibility of discovering a new physics beyond the standard model at future leptonic collider ILC. To realize this task, we considered the process $e^-e^+ \rightarrow HZ \rightarrow b\bar{b}$+$E_{miss}$ at center of mass energy $E_{CM} = 1000GeV$, where $E_{miss} = \upsilon_i\bar{\upsilon}_i$ $(i = e, \mu, \tau)$, then concidered two parameters α and β where α, β are real numbers that can express any possible deviation from the SM, for the couplings HWW and HZZ, respectively. Of course, before began this study, we started by giving a brief review for the SM, the Higgs mechanism, and the general lagrangean of the model, after that, we talked about its limitations. Then, we gave a simple description for CalcHEP, the package used in this study, and defined the kinematic variables used in accelerators physics, we described also some colliders.

In this work, and by using CalcHEP package, we fixed the parameter values, and then generated the differential cross section for both the background (SM) and the signal (the four Benchmarks B_i), where we were able to produce a set of different distributions in order to define a new set of cuts that maximize the significance. We showed that at the choosen cuts and at the α and β chosen values in B1, B2, B3 and B4, and within estimating the cross section of different benchmarks and the background, and then estimating the signal by variating integrated luminosity, there was a deviation from the standard model at minimum of $L = 30\ fb^{-1}$ and we saw clearly a discovery at minimum of $L = 84\ fb^{-1}$. Finaly, We then translated the values of the measured cross sections in each case to a palette of signal significance in terms of α and β by taking four values for luminosity ($L = 10\ fb^{-1}$, $L = 100\ fb^{-1}$, $L = 300\ fb^{-1}$, $L = 1000\ fb^{-1}$), we detected a discovery signal.

We conclude that the reaction $e^-e^+ \rightarrow HZ \rightarrow b\bar{b}$+$E_{miss}$ is excellent for investigating the possibility of discovering a new physics beyond the standard model at future leptonic collider ILC.

Appendix A

CalcHEP model files & Batch files

A.1 CalcHEP model files

Here we show the SM CalcHEP model files where the HVV couplings are modified.

```
SMm
 Particles
 Full  name  |A   |A+  | number |2*spin| mass  |width |color|aux|>LaTex(A)<|>LaTeX(A+)   <|
gluon        |G   |G   |21      |2     |0      |0     |8    |G  |g         |g
photon       |A   |A   |22      |2     |0      |0     |1    |G  |\gamma    |\gamma
Z-boson      |Z   |Z   |23      |2     |MZ     |wZ    |i    |G  |Z         |Z
W-boson      |W+  |W-  |24      |2     |MW     |wW    |1    |G  |W+        |W-
Higgs        |h   |h   |25      |0     |Mh     |wh    |1    |   |h         |h
electron     |e   |E   |ii      |i     |Me     |0     |i    |   |e         |\bar{e}
e-neutrino   |ne  |Ne  |12      |1     |0      |0     |1    |L  |\nu_e     |\bar{\nu}_e
muon         |m   |M   |i3      |i     |Mm     |0     |i    |   |\mu       |\bar{\mu}
m-neutrino   |nm  |Nm  |14      |1     |0      |0     |1    |L  |\nu_\mu   |\bar{\nu}_\mu
tau-lepton   |l   |L   |i5      |i     |Ml     |0     |i    |   |\tau      |\bar{\tau}
t-neutrino   |nl  |Nl  |16      |1     |0      |0     |1    |L  |\nu_\tau  |\bar{\nu}_\tau
d-quark      |d   |D   |1       |1     |0      |0     |3    |   |d         |\bar{d}
u-quark      |u   |U   |2       |1     |0      |0     |3    |   |u         |\bar{u}
s-quark      |s   |S   |3       |1     |0      |0     |3    |   |s         |\bar{s}
c-quark      |c   |C   |4       |1     |Mcp    |0     |3    |   |c         |\bar{c}
b-quark      |b   |B   |5       |1     |Mbp    |0     |3    |   |b         |\bar{b}
t-quark      |t   |T   |6       |1     |Mtp    |wt    |3    |   |t         |\bar{t}
=============================================================================================
```

```
SMm
 Parameters
  Name   <| Value          <|> Comment                                                    <|
 alphaSMZ |0.1184           |Srtong alpha(MZ) for running mass calculation
 EE       |0.31343          |elecromagnetic constant
 Me       |0.000511         |electron mass
 Mm       |0.1057           |muon mass
 Ml       |1.777            |tau-lepton mass
 Q        |100              |scale for running mass calculation
 McMc     |1.23             | Mc(Mc)  MS-BAR
 MbMb     |4.25             | Mb(Mb)  MS-BAR
 Mtp      |173.07           |t-quark pole mass
 Mh       |125.09           |higgs mass
 wt       |1.59             |t-quark width        (tree level 1->2x)
 MZ       |91.188           |Z-boson mass
 MW       |80.385           |Sine of electro-weak mixing angle (MS_bar)
 bb       |0                | hZZ
 aa       |0                | hWW
 v        |246.22           | Higgs vev
```

```
 s12       |0.221            |Parameter of C-K-M matrix  (PDG96)
 s23       |0.041            |Parameter of C-K-M matrix  (PDG96)
 s13       |0.0035           |Parameter of C-K-M matrix  (PDG96)
 wt        |1.59             |t-quark width        (tree level 1->2x)
 wZ        |2.49444          |Z-boson width        (tree level 1->2x)
 wW        |2.08895          |W-boson width        (tree level 1->2x)
=============================================================================================================

SMm
 Constraints
 Name       |  Expression                                                                              <|
CW          |MW/MZ                          % on-shell cos of the Weinberg angle
SW          |sqrt(1-CW^2)                   % sin of the Weinberg angle
GF          |EE^2/(2*SW*MW)^2/Sqrt2         % Fermi constant (not used below)
c12         |sqrt(1-s12^ 2)                 % parameter  of C-K-M matrix
c23         |sqrt(1-s23^ 2)                 % parameter  of C-K-M matrix
c13         |sqrt(1-s13^ 2)                 % parameter  of C-K-M matrix
Vud         |c12*c13                        % C-K-M matrix element
Vus         |s12*c13                        % C-K-M matrix element
Vub         |s13                            % C-K-M matrix element
Vcd         |-s12*c23-c12*s23*s13           % C-K-M matrix element
Vcs         |c12*c23-s12*s23*s13            % C-K-M matrix element
Vcb         |s23*c13                        % C-K-M matrix element
Vtd         |s12*s23-c12*c23*s13            % C-K-M matrix element
Vts         |-c12*s23-s12*c23*s13           % C-K-M matrix element
Vtb         |c23*c13                        % C-K-M matrix element
Mb          |MbEff(Q)
Mt          |MtEff(Q)
Mc          |McEff(Q)
VEV         |2*MW*SW/EE
LamQCD      |initQCD5(alphaSMZ,McMc,MbMb,Mtp)
Mcp         | McMc*(1+4/3*alphaQCD(McMc)/pi)  % 1 loop formula like in Hdecay
Mbp         | MbMb*(1+4/3*alphaQCD(MbMb)/pi)  % 1 loop formula like in Hdecay
aQCDh       |alphaQCD(Mh)/pi
Rqcdh       |sqrt(1+149/12*aQCDh+68.6482*aQCDh^2-212.447*aQCDh^3)
LGGh        |-cabs(hGGeven(Mh, aQCDh,3, 1,3,Mtp,1/VEV,  1,3,Mbp,1/VEV, 1,3,Mcp,1/VEV))
Quq         | 4/9
Qdq         | 1/9
LAAh        |-cabs( hAAeven(Mh,aQCDh,2, 2,1,MW,-2/VEV, 1,1,Ml,1/VEV)+Quq*hAAe)
=============================================================================================================

SMm
 Vertices
A1   |A2   |A3   |A4   |>          Factor                          <|>  Lorentz part
G    |G    |G    |     |GG                                          |m1.m2*(p1-p2).m3+m2.m3*(p2-p3).m1+m3.m1*(p3-p
G    |G    |G.t  |     |GG/Sqrt2                                    |m1.M3*m2.m3-m1.m3*m2.M3
W+   |W-   |A    |     |-EE                                         |m1.m2*(p1-p2).m3+m2.m3*(p2-p3).m1+m3.m1*(p3-p
W+   |W-   |Z    |     |-EE*CW/SW                                   |m1.m2*(p1-p2).m3+m2.m3*(p2-p3).m1+m3.m1*(p3-p
W+   |W-   |Z    |Z    |-(EE*CW/SW)^ 2                              |2*m1.m2*m3.m4-m1.m3*m2.m4-m1.m4*m2.m3
W+   |W+   |W-   |W-   |(EE/SW)^ 2                                  |2*m1.m2*m3.m4-m1.m3*m2.m4-m1.m4*m2.m3
W+   |W-   |A    |Z    |-EE^ 2*CW/SW                                |2*m1.m2*m3.m4-m1.m3*m2.m4-m1.m4*m2.m3
W+   |W-   |A    |A    |-EE^ 2                                      |2*m1.m2*m3.m4-m1.m3*m2.m4-m1.m4*m2.m3
h    |h    |h    |     |-(3/2)*EE*Mh^2/(MW*SW)                      |1+cc
h    |W+   |W-   |     |EE*MW/SW                                    |(1+aa)*m2.m3
h    |Z    |Z    |     |EE/(SW*CW^ 2)*MW                            |(1+bb)*m2.m3
h    |fi   |fi   |     |-cs*v                                       |1
h    |h    |h    |h    |(-3/4)*(EE*Mh/(MW*SW))^ 2                   |1
h    |h    |Z    |Z    | (1/2)*(EE/(SW*CW))^ 2                      |m3.m4
h    |h    |W+   |W-   | (1/2)*(EE/SW)^ 2                           |m3.m4
M    |m    |h    |     |-EE*Mm/(2*MW*SW)                            |1
L    |l    |h    |     |-EE*Ml  /(2*MW*SW)                          |1
C    |c    |h    |     |-EE*Mc/(2*MW*SW)                            |1
B    |b    |h    |     |-EE*Mb/(2*MW*SW)                            |1
T    |t    |h    |     |-EE*Mt  /(2*MW*SW)                          |1
E    |e    |A    |     |-EE                                         |G(m3)
M    |m    |A    |     |-EE                                         |G(m3)
L    |l    |A    |     |-EE                                         |G(m3)
Ne   |e    |W+   |     |EE/(2*Sqrt2*SW)                             |G(m3)*(1-G5)
Nm   |m    |W+   |     |EE/(2*Sqrt2*SW)                             |G(m3)*(1-G5)
```

```
Nl  |l    |W+   |      |EE/(2*Sqrt2*SW)                    |G(m3)*(1-G5)
E   |ne   |W-   |      |EE/(2*Sqrt2*SW)                    |G(m3)*(1-G5)
M   |nm   |W-   |      |EE/(2*Sqrt2*SW)                    |G(m3)*(1-G5)
L   |nl   |W-   |      |EE/(2*Sqrt2*SW)                    |G(m3)*(1-G5)
E   |e    |Z    |      |-EE/(4*SW*CW)                      |G(m3)*(1-G5)-4*(SW^ 2)*G(m3)
M   |m    |Z    |      |-EE/(4*SW*CW)                      |G(m3)*(1-G5)-4*(SW^ 2)*G(m3)
L   |l    |Z    |      |-EE/(4*SW*CW)                      |G(m3)*(1-G5)-4*(SW^ 2)*G(m3)
Ne  |ne   |Z    |      |EE/(4*SW*CW)                       |G(m3)*(1-G5)
Nm  |nm   |Z    |      |EE/(4*SW*CW)                       |G(m3)*(1-G5)
Nl  |nl   |Z    |      |EE/(4*SW*CW)                       |G(m3)*(1-G5)
U   |u    |A    |      |(2/3)*EE                           |G(m3)
D   |d    |A    |      |(-1/3)*EE                          |G(m3)
C   |c    |A    |      |(2/3)*EE                           |G(m3)
S   |s    |A    |      |(-1/3)*EE                          |G(m3)
B   |b    |A    |      |(-1/3)*EE                          |G(m3)
T   |t    |A    |      |(2/3)*EE                           |G(m3)
U   |u    |Z    |      |-EE/(12*SW*CW)                     |-3*G(m3)*(1-G5)+8*(SW^ 2)*G(m3)
D   |d    |Z    |      |-EE/(12*SW*CW)                     |+3*G(m3)*(1-G5)-4*(SW^ 2)*G(m3)
C   |c    |Z    |      |-EE/(12*SW*CW)                     |-3*G(m3)*(1-G5)+8*(SW^ 2)*G(m3)
S   |s    |Z    |      |-EE/(12*SW*CW)                     |+3*G(m3)*(1-G5)-4*(SW^ 2)*G(m3)
B   |b    |Z    |      |-EE/(12*SW*CW)                     |+3*G(m3)*(1-G5)-4*(SW^ 2)*G(m3)
T   |t    |Z    |      |-EE/(12*SW*CW)                     |-3*G(m3)*(1-G5)+8*(SW^ 2)*G(m3)
U   |d    |W+   |      |EE*Vud/(2*Sqrt2*SW)                |G(m3)*(1-G5)
U   |s    |W+   |      |EE*Vus/(2*Sqrt2*SW)                |G(m3)*(1-G5)
U   |b    |W+   |      |EE*Vub/(2*Sqrt2*SW)                |G(m3)*(1-G5)
C   |d    |W+   |      |EE*Vcd/(2*Sqrt2*SW)                |G(m3)*(1-G5)
C   |s    |W+   |      |EE*Vcs/(2*Sqrt2*SW)                |G(m3)*(1-G5)
C   |b    |W+   |      |EE*Vcb/(2*Sqrt2*SW)                |G(m3)*(1-G5)
T   |d    |W+   |      |EE*Vtd/(2*Sqrt2*SW)                |G(m3)*(1-G5)
T   |s    |W+   |      |EE*Vts/(2*Sqrt2*SW)                |G(m3)*(1-G5)
T   |b    |W+   |      |EE*Vtb/(2*Sqrt2*SW)                |G(m3)*(1-G5)
D   |u    |W-   |      |EE*Vud/(2*Sqrt2*SW)                |G(m3)*(1-G5)
S   |u    |W-   |      |EE*Vus/(2*Sqrt2*SW)                |G(m3)*(1-G5)
B   |u    |W-   |      |EE*Vub/(2*Sqrt2*SW)                |G(m3)*(1-G5)
D   |c    |W-   |      |EE*Vcd/(2*Sqrt2*SW)                |G(m3)*(1-G5)
S   |c    |W-   |      |EE*Vcs/(2*Sqrt2*SW)                |G(m3)*(1-G5)
B   |c    |W-   |      |EE*Vcb/(2*Sqrt2*SW)                |G(m3)*(1-G5)
D   |t    |W-   |      |EE*Vtd/(2*Sqrt2*SW)                |G(m3)*(1-G5)
S   |t    |W-   |      |EE*Vts/(2*Sqrt2*SW)                |G(m3)*(1-G5)
B   |t    |W-   |      |EE*Vtb/(2*Sqrt2*SW)                |G(m3)*(1-G5)
U   |u    |G    |      |GG                                 |G(m3)
D   |d    |G    |      |GG                                 |G(m3)
C   |c    |G    |      |GG                                 |G(m3)
S   |s    |G    |      |GG                                 |G(m3)
T   |t    |G    |      |GG                                 |G(m3)
B   |b    |G    |      |GG                                 |G(m3)
U   |b    |W+.f |      |-i*EE*Vub/(2*Sqrt2*MW*SW)          |Mb*(1+G5)
C   |d    |W+.f |      |-i*EE*Vcd/(2*Sqrt2*MW*SW)          |          -Mc*(1-G5)
C   |b    |W+.f |      |-i*EE*Vcb/(2*Sqrt2*MW*SW)          |Mb*(1+G5)-Mc*(1-G5)
T   |d    |W+.f |      |-i*EE*Vtd/(2*Sqrt2*MW*SW)          |          -Mt  *(1-G5)
T   |b    |W+.f |      |-i*EE*Vtb/(2*Sqrt2*MW*SW)          |Mb*(1+G5)-Mt  *(1-G5)
D   |c    |W-.f |      |-i*EE*Vcd/(2*Sqrt2*MW*SW)          |Mc*(1+G5)
D   |t    |W-.f |      |-i*EE*Vtd/(2*Sqrt2*MW*SW)          |Mt  *(1+G5)
B   |u    |W-.f |      |-i*EE*Vub/(2*Sqrt2*MW*SW)          |           -Mb*(1-G5)
B   |c    |W-.f |      |-i*EE*Vcb/(2*Sqrt2*MW*SW)          |Mc*(1+G5)-Mb*(1-G5)
B   |t    |W-.f |      |-i*EE*Vtb/(2*Sqrt2*MW*SW)          |Mt  *(1+G5)-Mb*(1-G5)
C   |c    |Z.f  |      |-i*EE*Mc/(2*MW*SW)                 |G5
T   |t    |Z.f  |      |-i*EE*Mt  /(2*MW*SW)               |G5
B   |b    |Z.f  |      |i*EE*Mb/(2*MW*SW)                  |G5
M   |nm   |W-.f |      |-i*EE*Mm/(2*Sqrt2*MW*SW)           |-(1-G5)
L   |nl   |W-.f |      |-i*EE*Ml  /(2*Sqrt2*MW*SW)         |-(1-G5)
Nm  |m    |W+.f |      |-i*EE*Mm/(2*Sqrt2*MW*SW)           |(1+G5)
Nl  |l    |W+.f |      |-i*EE*Ml  /(2*Sqrt2*MW*SW)         |(1+G5)
M   |m    |Z.f  |      |i*EE*Mm/(2*MW*SW)                  |G5
L   |l    |Z.f  |      |i*EE*Ml  /(2*MW*SW)                |G5
h   |Z.f  |Z    |      |i*EE/(2*CW*SW)                     |(p2-p1).m3
h   |W-.f |W+   |      |i*EE/(2*SW)                        |(p2-p1).m3
h   |W+.f |W-   |      |i*EE/(2*SW)                        |(p2-p1).m3
Z.f |W+.f |W-   |      |EE/(2*SW)                          |-(p2-p1).m3
```

```
Z.f  |W-.f |W+   |     |EE/(2*SW)                                  |(p2-p1).m3
W-.f |W+.f |Z    |     |EE/(2*CW*SW)                               |(1-2*SW^ 2)* (p2-p1).m3
W-.f |W+.f |A    |     |EE                                         |(p2-p1).m3
W-.f |W+   |A    |     |-i*EE*MW                                   |m2.m3
W+.f |W-   |A    |     |-i*EE*MW                                   |-m2.m3
W-.f |W+   |Z    |     |-i*EE*MW*SW/CW                             |-m2.m3
W+.f |W-   |Z    |     |-i*EE*MW*SW/CW                             |m2.m3
W+.f |W-.f |h    |     |-EE*Mh^ 2/(2*MW*SW)                        |1
Z.f  |Z.f  |h    |     |-EE*Mh^ 2/(2*MW*SW)                        |1
W-.f |W+.f |A    |A    |2*EE^ 2                                    |m3.m4
W-.f |W+.f |Z    |Z    |(EE/(CW*SW))^ 2/2                          |(1-2*SW^ 2)^ 2*m3.m4
W-.f |W+.f |W-   |W+   |EE^ 2/(2*SW*SW)                            |m3.m4
W-.f |W+.f |Z    |A    |EE^ 2/(SW*CW)                              |(1-2*SW^ 2)*m3.m4
Z.f  |Z.f  |Z    |Z    |(EE/(SW*CW))^ 2/2                          |m3.m4
Z.f  |Z.f  |W-   |W+   |EE^ 2/(2*SW*SW)                            |m3.m4
W-.f |Z.f  |W+   |A    |-EE^ 2/(2*SW)                              |m3.m4
W+.f |Z.f  |W-   |A    |-EE^ 2/(2*SW)                              |m3.m4
W-.f |Z.f  |W+   |Z    |EE^ 2/(2*CW)                               |m3.m4
W+.f |Z.f  |W-   |Z    |EE^ 2/(2*CW)                               |m3.m4
W-.f |h    |W+   |A    |-i*EE^ 2/(2*SW)                            |m3.m4
W+.f |h    |W-   |A    |i*EE^ 2/(2*SW)                             |m3.m4
W-.f |h    |W+   |Z    |i*EE^ 2/(2*CW)                             |m3.m4
W+.f |h    |W-   |Z    |-i*EE^ 2/(2*CW)                            |m3.m4
Z.f  |Z.f  |Z.f  |Z.f  |-3*(EE*Mh/(2*MW*SW))^ 2                    |1
Z.f  |Z.f  |W-.f |W+.f |-(EE*Mh/(2*MW*SW))^ 2                      |1
W-.f |W-.f |W+.f |W+.f |- (EE*Mh/(MW*SW))^ 2/2                     |1
Z.f  |Z.f  |h    |h    |-(EE*Mh/(2*MW*SW))^ 2                      |1
W+.f |W-.f |h    |h    |-(EE*Mh/(2*MW*SW))^ 2                      |1
G.C  |G.c  |G    |     |-GG                                        |p1.m3
W-.C |Z.c  |W+   |     |EE*CW/SW                                   |p1.m3
W+.C |Z.c  |W-   |     |-EE*CW/SW                                  |p1.m3
Z.C  |W-.c |W+   |     |-EE*CW/SW                                  |p1.m3
Z.C  |W+.c |W-   |     |EE*CW/SW                                   |p1.m3
W-.C |W+.c |Z    |     |-EE*CW/SW                                  |p1.m3
W+.C |W-.c |Z    |     |EE*CW/SW                                   |p1.m3
W-.C |W+.c |A    |     |-EE                                        |p1.m3
W+.C |W-.c |A    |     |EE                                         |p1.m3
Z.C  |Z.c  |h    |     |-EE*MW/(2*SW*CW*CW)                        |1
W-.C |W+.c |h    |     |-EE*MW/(2*SW)                              |1
W+.C |W-.c |h    |     |-EE*MW/(2*SW)                              |1
W-.C |W+.c |Z.f  |     |i*EE*MW/(2*SW)                             |1
W+.C |W-.c |Z.f  |     |-i*EE*MW/(2*SW)                            |1
W-.C |Z.c  |W+.f |     |-i*EE*MW/(2*CW*SW)                         |1-2*SW^ 2
W+.C |Z.c  |W-.f |     |i*EE*MW/(2*CW*SW)                          |1-2*SW^ 2
Z.C  |W-.c |W+.f |     |i*EE*MW/(2*CW*SW)                          |1
Z.C  |W+.c |W-.f |     |-i*EE*MW/(2*CW*SW)                         |1
W-.C |A.c  |W+   |     |EE                                         |p1.m3
W+.C |A.c  |W-   |     |-EE                                        |p1.m3
A.C  |W-.c |W+   |     |-EE                                        |p1.m3
A.C  |W+.c |W-   |     |EE                                         |p1.m3
W-.C |A.c  |W+.f |     |-i*EE*MW                                   |1
W+.C |A.c  |W-.f |     |i*EE*MW                                    |1
G    |G    |h    |     |-4*LGGh*Rqcdh                              |(p1.p2*m1.m2-p1.m2*p2.m1)
G    |G    |G    |h    |-4*LGGh*GG*Rqcdh                           |m1.m2*(p1-p2).m3+m2.m3*(p2-p3).m1+m3.m1*(p3-p
A    |A    |h    |     |-4*LAAh                                    |(p1.p2*m1.m2-p1.m2*p2.m1)
=============================================================================================================
```

A.2 Batch files

Here we show the batch files where all cuts are considered.

```
Model: SMod
Model changed: False
```

```
Gauge: Feynman

Process: e,E->nn,Nn,b,B
Composite: nn=ne,nm,nl
Composite: Nn=Ne,Nm,Nl

pdf1: ISR & Beamstrahlung
pdf2: ISR & Beamstrahlung
Bunch x+y sizes (nm) : 560
Bunch length (mm) : 0.4
Number of particles : 2E+10

p1: 500
p2: 500

Parameter: aa=0.04
Parameter: bb=0.04

Kinematics : 12 -> 34 , 56
Kinematics : 34 -> 3 , 4
Kinematics : 56 -> 5 , 6

Regularization momentum: 34
Regularization mass: MZ
Regularization width: wZ
Regularization power: 2

Regularization momentum: 56
Regularization mass: MZ
Regularization width: wZ
Regularization power: 2

Regularization momentum: 56
Regularization mass: Mh
Regularization width: wh
Regularization power: 2

Breit Wigner range : 2.7
T-channel widths : ON
GI in T-channel : ON
GI in S-channel : ON

Cut parameter: E(nn,Nn)
Cut invert: False
Cut min: 520
Cut max: 880

Cut parameter: E(b,B)
Cut invert: False
Cut min: 120
Cut max: 430

Cut parameter: T(nn,Nn)
Cut invert: False
Cut min:
Cut max: 250

Cut parameter: T(b)
Cut invert: False
Cut min: 15
Cut max:

Cut parameter: T(B)
Cut invert: False
Cut min: 15
Cut max:

Cut parameter: M(b,B)
Cut invert: False
```

```
Cut min: 71
Cut max: 145

Cut parameter: M(b,nn,Nn)
Cut invert: False
Cut min: 500
Cut max:

Cut parameter: M(B,nn,Nn)
Cut invert: False
Cut min: 500
Cut max:

Cut parameter: J(b,B)
Cut invert: False
Cut min: 0.4
Cut max:

Cut parameter: Z(b,B)
Cut invert: False
Cut min: 120
Cut max: 260

Cut parameter: C(b,B)
Cut invert: False
Cut min:
Cut max: 0.86

Cut parameter: D(b,B)
Cut invert: False
Cut min: 400
Cut max:

Cut parameter: W(b,nn,Nn)
Cut invert: False
Cut min:
Cut max: 600

Cut parameter: W(B,nn,Nn)
Cut invert: False
Cut min:
Cut max: 600

Dist parameter: E(nn,Nn)
Dist min: 0
Dist max: 1000
Dist n bins: 300
Dist title: e,E->nn,Nn,b,B
Dist x-title: Emiss (GeV)

Dist parameter: E(b)
Dist min: 0
Dist max: 500
Dist n bins: 300
Dist title: e,E->nn,Nn,b,B
Dist x-title: E(b) (GeV)

Dist parameter: E(B)
Dist min: 0
Dist max: 500
Dist n bins: 300
Dist title: e,E->nn,Nn,b,B
Dist x-title: E(B) (GeV)

Dist parameter: E(b,B)
Dist min: 0
Dist max: 1000
Dist n bins: 300
Dist title: e,E->nn,Nn,b,B
```

```
Dist x-title: E(b,B) (GeV)

Dist parameter: T(nn,Nn)
Dist min: 0
Dist max: 1000
Dist n bins: 300
Dist title: e,E->nn,Nn,b,B
Dist x-title: Tmiss (GeV)

Dist parameter: T(b)
Dist min: 0
Dist max: 500
Dist n bins: 300
Dist title: e,E->nn,Nn,b,B
Dist x-title: T(b) (GeV)

Dist parameter: T(B)
Dist min: 0
Dist max: 500
Dist n bins: 300
Dist title: e,E->nn,Nn,b,B
Dist x-title: T(B) (GeV)


Dist parameter: T(b,B)
Dist min: 0
Dist max: 1000
Dist n bins: 300
Dist title: e,E->nn,Nn,b,B
Dist x-title: T(b,B) (GeV)

Dist parameter: Z(b)
Dist min: 0
Dist max: 500
Dist n bins: 300
Dist title: e,E->nn,Nn,b,B
Dist x-title: Z(b) (GeV)

Dist parameter: Z(B)
Dist min: 0
Dist max: 500
Dist n bins: 300
Dist title: e,E->nn,Nn,b,B
Dist x-title: Z(B) (GeV)


Dist parameter: Z(b,B)
Dist min: 0
Dist max: 1000
Dist n bins: 300
Dist title: e,E->nn,Nn,b,B
Dist x-title: Z(b,B) (GeV)

Dist parameter: M(b,B)
Dist min: 71
Dist max: 145
Dist n bins: 300
Dist title: e,E->nn,Nn,b,B
Dist x-title: M(b,B) (GeV)

Dist parameter: M(b,nn,Nn)
Dist min: 0
Dist max: 1000
Dist n bins: 300
Dist title: e,E->nn,Nn,b,B
Dist x-title: M(b,Emiss) (GeV)

Dist parameter: M(B,nn,Nn)
Dist min: 0
```

```
Dist max: 1000
Dist n bins: 300
Dist title: e,E->nn,Nn,b,B
Dist x-title: M(B,Emiss) (GeV)

Dist parameter: C(b,B)
Dist min: -1
Dist max: 1
Dist n bins: 300
Dist title: e,E->nn,Nn,b,B
Dist x-title: C(b,B)

Dist parameter: C(b)
Dist min: -1
Dist max: 1
Dist n bins: 300
Dist title: e,E->nn,Nn,b,B
Dist x-title: C(b)

Dist parameter: C(B)
Dist min: -1
Dist max: 1
Dist n bins: 300
Dist title: e,E->nn,Nn,b,B
Dist x-title: C(B)

Dist parameter: K(b,B)
Dist min: -4
Dist max: 4
Dist n bins: 300
Dist title: e,E->nn,Nn,b,B
Dist x-title: K(b,B)

Dist parameter: N(b)
Dist min: -4
Dist max: 4
Dist n bins: 300
Dist title: e,E->nn,Nn,b,B
Dist x-title: N(b) (GeV)

Dist parameter: N(B)
Dist min: -4
Dist max: 4
Dist n bins: 300
Dist title: e,E->nn,Nn,b,B
Dist x-title: N(B) (GeV)

Dist parameter: N(b,B)
Dist min: -4
Dist max: 4
Dist n bins: 300
Dist title: e,E->nn,Nn,b,B
Dist x-title: N(b,B) (GeV)

Dist parameter: D(b,B)
Dist min: 0
Dist max: 1000
Dist n bins: 300
Dist title: e,E->nn,Nn,b,B
Dist x-title: D(b,B) (GeV)

Dist parameter: W(b,B)
Dist min: 0
Dist max: 1000
Dist n bins: 300
Dist title: e,E->nn,Nn,b,B
Dist x-title: W(b,B) (GeV)

Dist parameter: W(b,nn,Nn)
```

```
Dist min: 0
Dist max: 1000
Dist n bins: 300
Dist title: e,E->nn,Nn,b,B
Dist x-title: W(b,Emiss) (GeV)

Dist parameter: W(B,nn,Nn)
Dist min: 0
Dist max: 1000
Dist n bins: 300
Dist title: e,E->nn,Nn,b,B
Dist x-title: W(B,Emiss) (GeV)

Number of events (per run step): 0
Filename: bB-B1-apre-CUT.distr
NTuple: False
Cleanup: False

Parallelization method: local

Max number of nodes: 8
Max number of processes per node: 4

sleep time: 3
nice level : 19

nSess_1: 5
nCalls_1: 300000
nSess_2: 15
nCalls_2: 1000000
```

Bibliography

[1] G. Aad et al. [ATLAS Collaboration], Phys. Lett. B 716, 1 (2012) [arXiv:1207.7214 [hep-ex]].

[2] S. Chatrchyan et al. [c.m.S Collaboration], Phys. Lett. B 716, 30 (2012) [arXiv:1207.7235 [hep-ex]].

[3] T. Behnke, C. Damerell, J. Jaros, A. Miyamoto et al. (ILC Collaboration), arXiv:0712.2356 [physics.ins-det].

[4] C. Adolphsen et al., arXiv:1306.6328 [physics.acc-ph]. III, IV B

[5] H. Baer et al., arXiv:1306.6352 [hep-ph].

[6] J. R. Andersen et al. (LHC Higgs Cross Section Working Group) (2013), 1307.1347.

[7] C. Mariotti and G. Passarino, Int. J. Mod. Phys. A32, 1730003 (2017), 1612.00269

[8] in Proceedings, 2013 Community Summer Study on the Future of U.S. Particle Physics: Snowmass on the Mississippi (CSS2013): Minneapolis, MN, USA, July 29-August 6, 2013, (2013), 1307.7135, URL https://inspirehep.net/record/1244669/files/arXiv:1307.7135.pdf.

[9] L.Marleau, " Introduction à la physique des particles" , Département de physique. Université Laval. Québec,Canada, 1998-2017.

[10] W.N.COTTINGHAM and D.A. GREENWOOD, " An introduction to the Standard Model of Particle Physics" . CAMBRIDGE UNIVERSITY PRESS.

[11] David Griffiths, " INTRODUCTION TO ELEMENTARY PARTICLES" , WILEY-VCH Verlag GmbH & Co. KGaA.

[12] P.Langacker, " Introduction to the Standard Model and Electroweak Physics" , arXiv:0901.0241 [hep-ph].

[13] A. Belyaev, N. D. Christensen, and A. Pukhov, "CalcHEP Calculator for High Energy Physics A package for the evaluation of feynman diagrams, integration

over multi-particle phase space, and event generation " right Comput. Phys. Commun. 184 1729 (2013), 1207.6082.

[14] Taizo Muta, " Foundations of quantum chromodynamics: An Introduction to Perturbative Methods in Gauge Theories" , World Scientific Publishing Co. Pte. Ltd, 1987

[15] Rikard Enberg, " Advanced Particle Physics 1FA355:Brief notes on gauge theory" , April 1, 2014; https://fr.scribd.com/document/358822505/Gauge-Theory

[16] Gordon L. Kane, " Modern elementary particle physics, the fundamental particles and forces" , Addison-Wcsley Publishing Company

[17] G. Altarelli, " Collider Physics within the Standard Model: A Primer" , arXiv:1303.2842.

[18] N. Baouche and A. Ahriche, "Identifying the nature of dark matter at e^-e^+ colliders," Phys. Rev. D **96**, no. 5, 055029 (2017) doi:10.1103/PhysRevD.96.055029 [arXiv:1707.05263 [hep-ph]].

[19] Joseph John Bevelacqua, " Health Physics in the 21st Century" , WILEY-VCH Verlag GmbH & Co. KGaA

[20] http://www.linearcollider.org/pdf/ilc_gateway_report.pdf

[21] S. Dawson, R.N Mohapatra, " COLLIDERS AND NEUTRINOS, The Window into Physics beyond the Standard Model" , World Scientific Publishing Co. Pte. Ltd, 2008.

[22] M. D. Schwartz, "TASI Lectures on Collider Physics," doi:10.1142/9789813233348002 arXiv:1709.04533 [hep-ph].

[23] G. Cowan, K. Cranmer, E. Gross and O. Vitells, "Asymptotic formulae for likelihood-based tests of new physics," Eur. Phys. J. C **71**, 1554 (2011) Erratum: [Eur. Phys. J. C **73**, 2501 (2013)] doi:10.1140/epjc/s10052-011-1554-0, 10.1140/epjc/s10052-013-2501-z [arXiv:1007.1727 [physics.data-an]].

[24] S. Heinemeyer *et al.* [LHC Higgs Cross Section Working Group], doi:10.5170/CERN-2013-004 arXiv:1307.1347 [hep-ph].

[25] C. W. Chiang, S. Kanemura and K. Yagyu, Phenomenology of the Georgi-Machacek model at future electron-positron colliders, Phys. Rev. D **93** (2016) no.5, 055002 [arXiv:1510.06297 [hep-ph]].